X-ray Spectroscopy of Massive Stars: Constraints on Stellar Wind Mass-Loss Rates, Clumping, and Shock Physics

David Cohen
Swarthmore College

with Jon Sundqvist & Stan Owocki (U. Delaware), Maurice Leutenegger (GSFC),
Marc Gagné & Véronique Petit (West Chester University), Asif ud-Doula (Penn St.),
Alex Fullerton (STScI), Rich Townsend (Wisconsin)
and
Roban Kramer (Swarthmore ’03; ETH), Emma Wollman (Swarthmore ’09; Caltech),
Erin Martell (Swarthmore ’09; U. Chicago), James MacArthur (Swarthmore ’11; Sandia)

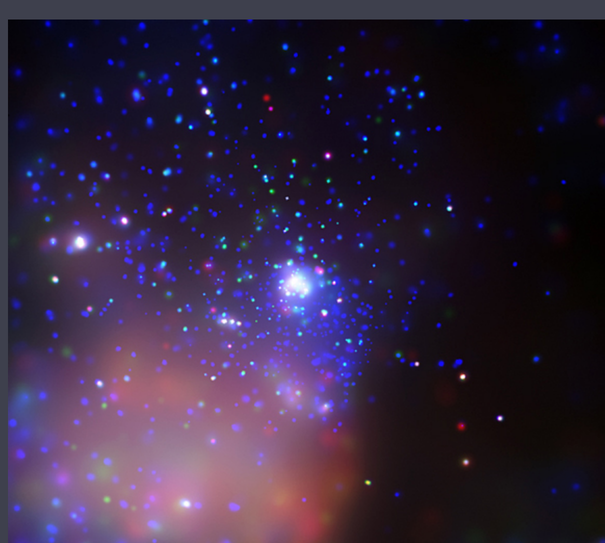

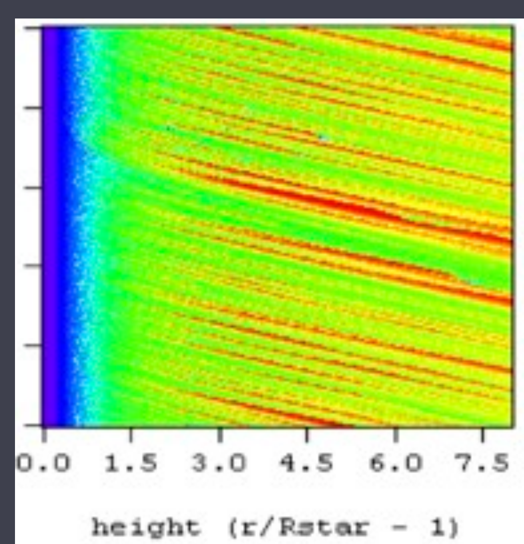

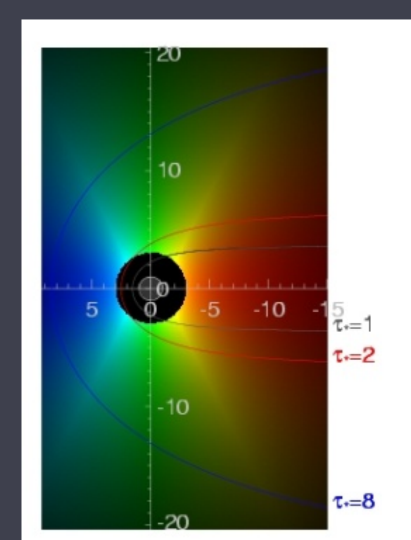

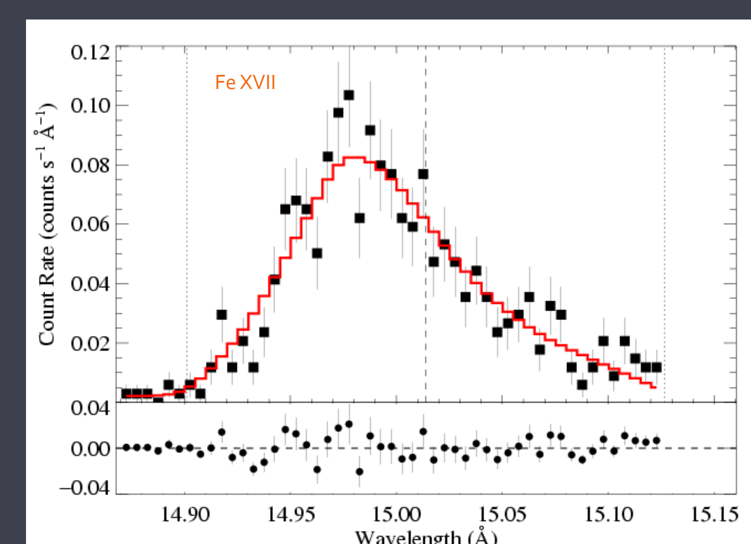

cool stars vs. hot stars

starfish, *in situ*, at the Monterey (California) Aquarium

The Sun's X-ray emission is associated with its magnetic dynamo (rotation + convection are key ingredients)

rotation

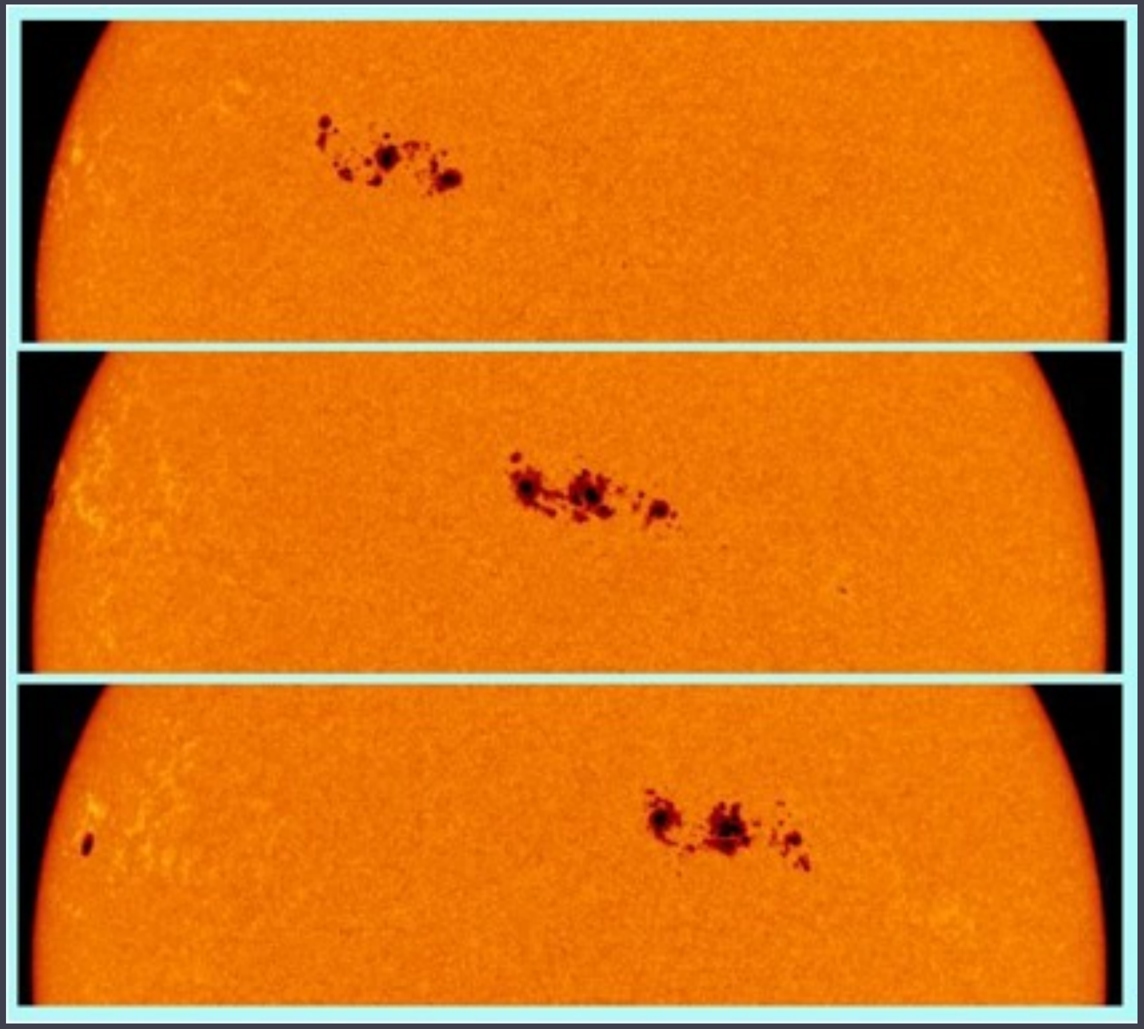

convection

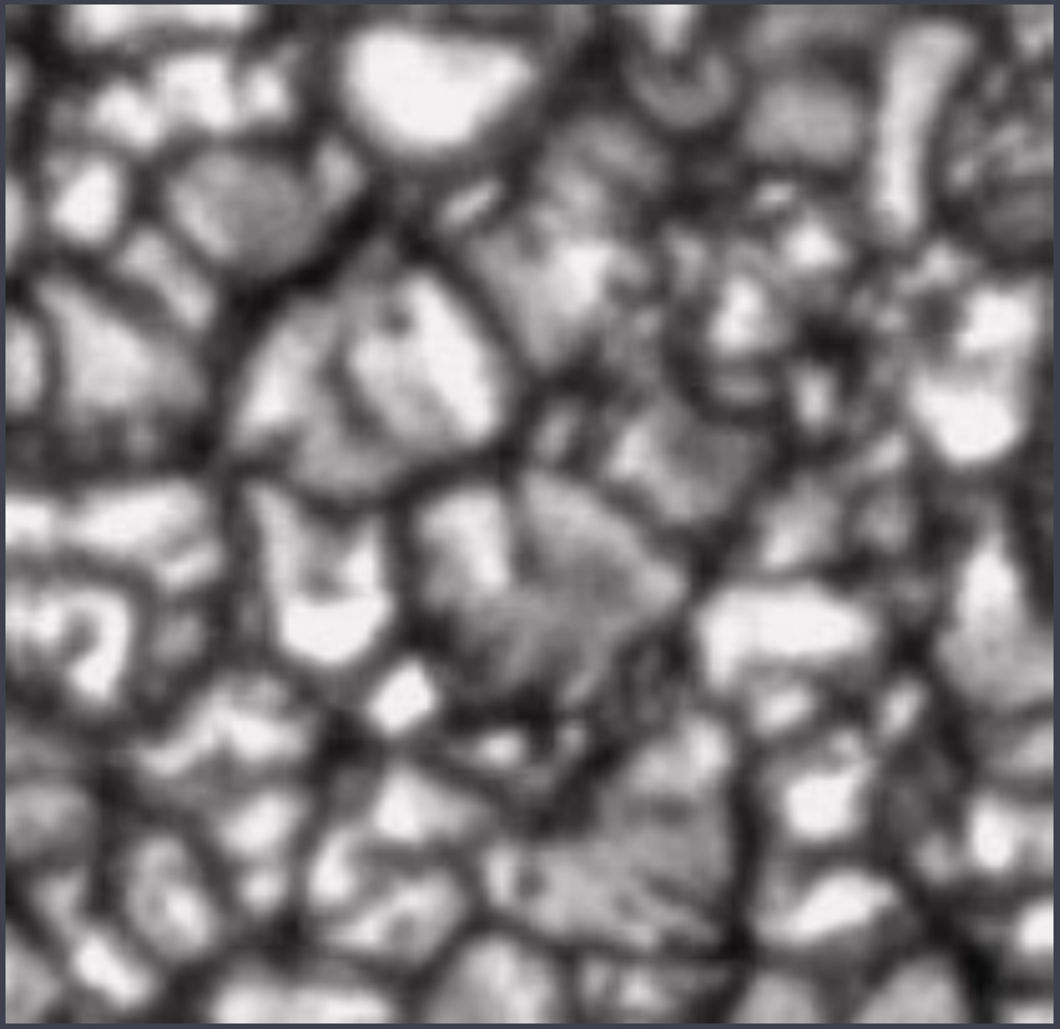

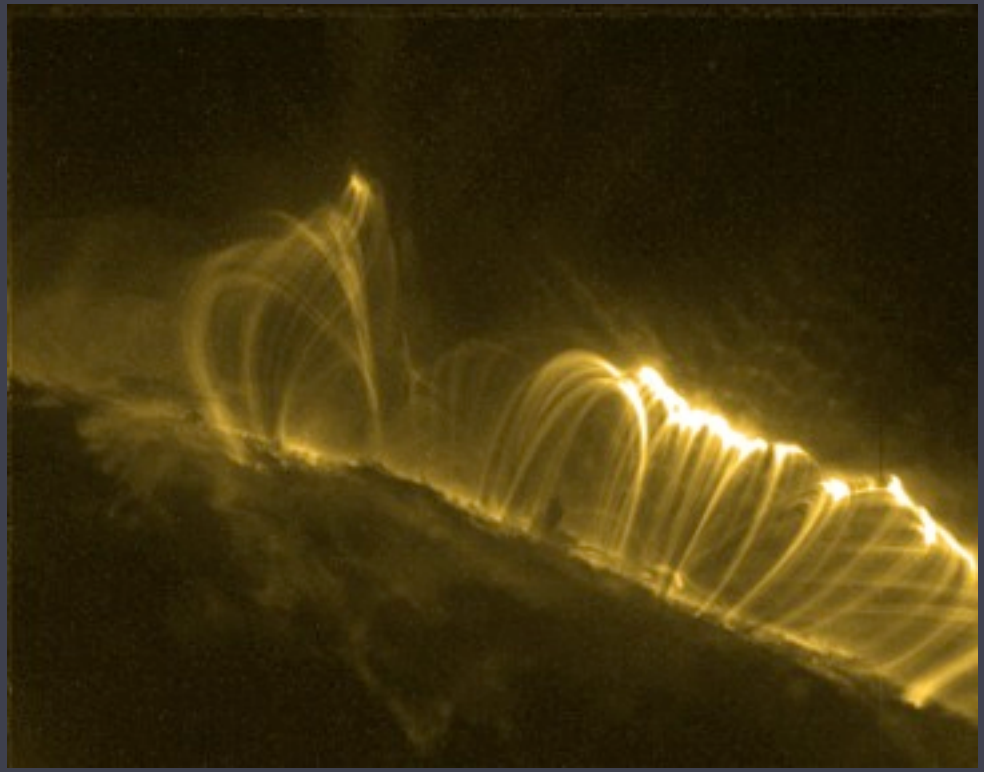

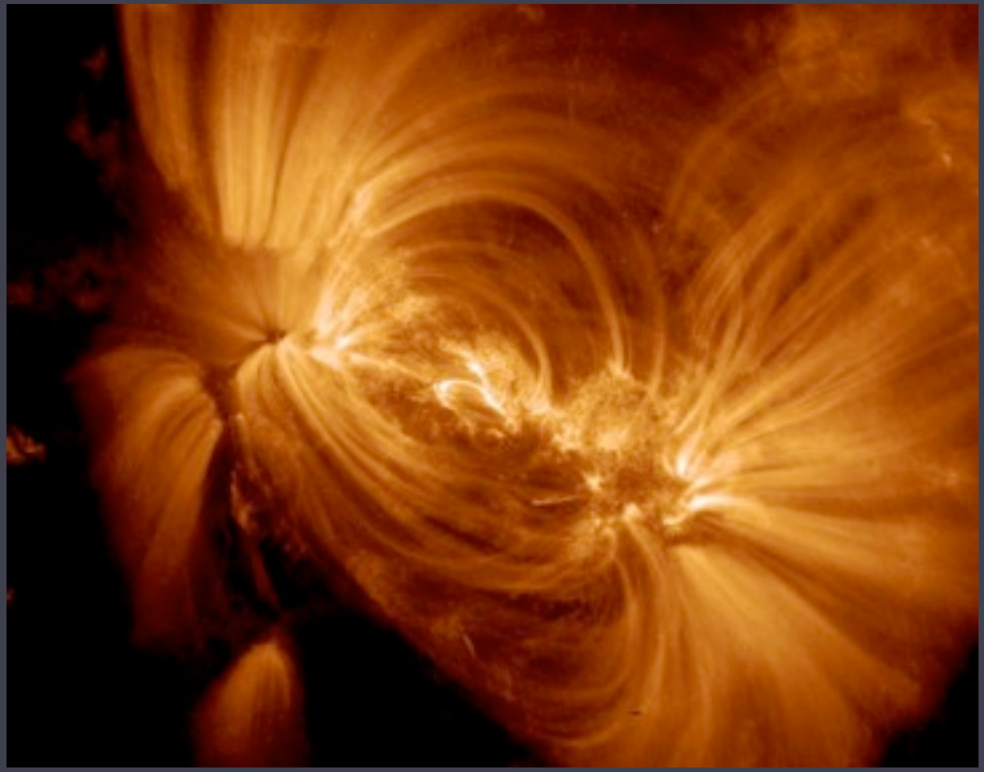

NASA: TRACE

Massive stars have some *other* X-ray production mechanism

Most massive stars do *not* have magnetic fields (theoretically understood as due to lack of convection)

No observed correlation between rotation and X-ray luminosity

low mass

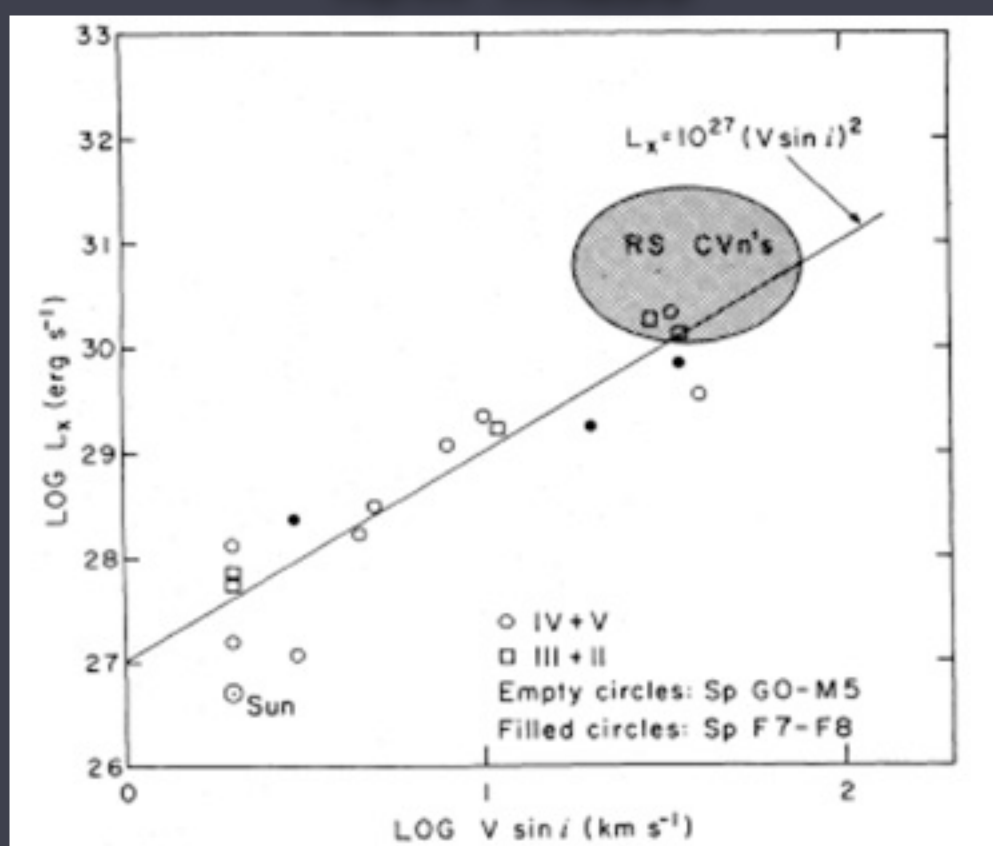

high mass

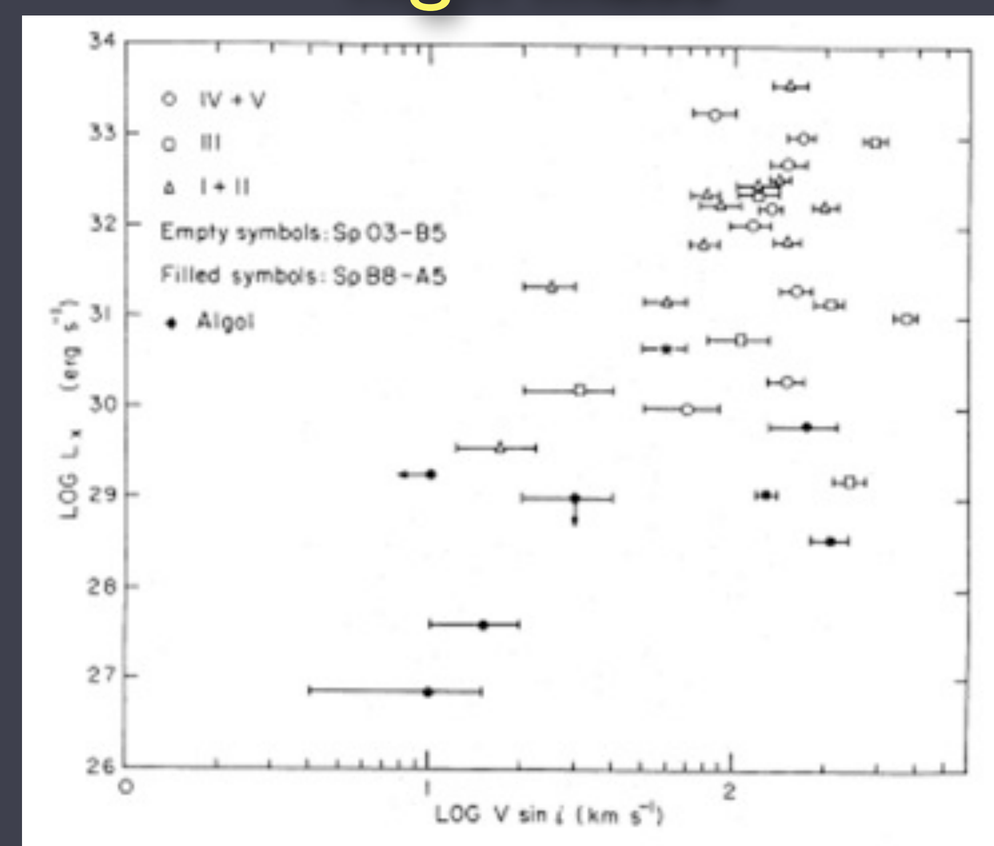

discovery of massive star X-ray emission in 1970s

THE ASTROPHYSICAL JOURNAL, 234:L51–54, 1979 November 15

DISCOVERY OF AN X-RAY STAR ASSOCIATION IN VI CYGNI (CYG OB2)

F. R. HARNDEN, JR., G. BRANDUARDI, M. ELVIS,[1] P. GORENSTEIN, J. GRINDLAY, J. P. PYE,[1] R. ROSNER, K. TOPKA, AND G. S. VAIANA[2]
Harvard-Smithsonian Center for Astrophysics, Cambridge, Massachusetts
Received 1979 June 26; accepted 1979 July 26

ABSTRACT

A group of six X-ray sources located within 0°.4 of Cygnus X-3 has been discovered with the *Einstein* Observatory. These sources have been positively identified and five of them correspond to stars in the heavily obscured OB association VI Cygni. The optical counterparts include four of the most luminous O stars within the field of view and a B5 supergiant. These sources are found to have typical X-ray luminosities L_x (0.2–4.0 keV) $\sim 5 \times 10^{33}$ ergs s^{-1}, with temperatures $T \sim 10^{6.8}$ K and hydrogen column densities $N_H \sim 10^{22}$ cm^{-2}, and therefore comprise a new class of low-luminosity galactic X-ray sources associated with early-type stars.

Basic properties of massive stars - O stars

mass ~ 50 M_{sun}
luminosity ~ 10^6 L_{sun}
surface temperature ~ 45,000 K

Basic properties of massive stars - O stars

mass ~ 50 M_{sun}
luminosity ~ 10^6 L_{sun}
surface temperature ~ 45,000 K

*significant **momentum** in the photospheric radiation field*

wind-blown bubble around a massive star

NGC 6888 Crescent Nebula - Tony Hallas

Radiation-driven O star winds

ζ Pup (O4 supergiant): $\dot{M}$ ~ few 10^{-6} M_{sun}/yr

UV spectrum: C IV 1548, 1551 Å

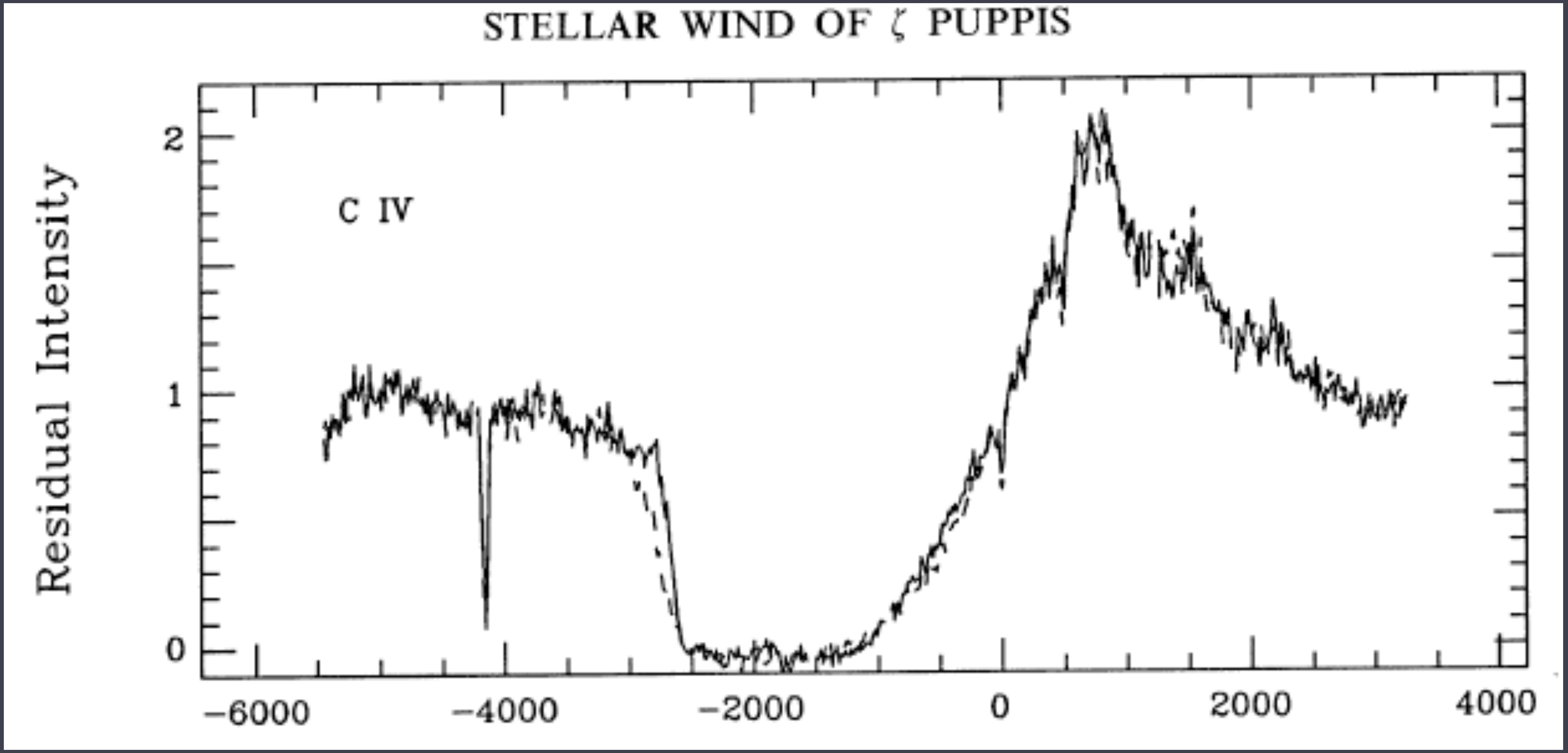

Velocity (km/s)

Prinja et al. 1992, ApJ, 390, 266

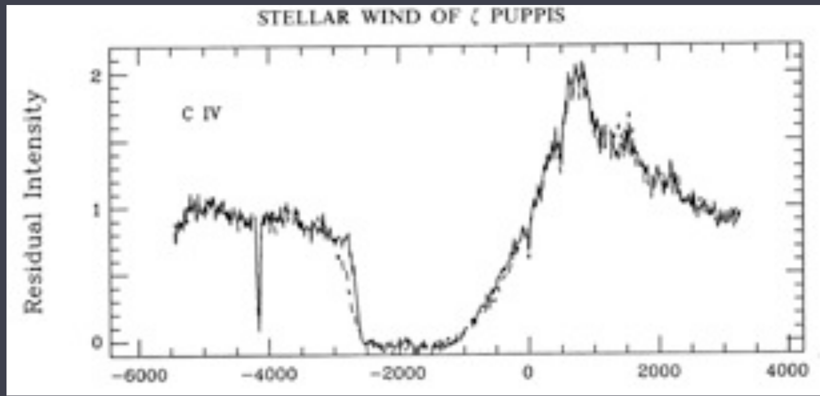
STELLAR WIND OF ζ PUPPIS
C IV
Residual Intensity
2
1
0
−6000
−4000
−2000
0
2000
4000

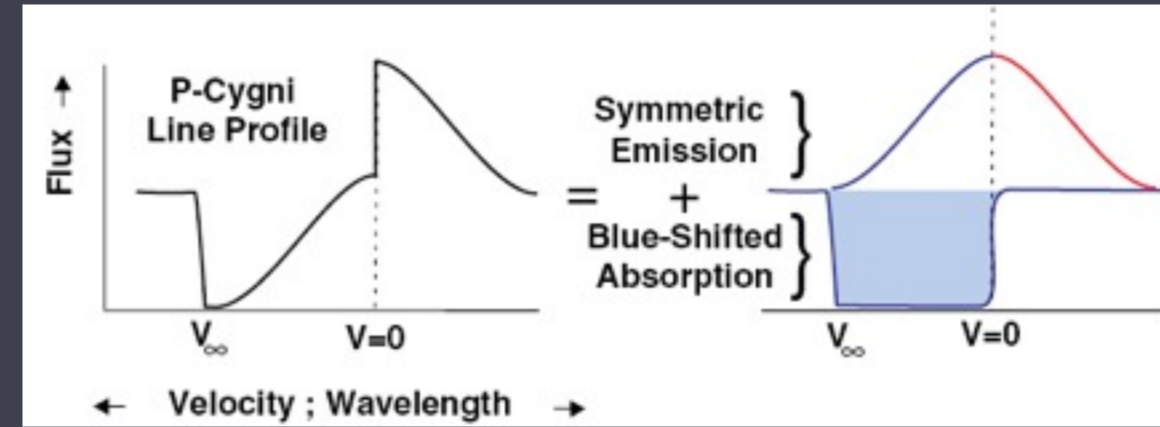
Flux
P-Cygni
Line Profile
V∞
V=0
Symmetric
Emission
=
+
Blue-Shifted
Absorption
V∞
V=0
Velocity ; Wavelength

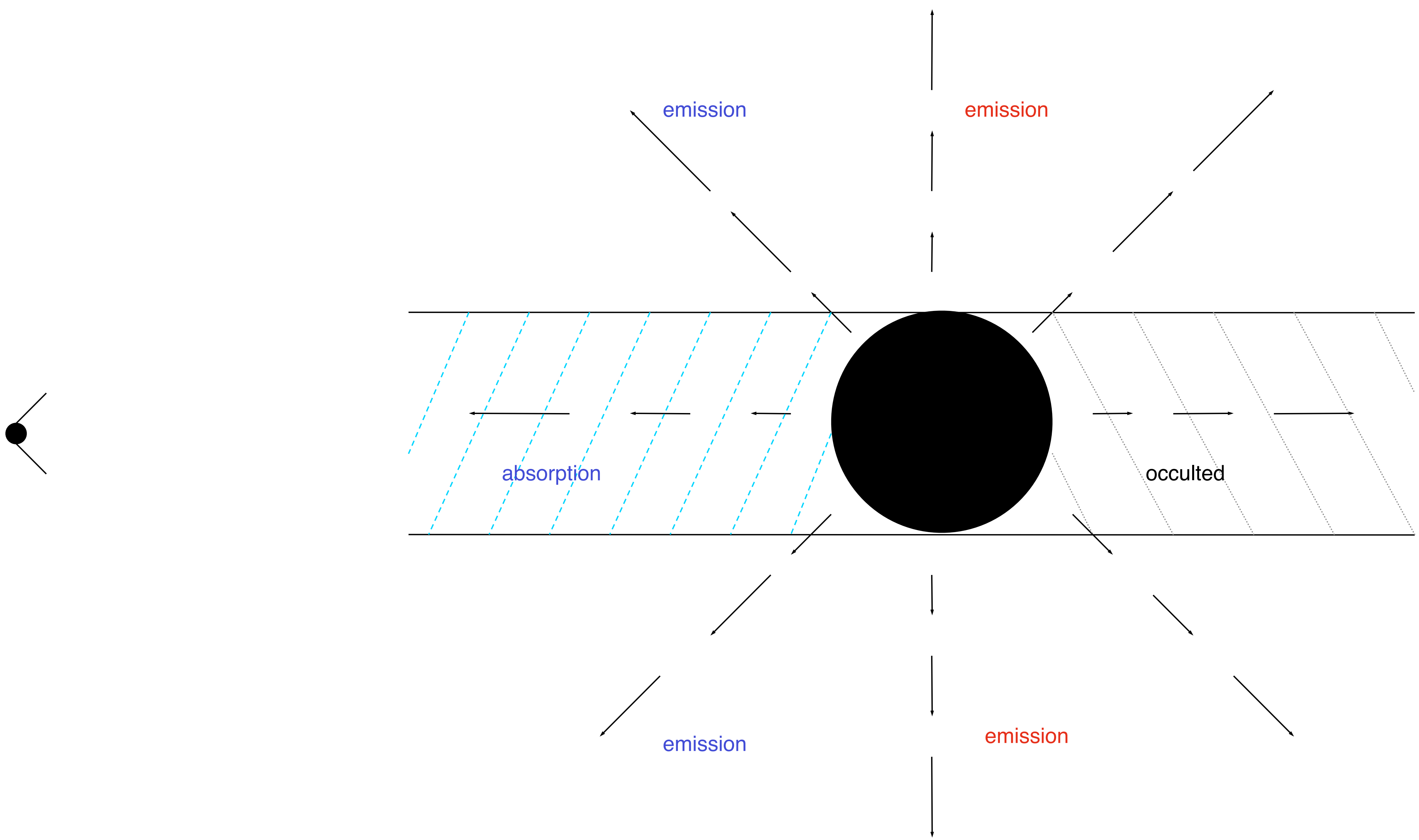
emission
emission
absorption
occulted
emission
emission

Radiation-driven O star winds

ζ Pup (O4 supergiant): $\dot{M} \sim$ few $10^{-6}\ M_{sun}/yr$

UV spectrum: C IV 1548, 1551 Å

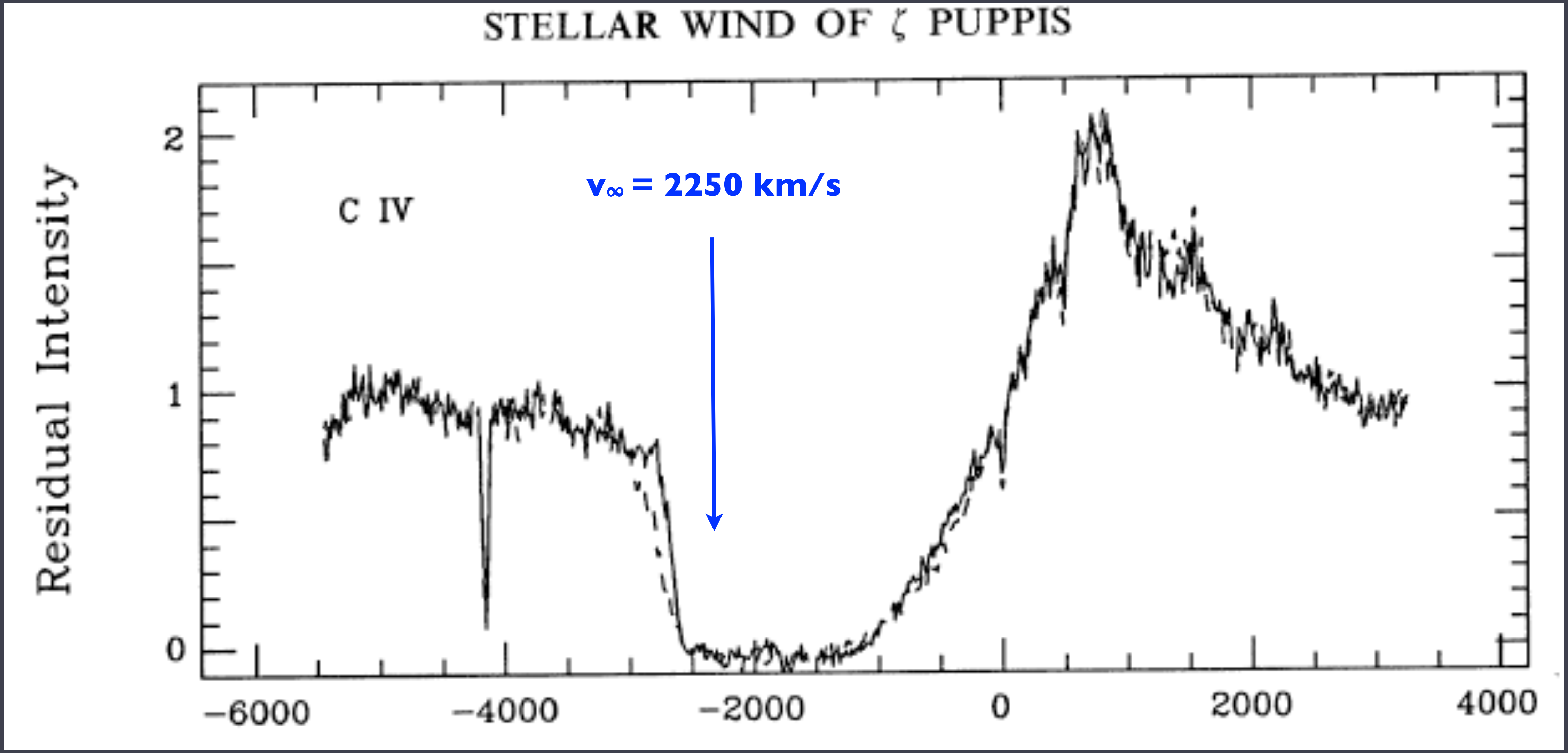

Prinja et al. 1992, ApJ, 390, 266

Velocity (km/s)

Wind mass-loss rates ($\dot{M}$) can be inferred from the strength of the absorption component

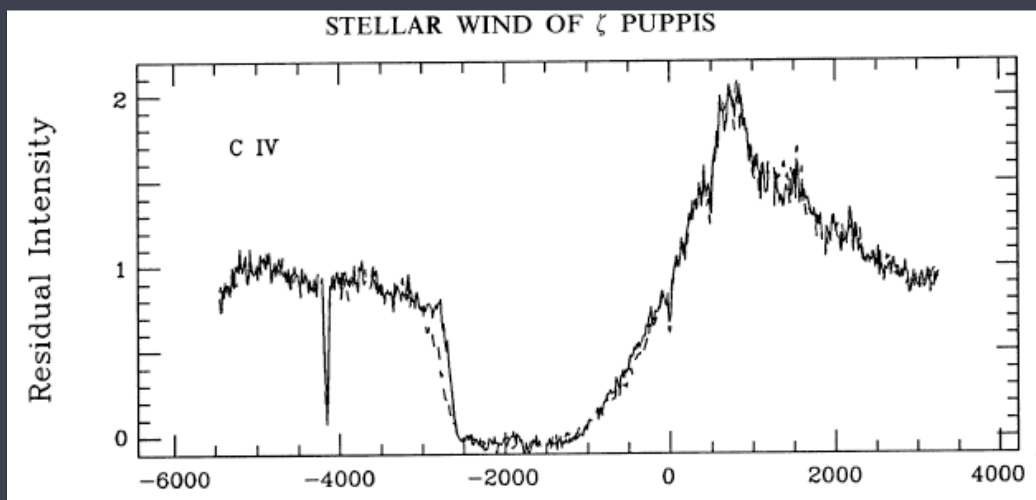

Velocity (km/s)

Prinja et al. 1992, ApJ, 390, 266

but, more reliable are emission lines such as Hα

emission from the wind, scales as density-squared

photosphere only, no wind

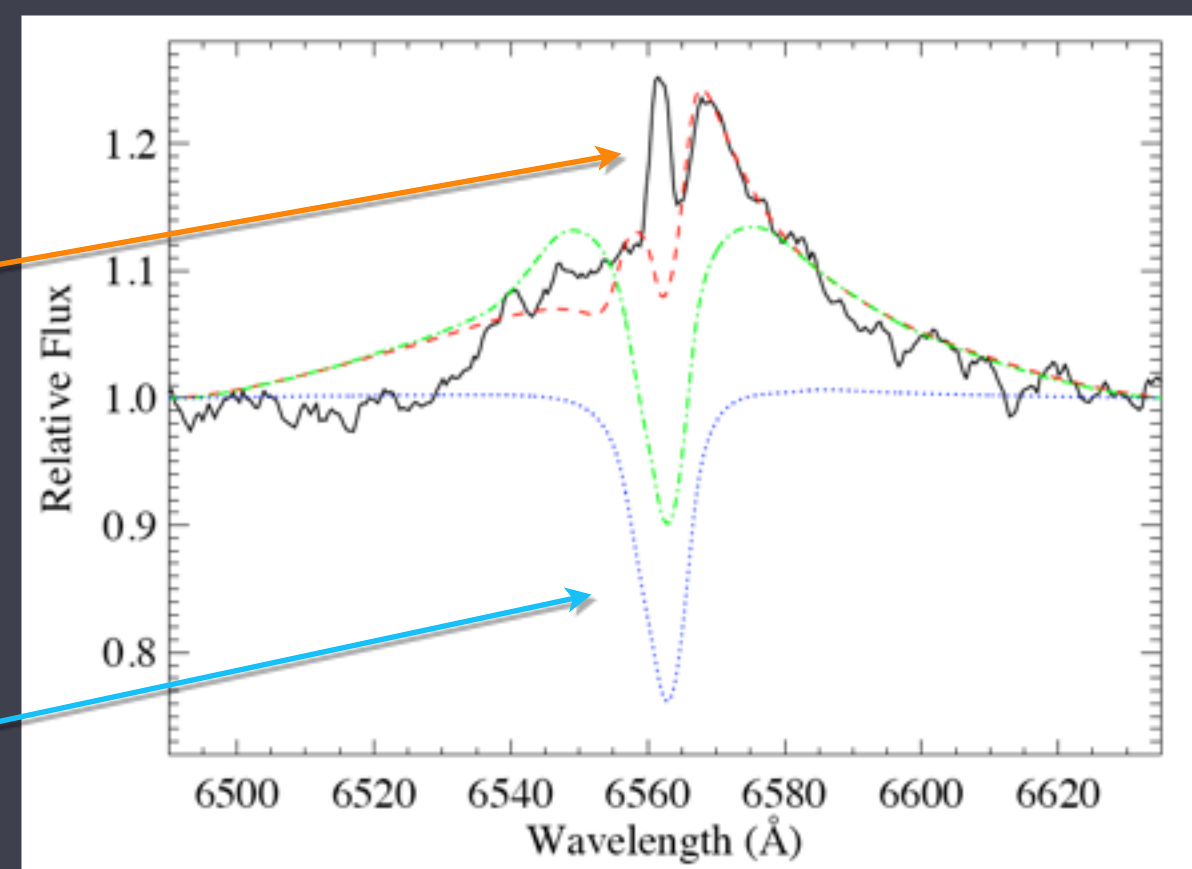

Radiation driving

L/c = momentum in the (mostly UV) radiation from the stellar surface < $\dot{M}v_\infty$ (wind momentum)

radiation couples to the matter in the wind via resonance line scattering

$\dot{M} \sim 10^{-6}\ M_{sun}/yr$ (10^8 times the Sun's value)

kinetic power in the wind = $1/2\ \dot{M}v_\infty^2$ ($\sim 10^{-3}\ L_{bol}$)

Doppler desaturation is key to line-driven winds

line opacity *increases* in a moving medium

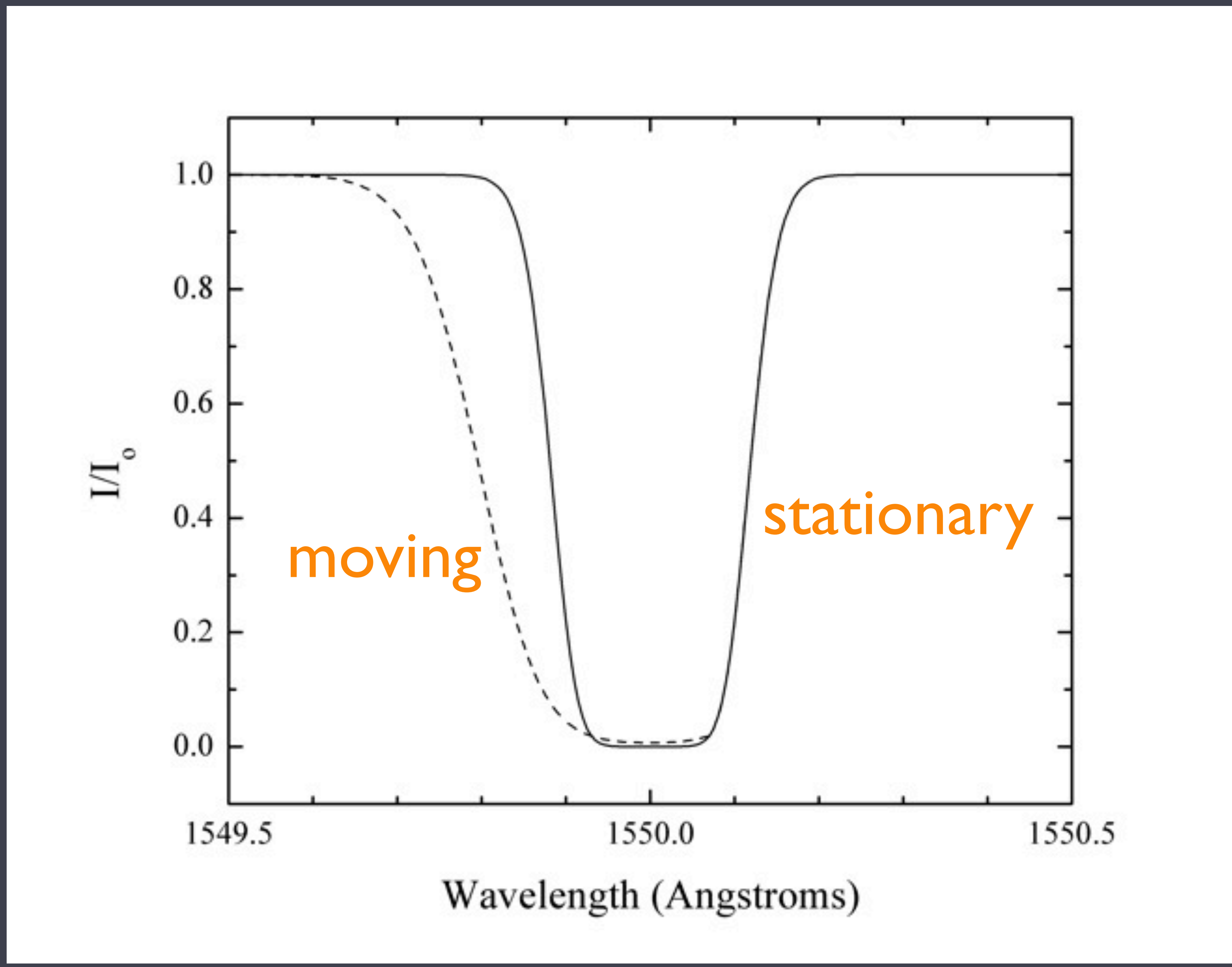

back to massive star **X-ray** emission

THE ASTROPHYSICAL JOURNAL, 234:L51–54, 1979 November 15

DISCOVERY OF AN X-RAY STAR ASSOCIATION IN VI CYGNI (CYG OB2)

F. R. HARNDEN, JR., G. BRANDUARDI, M. ELVIS,[1] P. GORENSTEIN, J. GRINDLAY,
J. P. PYE,[1] R. ROSNER, K. TOPKA, AND G. S. VAIANA[2]
Harvard-Smithsonian Center for Astrophysics, Cambridge, Massachusetts
Received 1979 June 26; accepted 1979 July 26

ABSTRACT

A group of six X-ray sources located within 0°.4 of Cygnus X-3 has been discovered with the *Einstein* Observatory. These sources have been positively identified and five of them correspond to stars in the heavily obscured OB association VI Cygni. The optical counterparts include four of the most luminous O stars within the field of view and a B5 supergiant. These sources are found to have typical X-ray luminosities L_x (0.2–4.0 keV) $\sim 5 \times 10^{33}$ ergs s^{-1}, with temperatures $T \sim 10^{6.8}$ K and hydrogen column densities $N_H \sim 10^{22}$ cm^{-2}, and therefore comprise a new class of low-luminosity galactic X-ray sources associated with early-type stars.

The Carina Complex

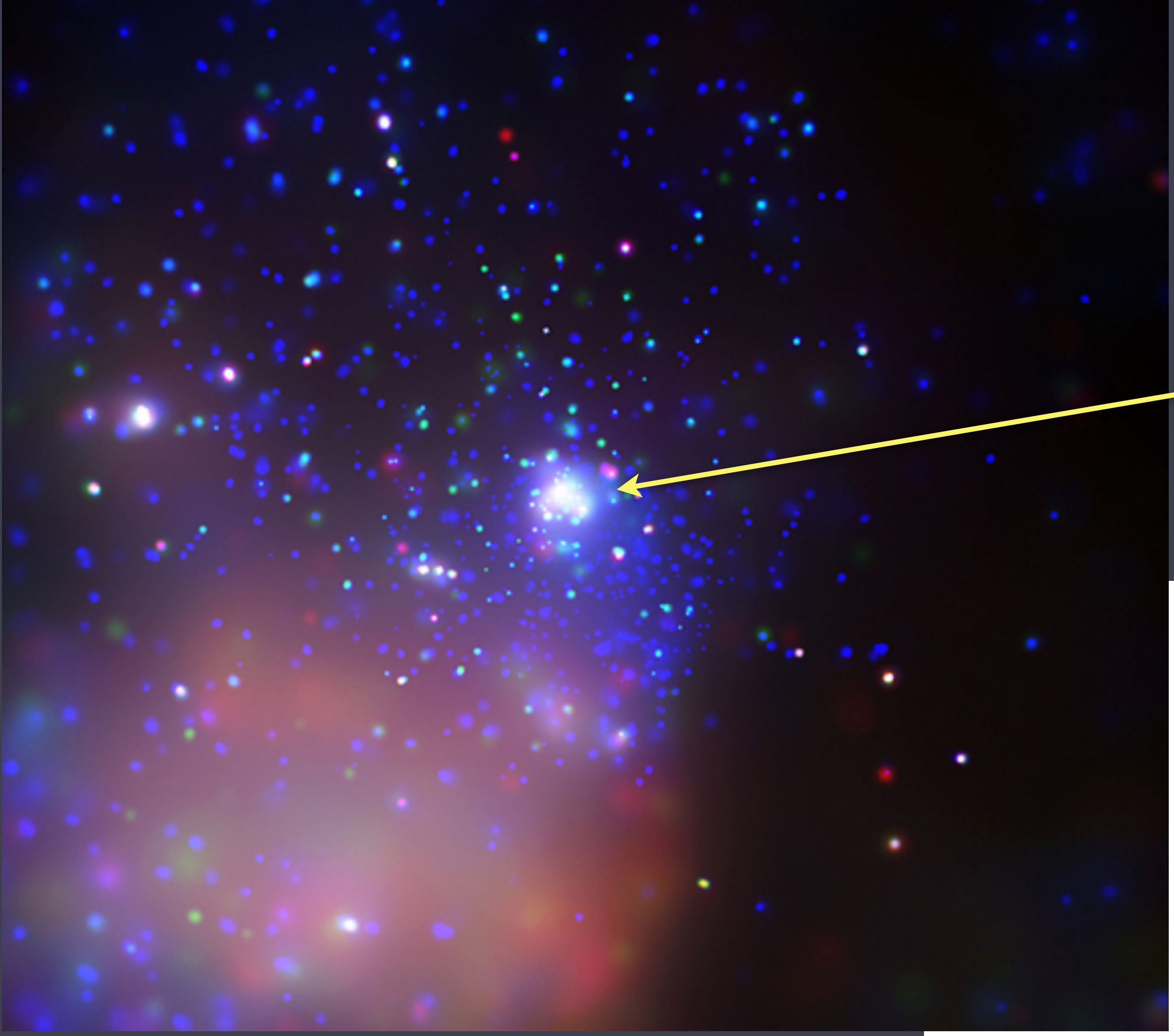

HD 93129A (O2If*)

Tr 14 in Carina: *Chandra*

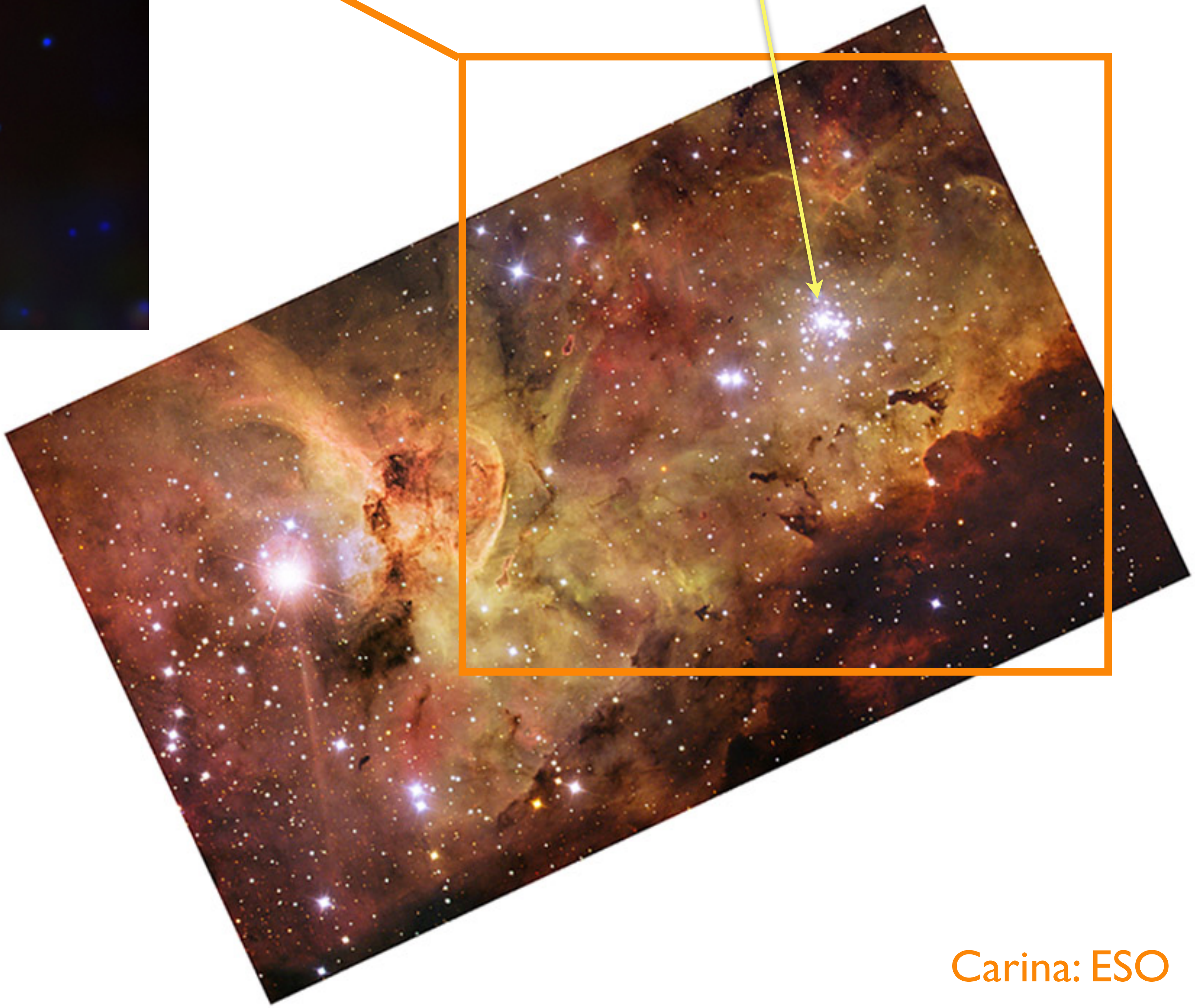

Carina: ESO

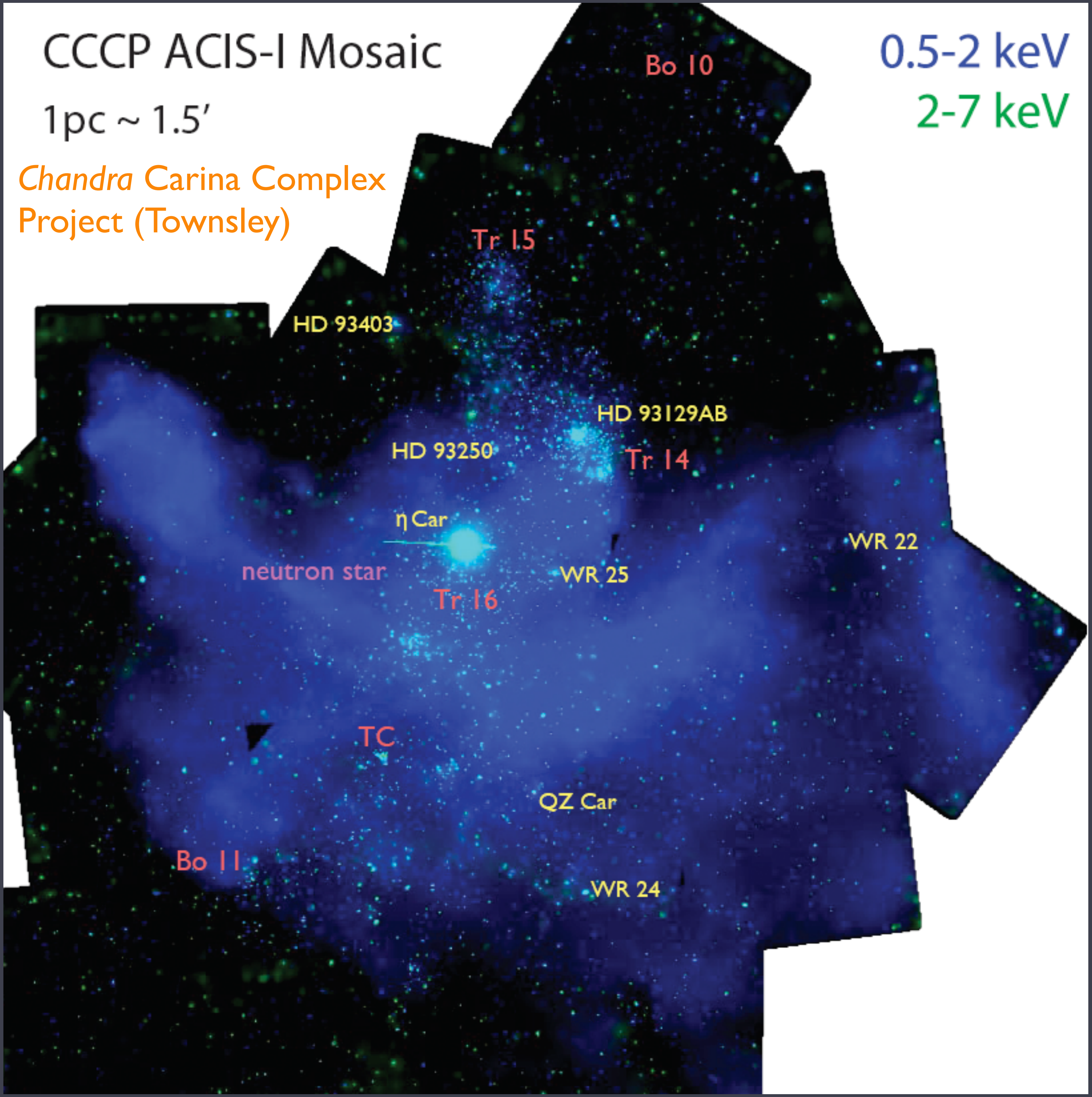
CCCP ACIS-I Mosaic
1pc ~ 1.5′
Chandra Carina Complex Project (Townsley)
0.5-2 keV
2-7 keV
Bo 10
Tr 15
HD 93403
HD 93129AB
HD 93250
Tr 14
η Car
WR 22
neutron star
WR 25
Tr 16
TC
QZ Car
Bo 11
WR 24

The wind kinetic power is typically 10^4 times larger than the observed L_x

some process - which doesn't have to be very efficient - converts a small fraction of this kinetic power to heat

the observed X-rays are the thermal radiation from this hot stellar wind plasma

The line-deshadowing instability (LDI)

causes fast, rarefied wind plasma to slam into slower, denser wind plasma

the resulting shocks heat the plasma

the X-rays we see are the thermal emission from this hot wind plasma

general result from shock theory:

$$T \sim 10^6(\Delta v_{shock}/300\ \mathrm{km/s})^2$$

the LDI was first proposed by Milne in the 1920's

larger heights require more blue-shifted photons to excite a given line transition

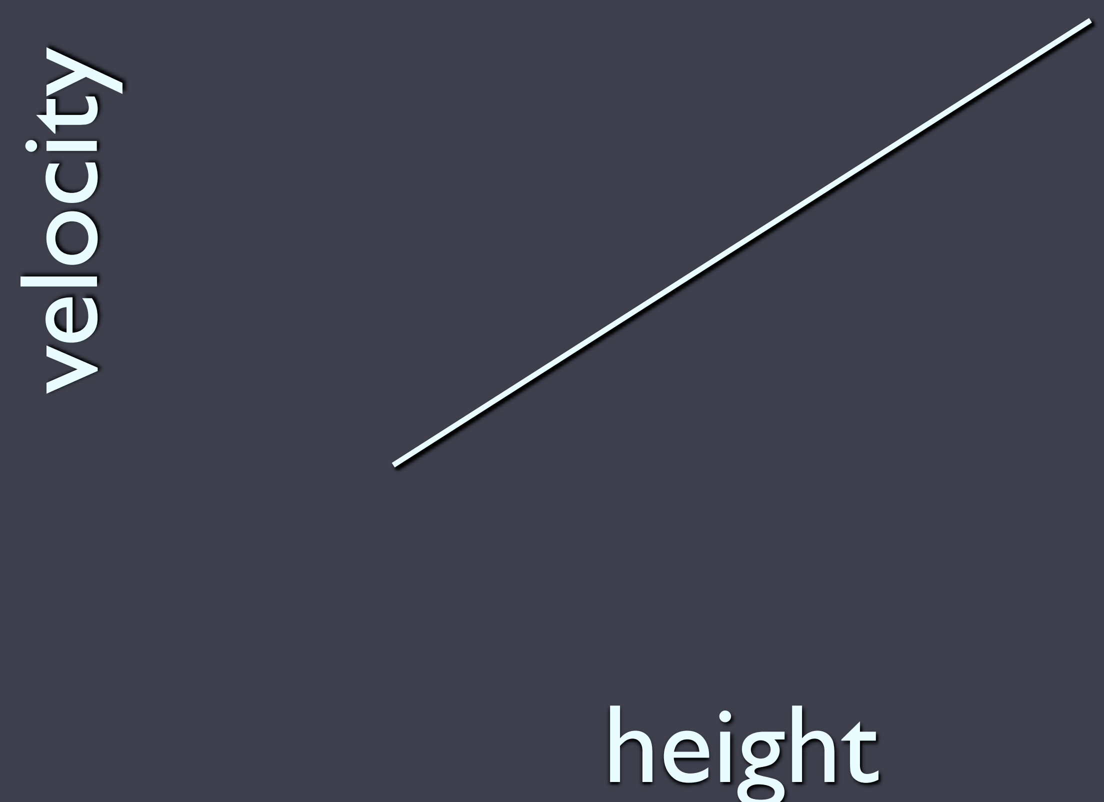

the LDI was first proposed by Milne in the 1920's

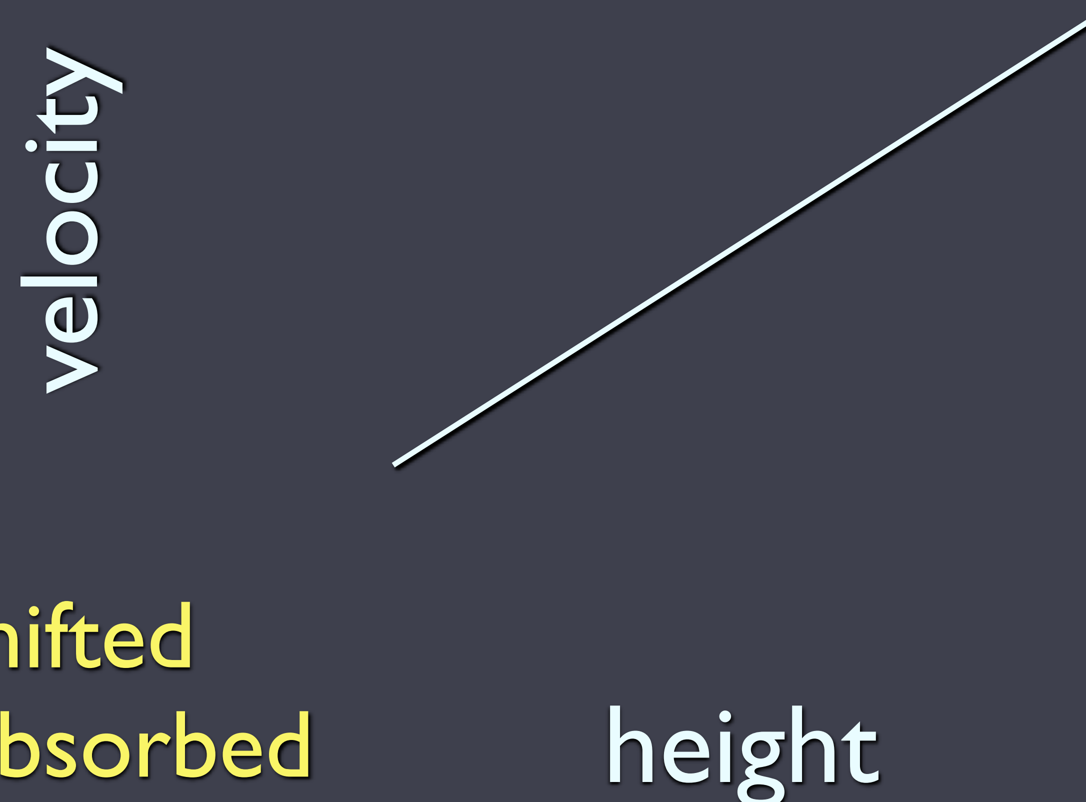

less blue-shifted
photons are absorbed
lower in the wind

the LDI was first proposed by Milne in the 1920's

there is a *Doppler shadow*, cast by the lower portion of the wind

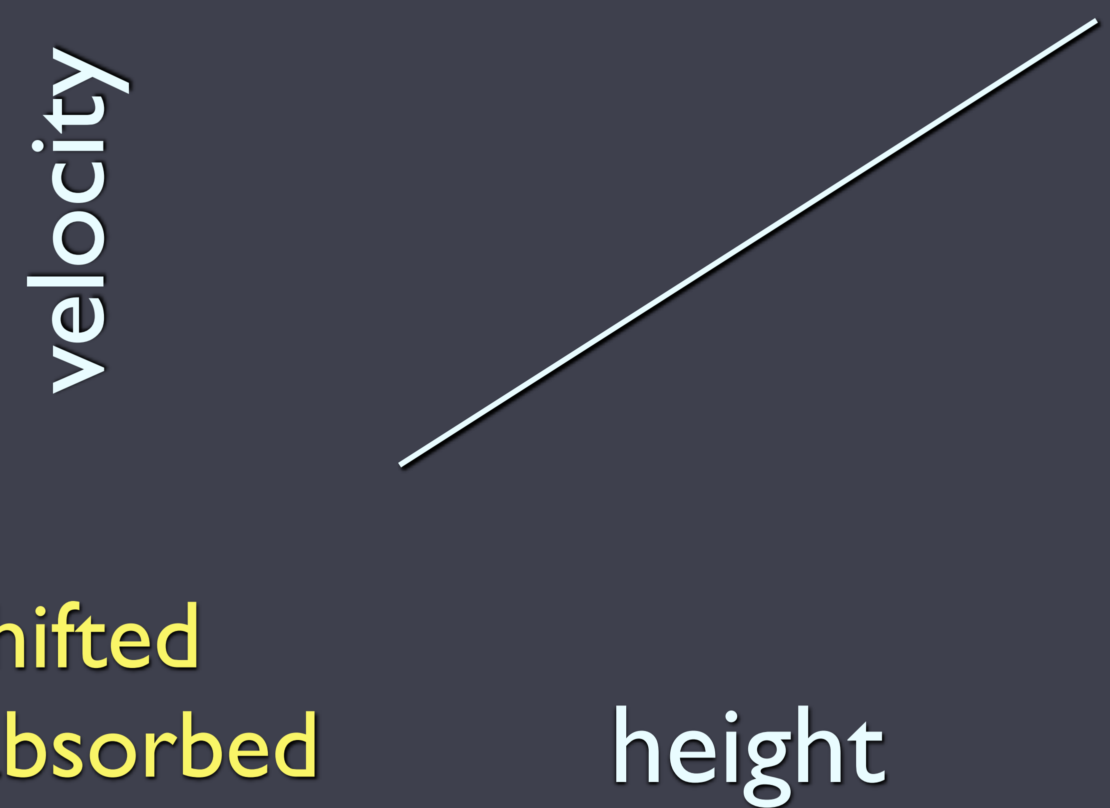

less blue-shifted photons are absorbed lower in the wind

the LDI was first proposed by Milne in the 1920's

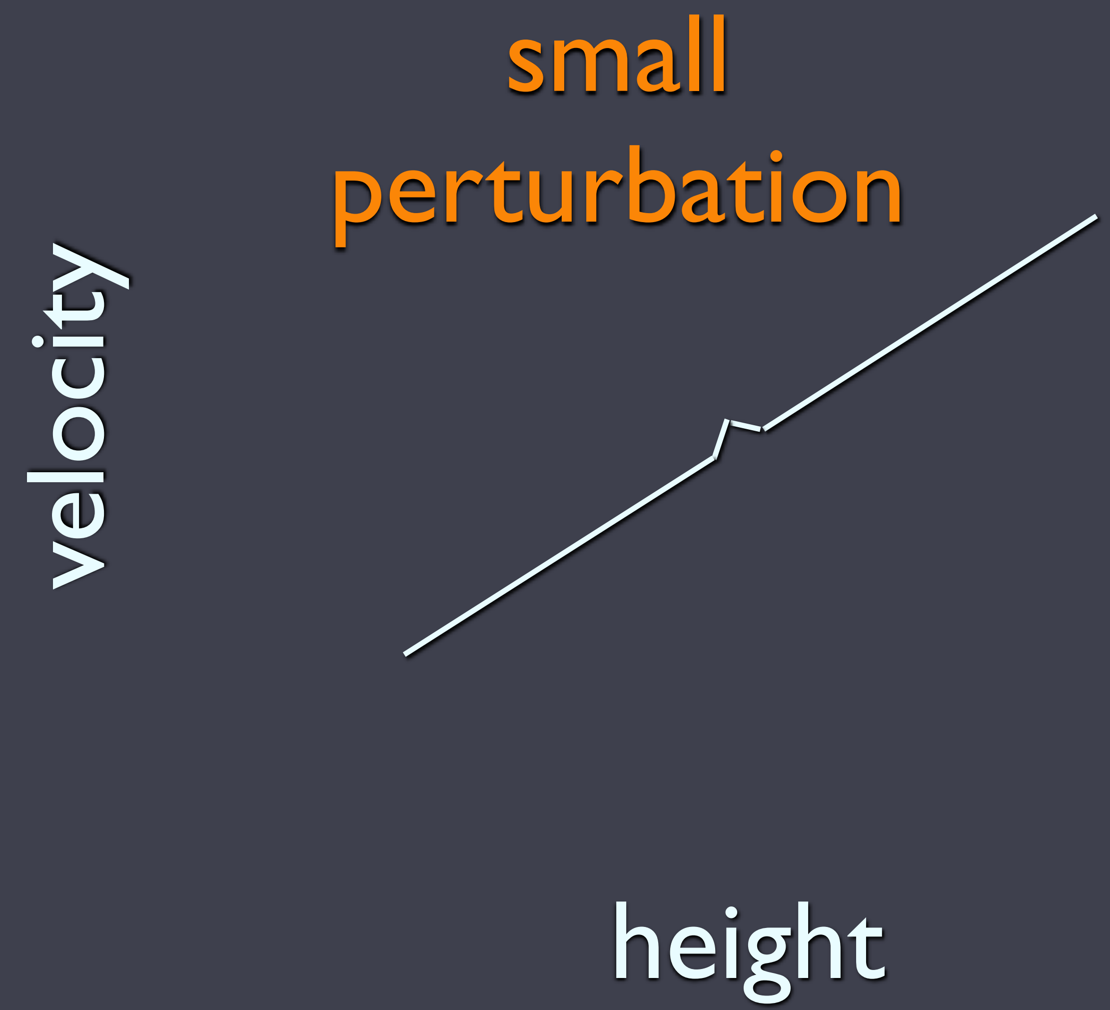

the LDI was first proposed by Milne in the 1920’s

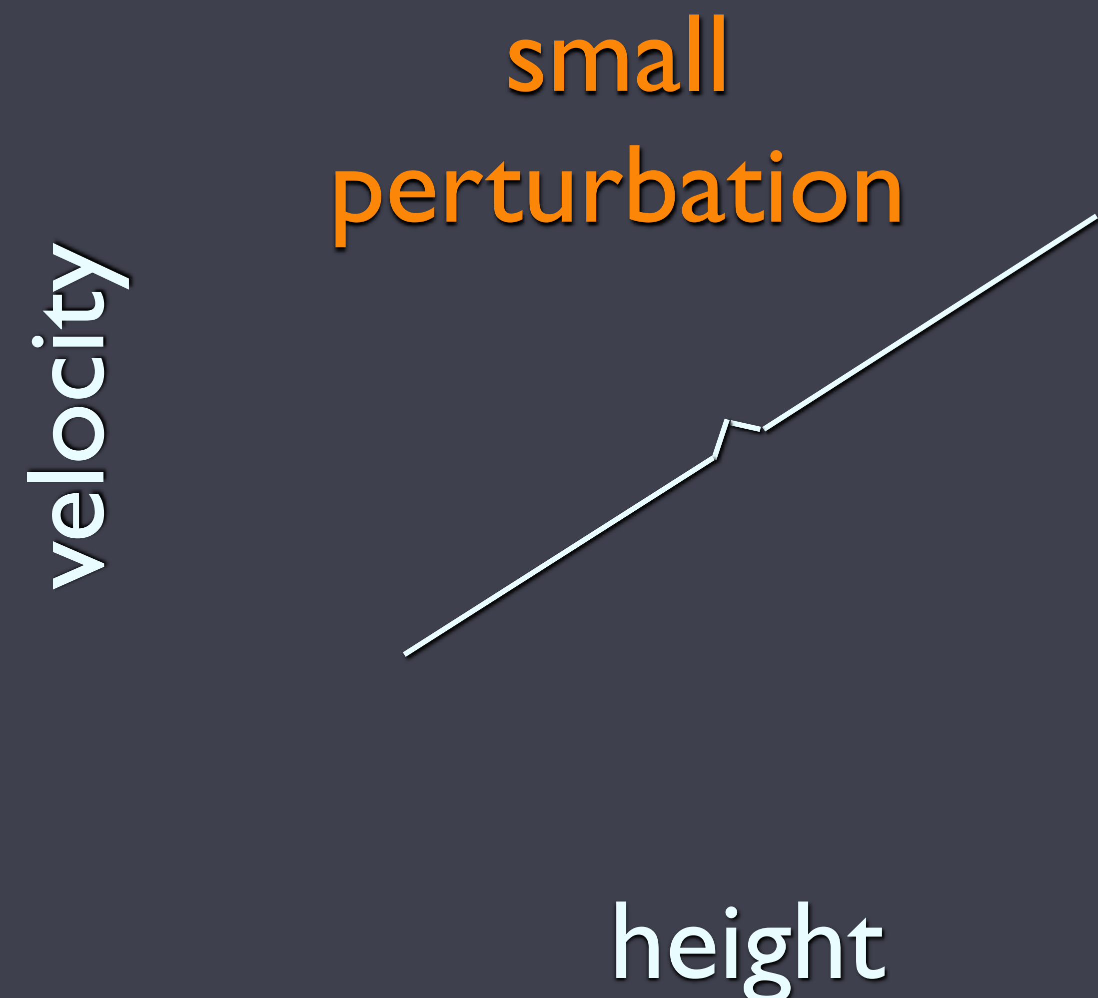

moves out of the *Doppler shadow* of the material below it

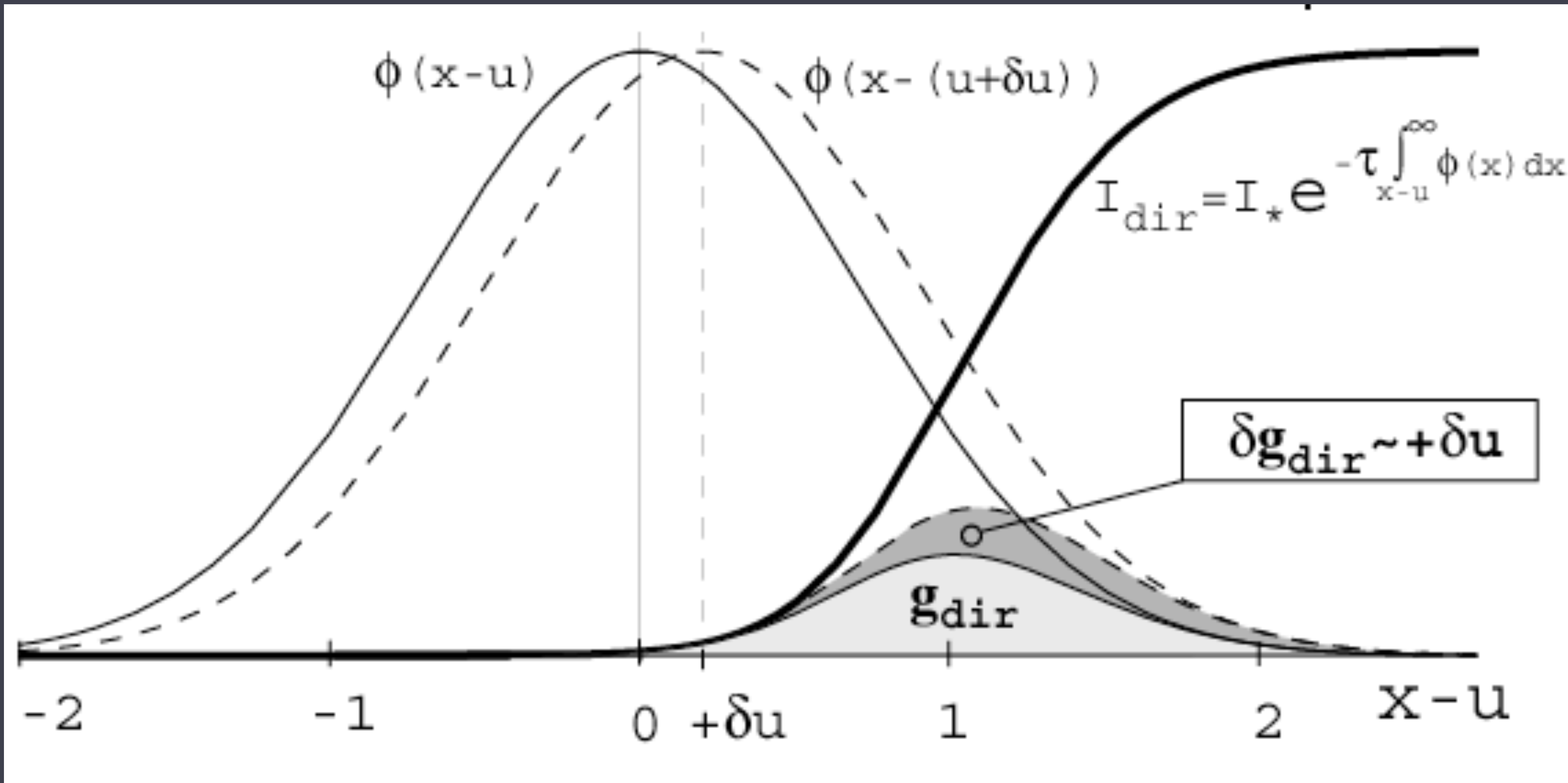

φ(x-u)
φ(x-(u+δu))
$I_{dir}=I_* e^{-\tau \int_{x-u}^{\infty} \phi(x)\,dx}$
$\delta g_{dir} \sim +\delta u$
g_{dir}
-2
-1
0
+δu
1
2
x-u

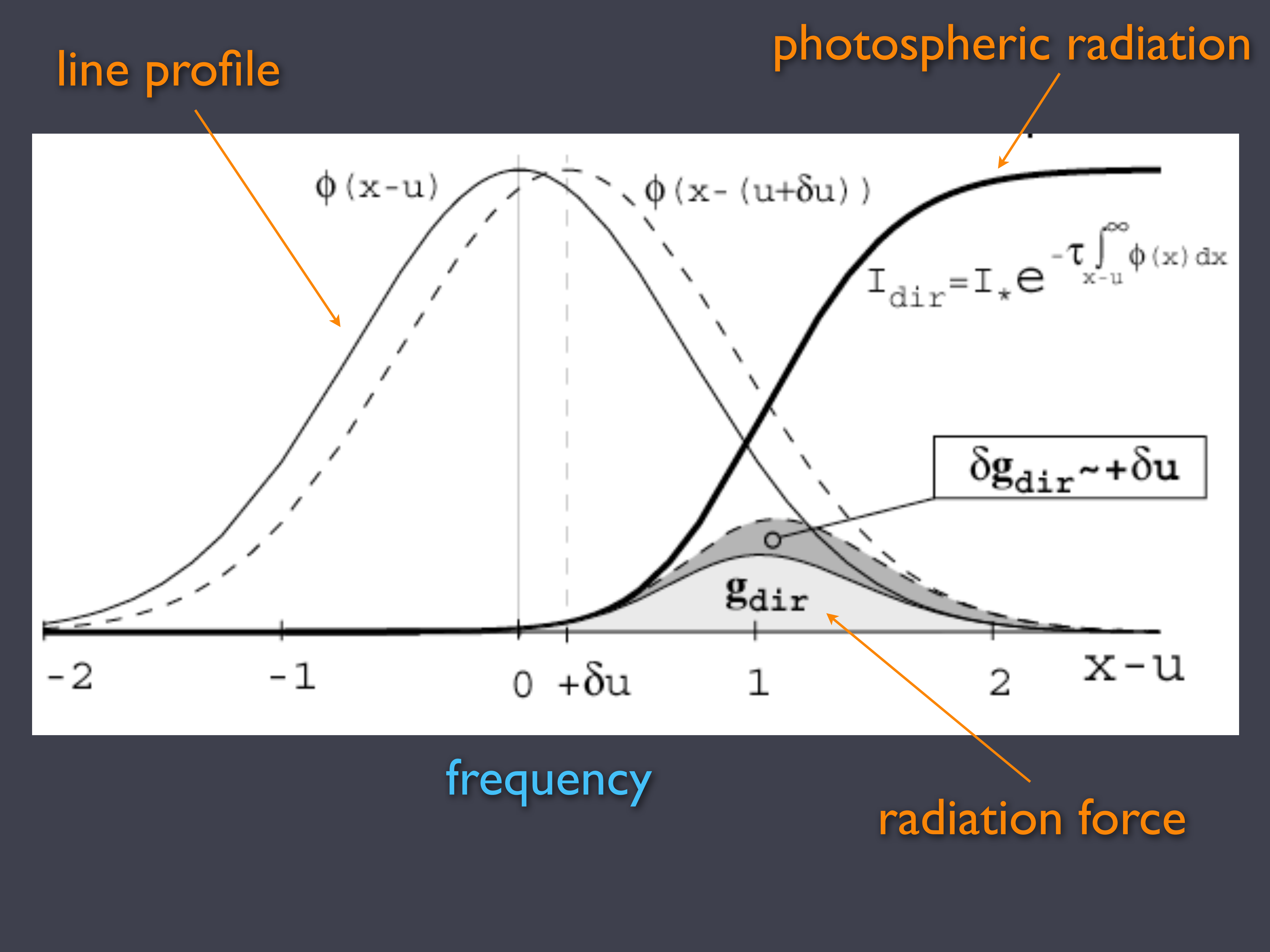

line profile
photospheric radiation
ϕ (x-u)
ϕ (x- (u+δu))
$I_{dir}=I_{*}e^{-\tau\int_{x-u}^{\infty}\phi(x)\,dx}$
$\delta g_{dir} \sim +\delta u$
g_{dir}
-2
-1
0
+δu
1
2
x-u
frequency
radiation force

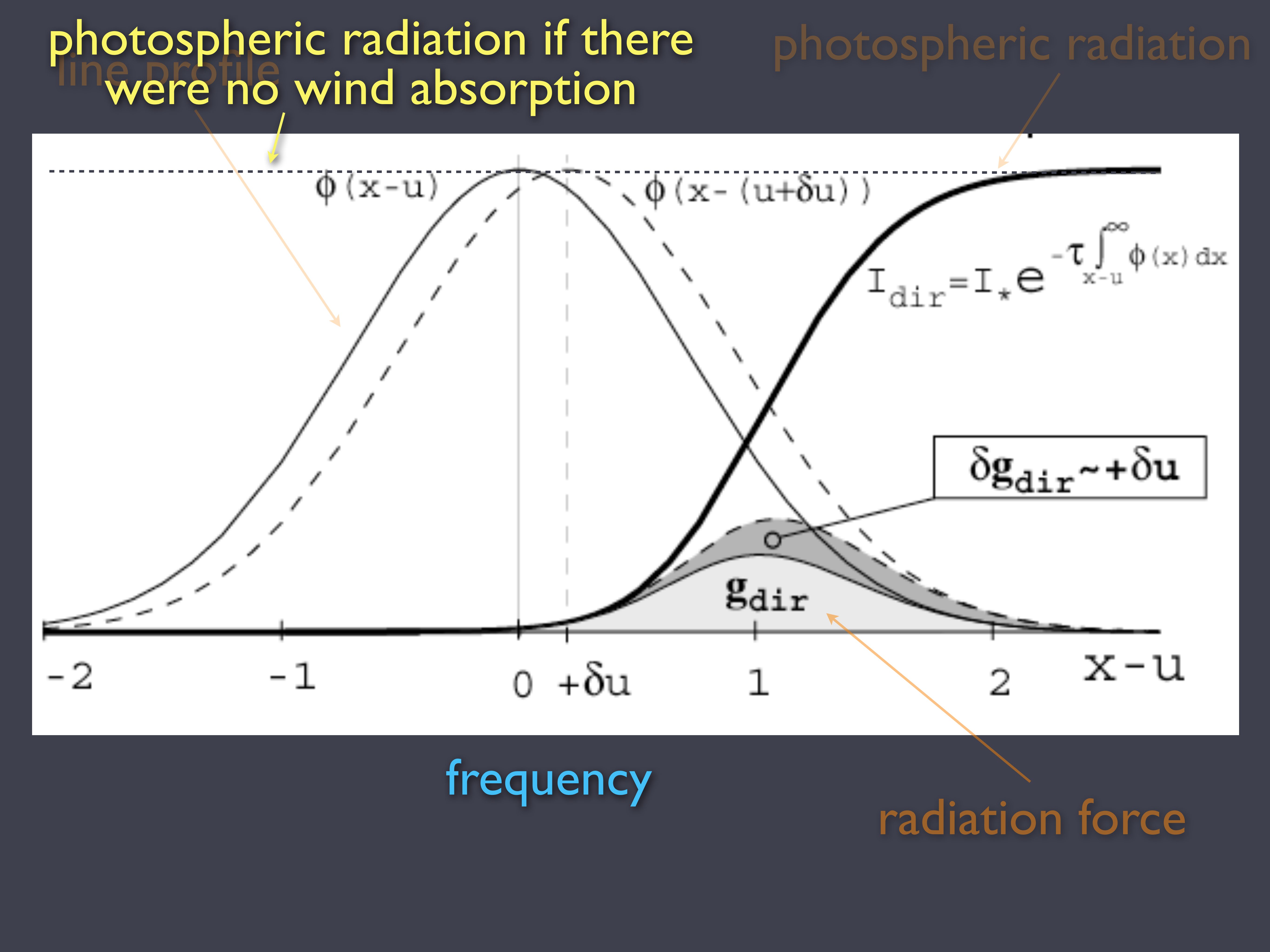

photospheric radiation if there were no wind absorption
line profile
photospheric radiation
ϕ (x-u)
ϕ (x- (u+δu))
$I_{dir} = I_* e^{-\tau \int_{x-u}^{\infty} \phi(x)\,dx}$
$\delta g_{dir} \sim +\delta u$
g_{dir}
-2
-1
0
+δu
1
2
x-u
frequency
radiation force

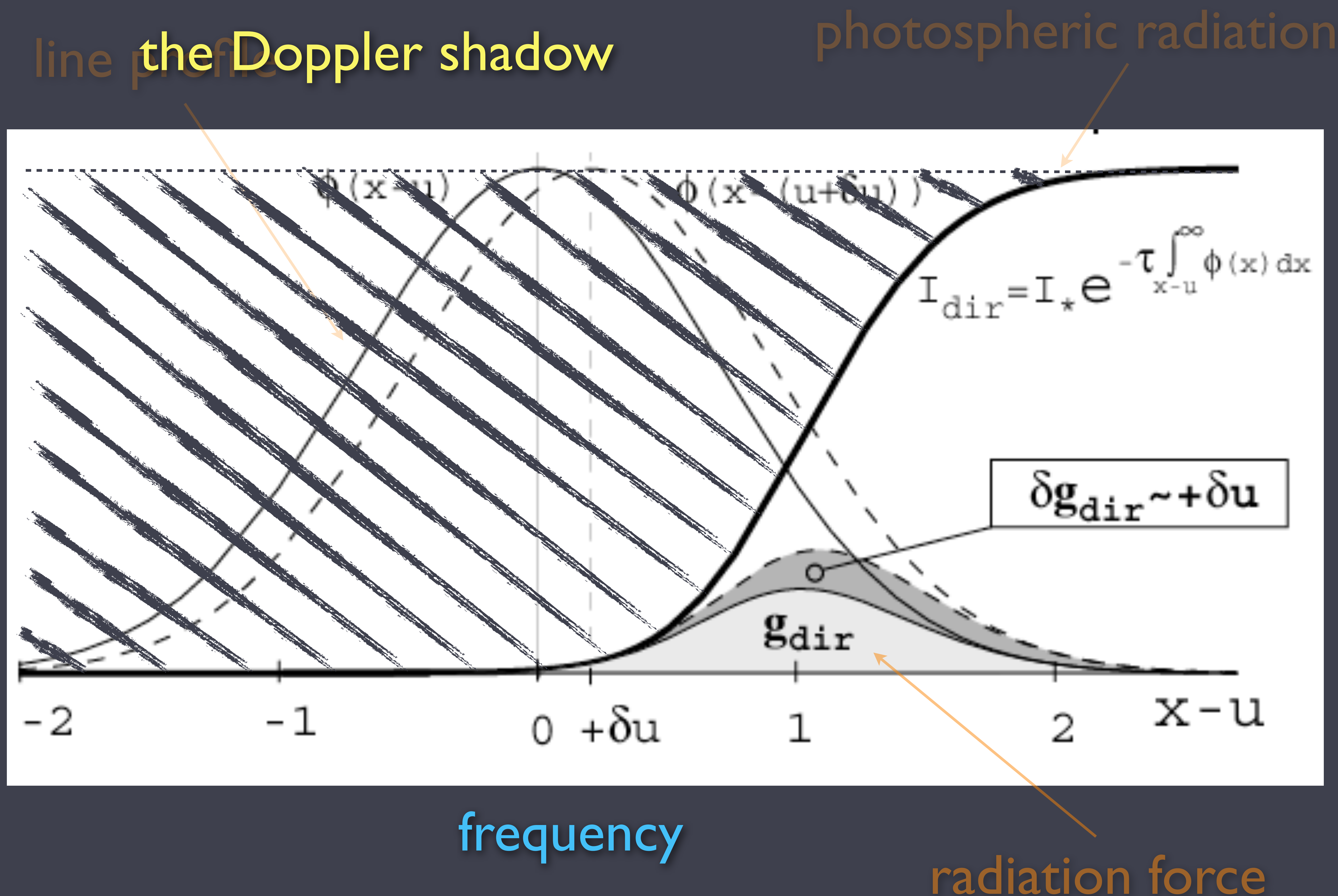
line profile
the Doppler shadow
photospheric radiation
φ(x-u)
φ(x-(u+δu))
$I_{dir} = I_* e^{-\tau \int_{x-u}^{\infty} \phi(x)\,dx}$
$\delta g_{dir} \sim +\delta u$
g_{dir}
-2
-1
0
+δu
1
2
x-u
frequency
radiation force

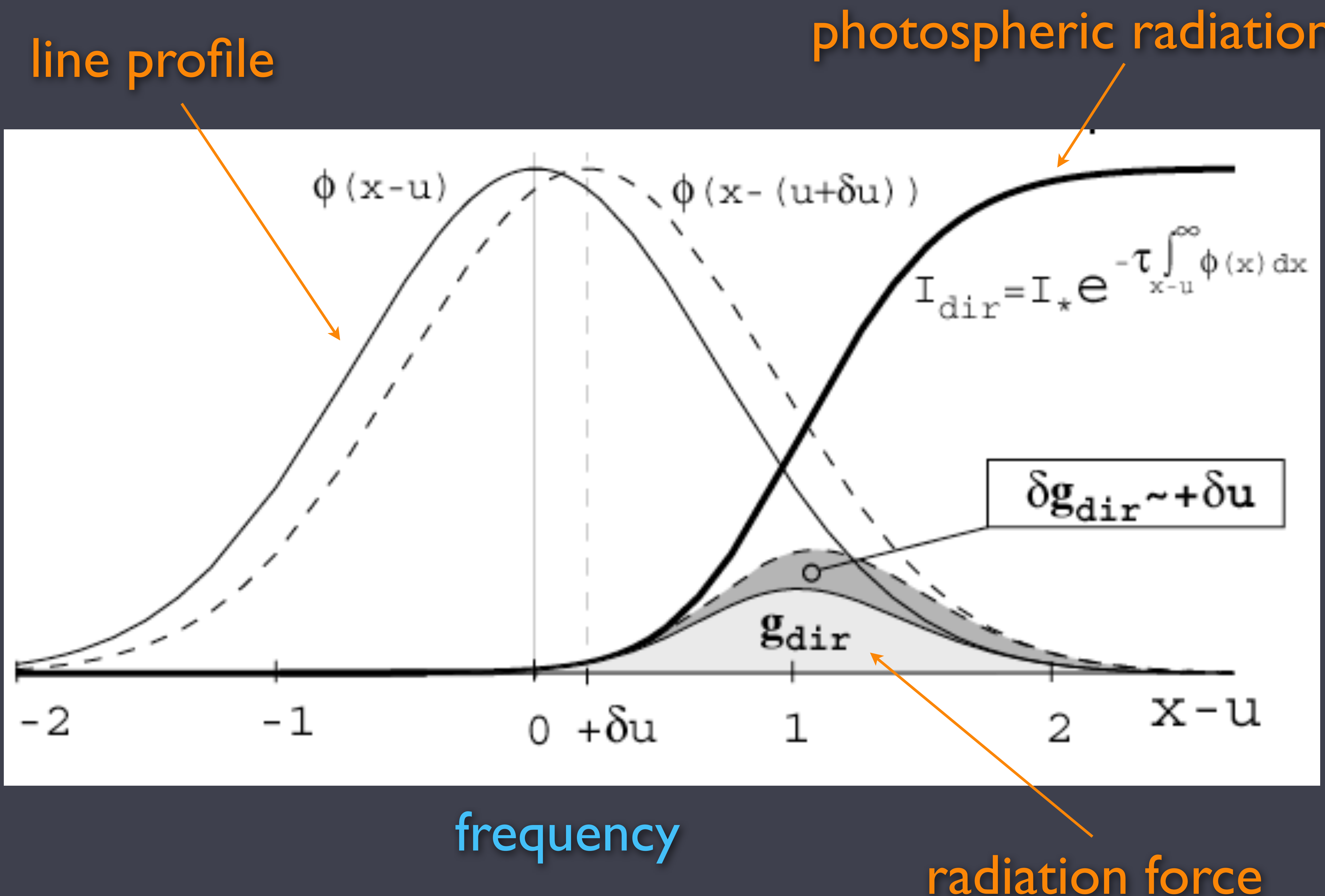

line profile
photospheric radiation
φ(x-u)
φ(x-(u+δu))
$I_{dir}=I_{*}e^{-\tau\int_{x-u}^{\infty}\phi(x)\,dx}$
$\delta g_{dir} \sim +\delta u$
g_{dir}
-2
-1
0
+δu
1
2
x-u
frequency
radiation force

positive velocity perturbation

line profile

photospheric radiation

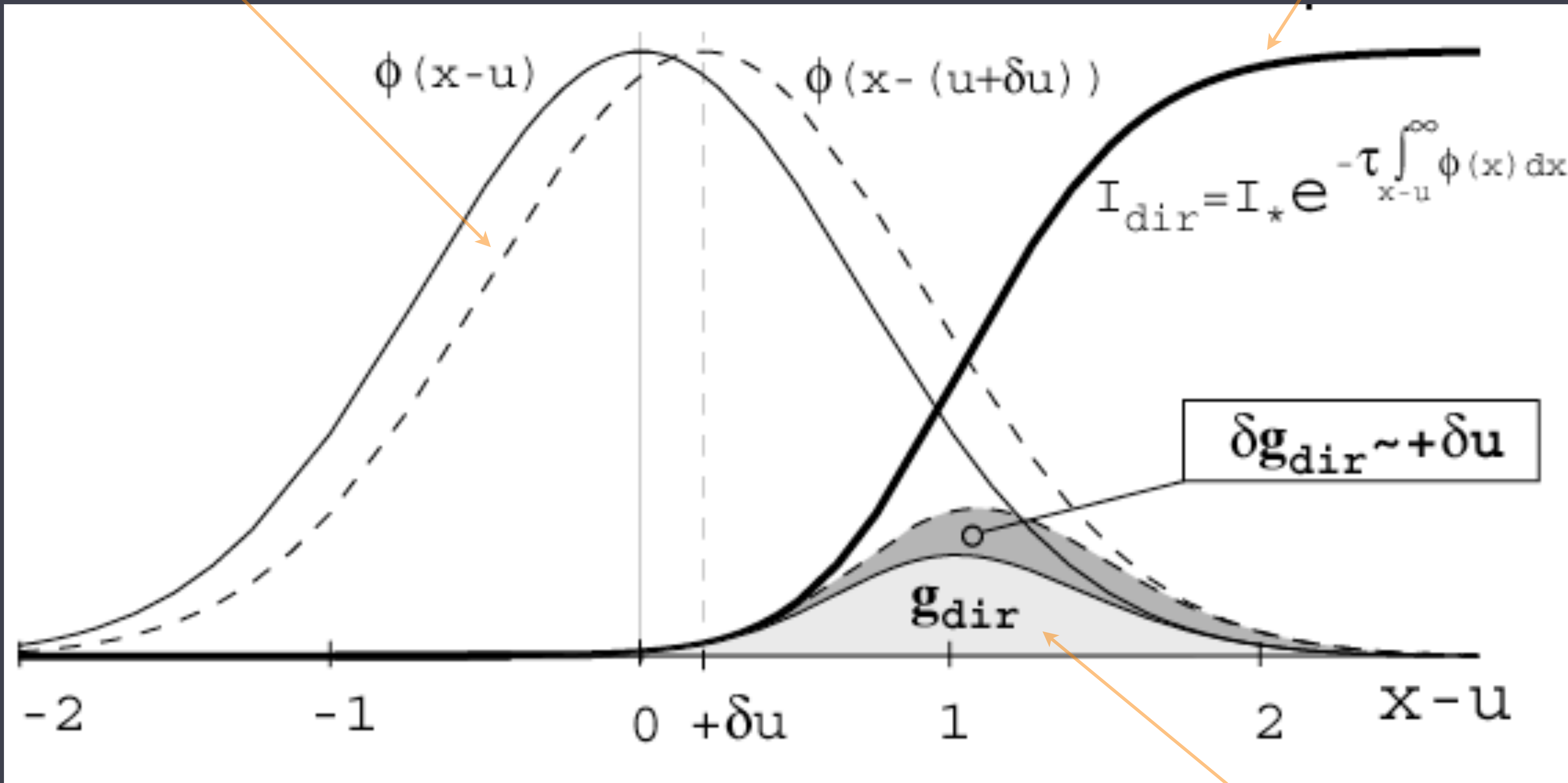

frequency

radiation force

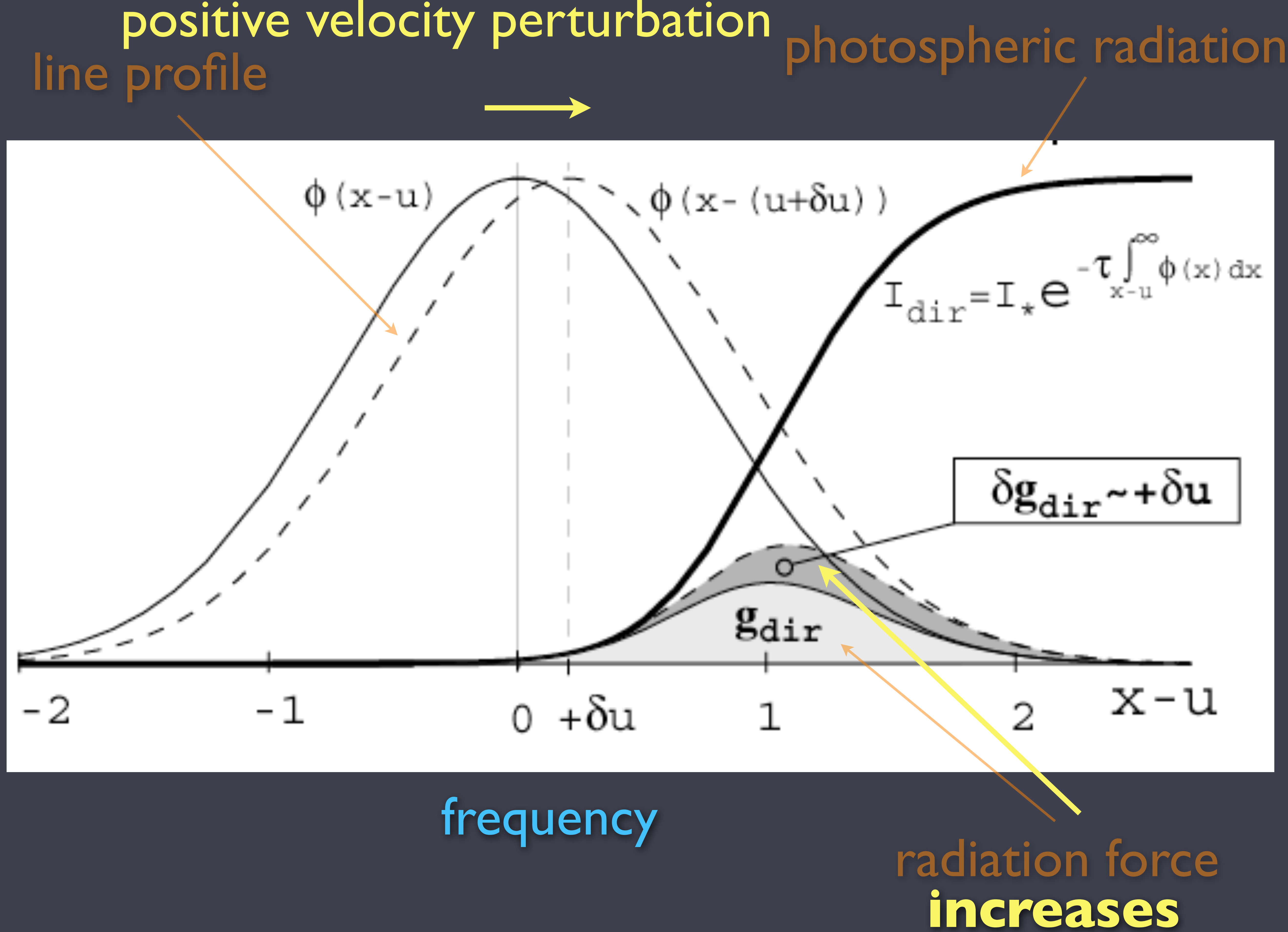
positive velocity perturbation
line profile
photospheric radiation
ϕ (x-u)
ϕ (x- (u+δu))
$I_{dir}=I_{*}e^{-\tau\int_{x-u}^{\infty}\phi(x)\,dx}$
$\delta g_{dir} \sim +\delta u$
g_{dir}
-2
-1
0
+δu
1
2
x-u
frequency
radiation force
increases

put detailed spectral line transport in a radiation-hydro code

2.1. Conservation equations

Consider an inviscid flow along the radial direction r from a central star. In Eulerian form, the one-dimensional (1D) time-dependent equations for conservation of mass, momentum, and energy are:

$$\frac{\partial \rho}{\partial t} + \frac{1}{r^2}\frac{\partial (r^2 \rho v)}{\partial r} = 0 \tag{1}$$

$$\frac{\partial (\rho v)}{\partial t} + \frac{1}{r^2}\frac{\partial (r^2 \rho v^2)}{\partial r} = -\frac{\partial p}{\partial r} - \rho g_* + \rho g_{\rm rad} \tag{2}$$

$$\frac{\partial e}{\partial t} + \frac{1}{r^2}\frac{\partial (r^2 e v)}{\partial r} = -\frac{p}{r^2}\frac{\partial (r^2 v)}{\partial r} - Q_{\rm rad}. \tag{3}$$

testable predictions from this model?

Numerous shock structures distributed above $r \sim 1.5\ R_\star$

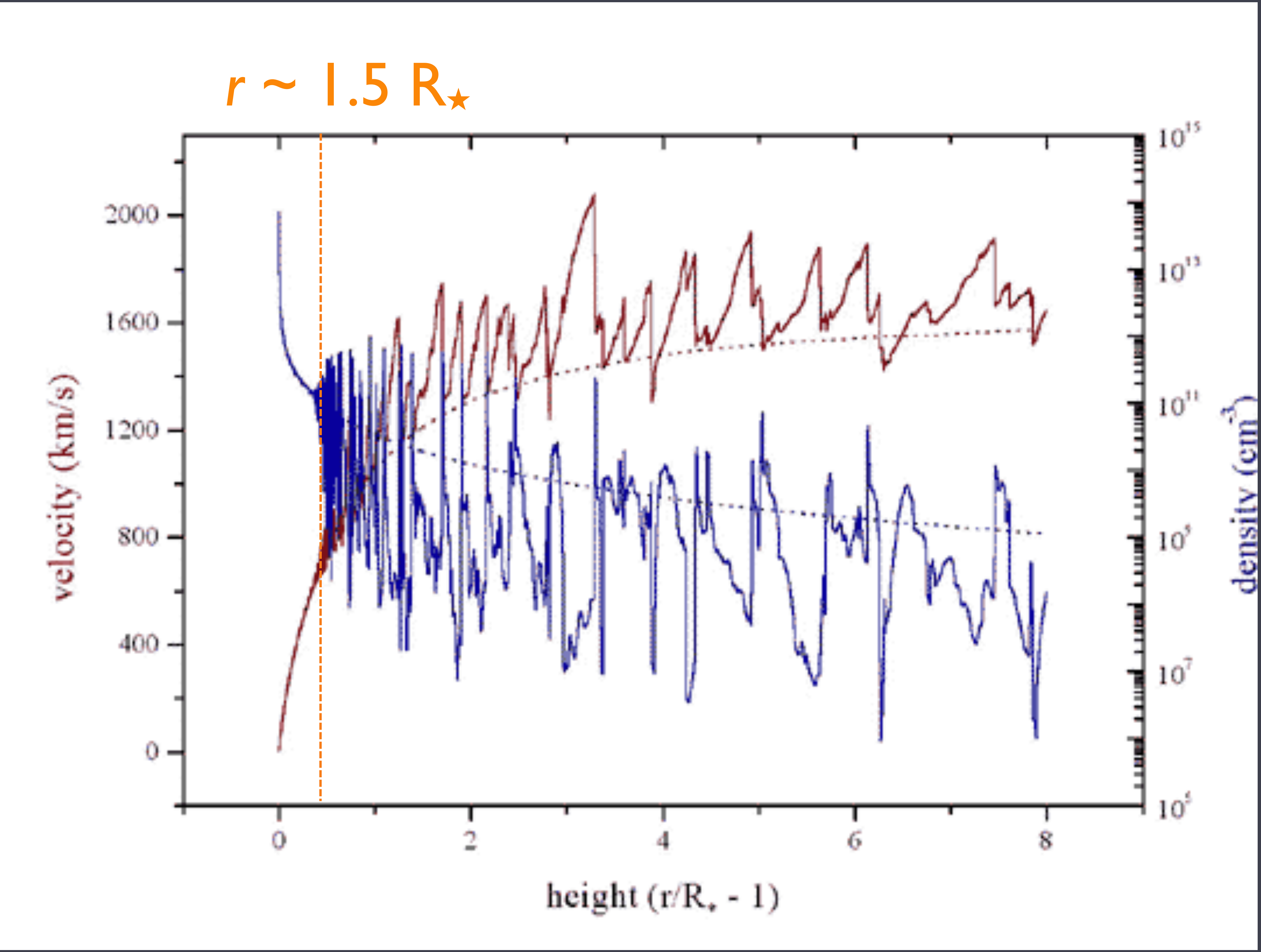

V_{shock} ~ 300 km/s : T ~ 10^6 K

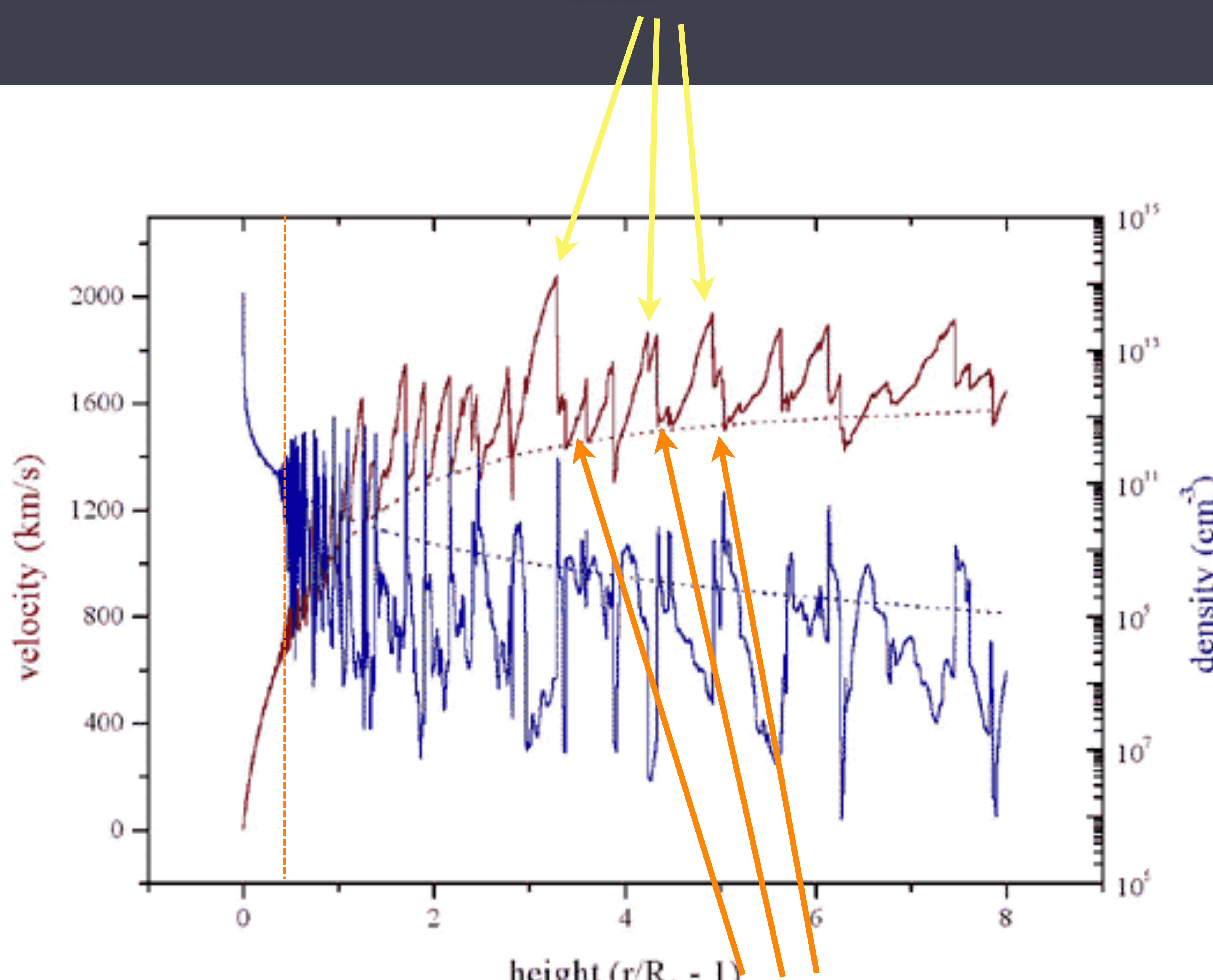

shocked wind plasma is decelerated back down to the local CAK wind velocity

Shocked plasma is moving at v ~ 1000 km/s

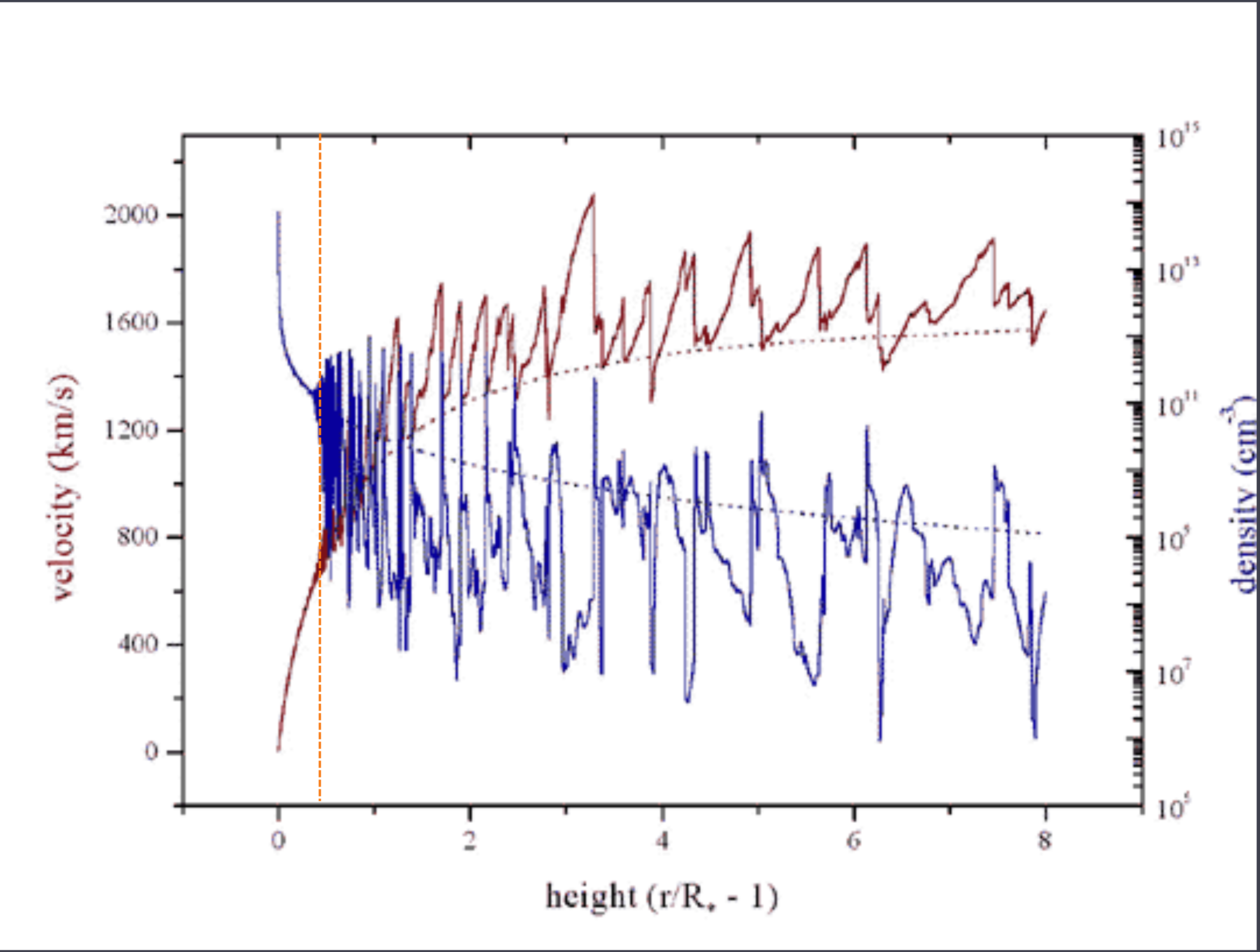

X-ray emission lines should be **Doppler broadened**

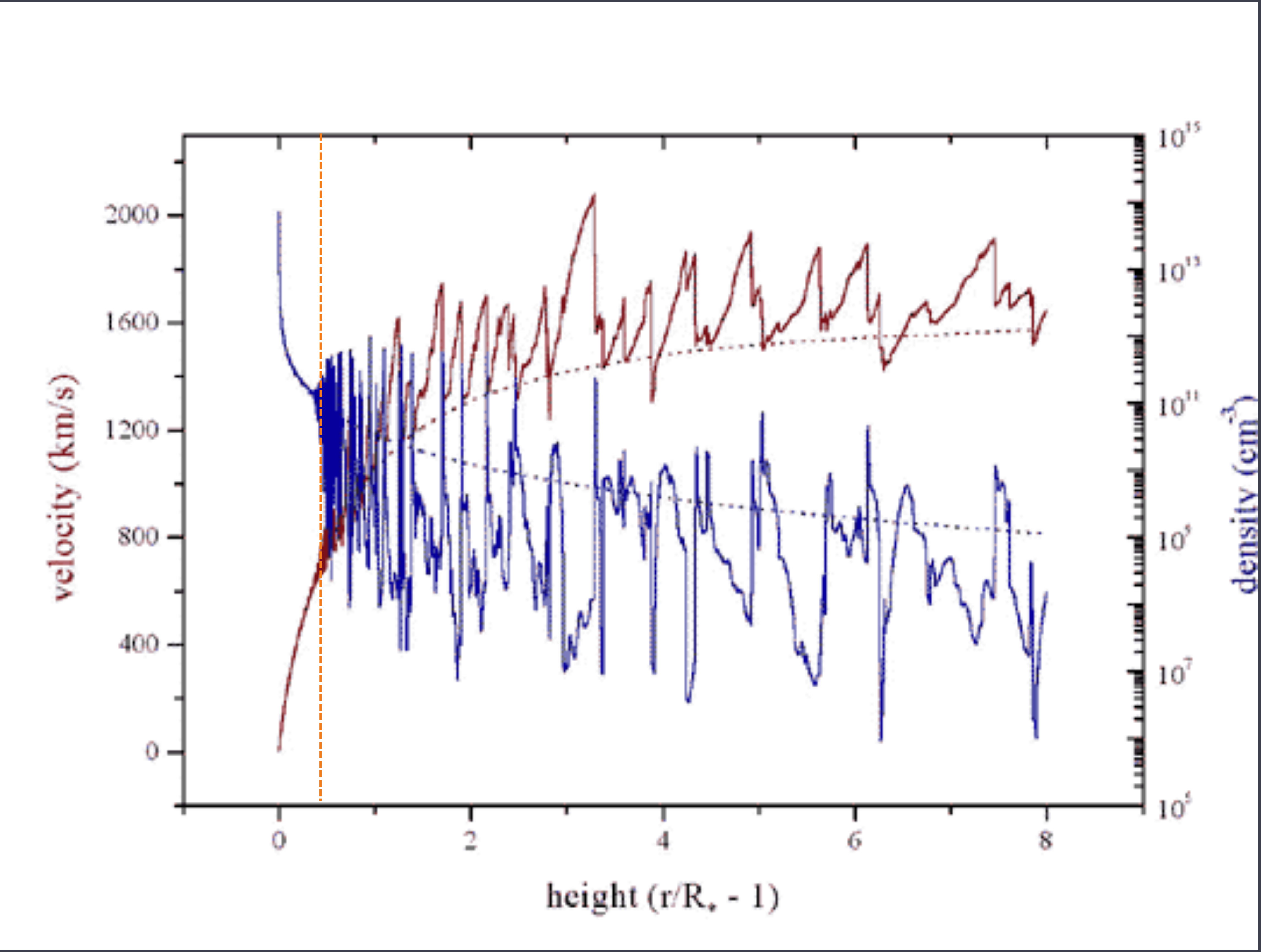

Less than 1% of the wind is emitting X-rays

>99% of the wind is cold and X-ray *absorbing*

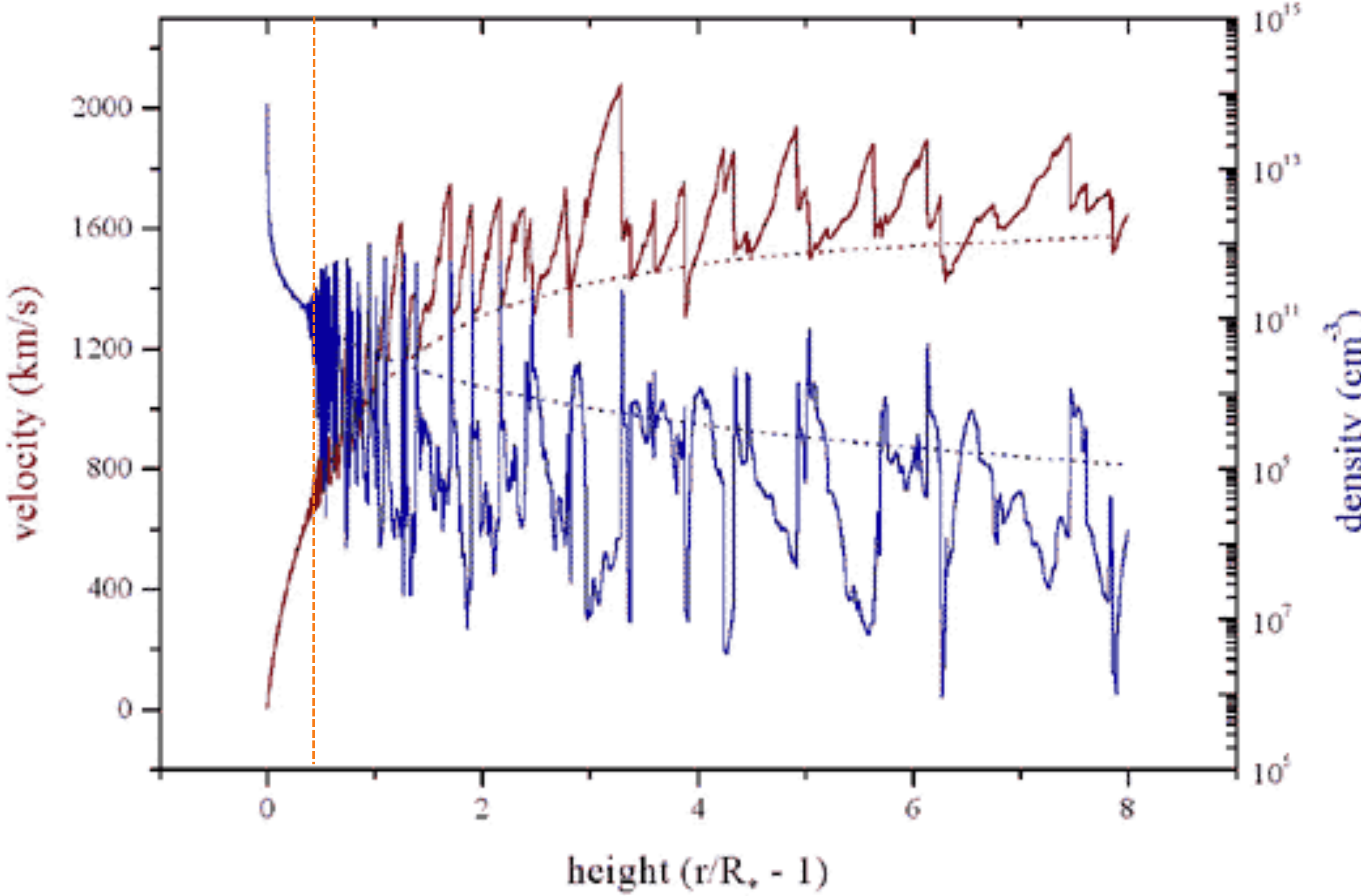

1-D is a severe limitation

e.g. the simulations show huge X-ray variability

but, the lack of observed time variability suggests numerous (>100) individual post-shock cooling volumes in the wind

2-D simulations

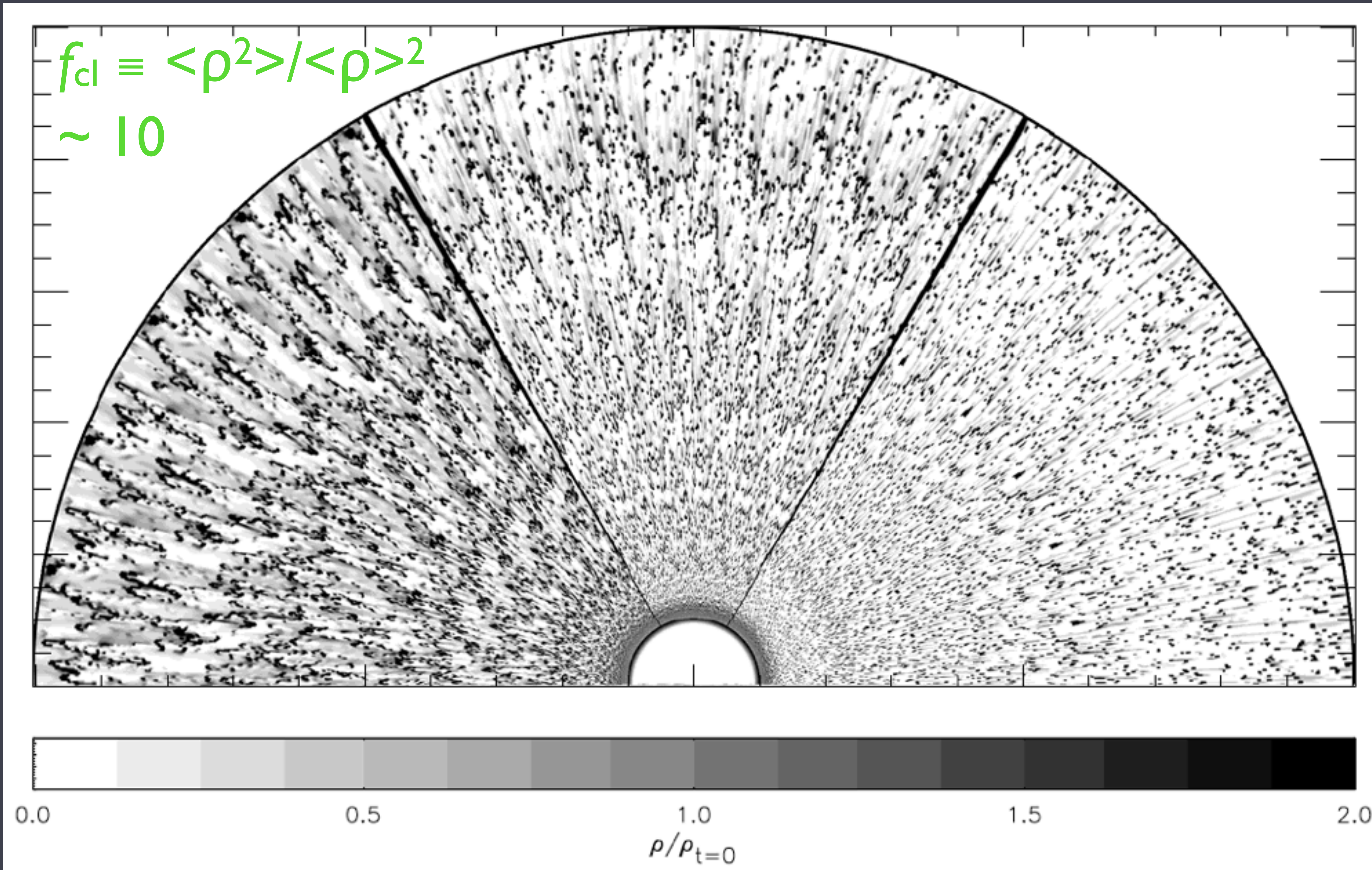

Dessart & Owocki 2003

Statistics (time-average quantities) from 2-D simulations

clumping factor, f_{cl} velocity dispersion, v_{rms}

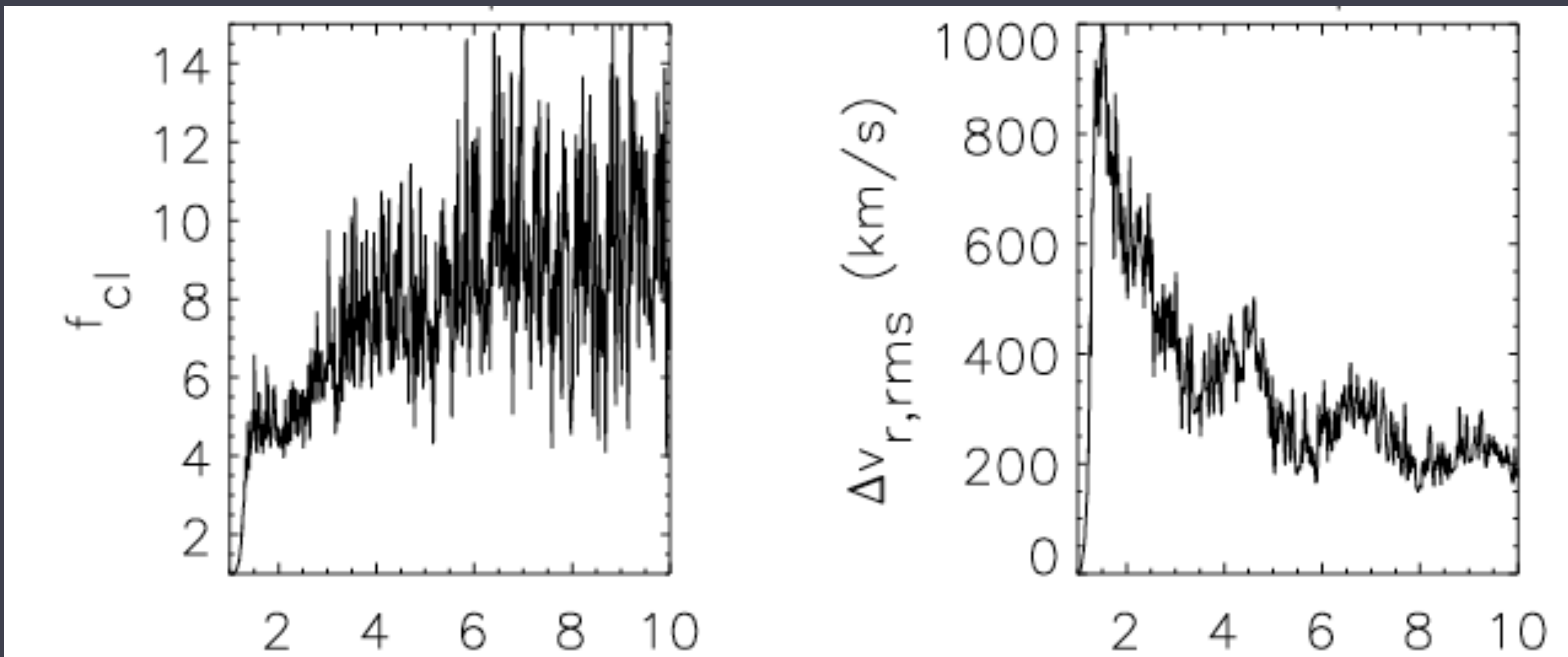

height ($R_\star$) height ($R_\star$)

basic definition: $f_{cl} \equiv \langle\rho^2\rangle / \langle\rho\rangle^2$

Dessart & Owocki 2005

now for some X-ray data...

ROSAT 1991

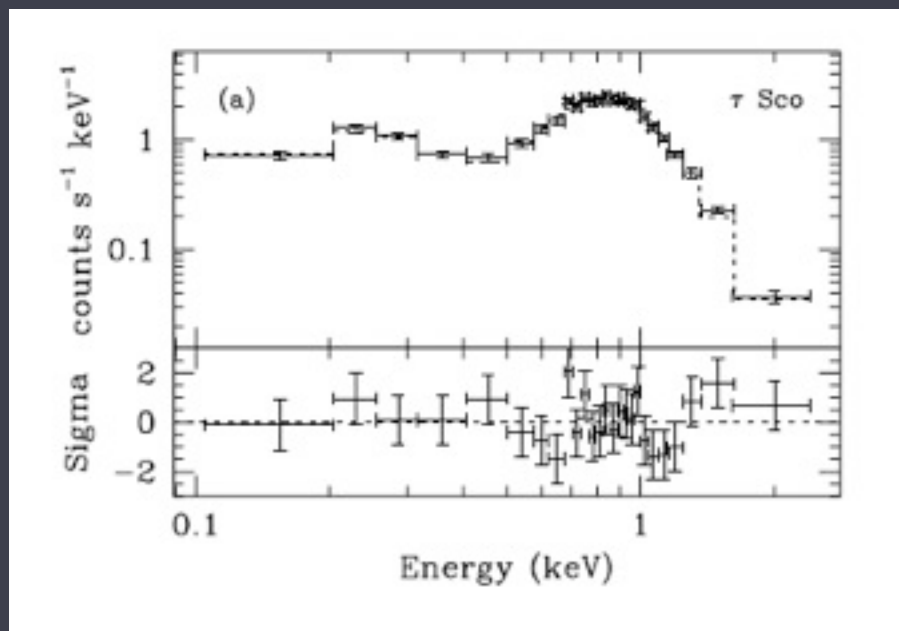

ASCA 1994

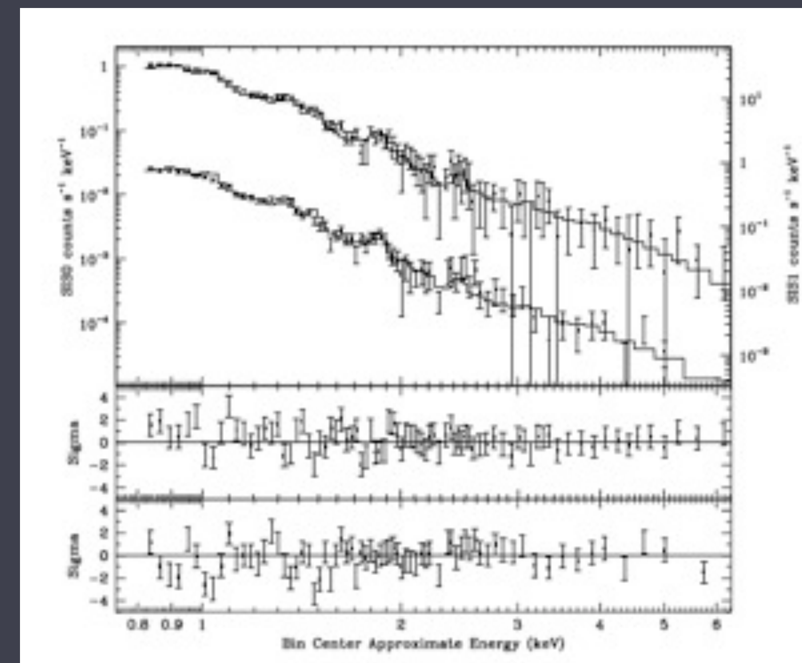

Chandra 2001

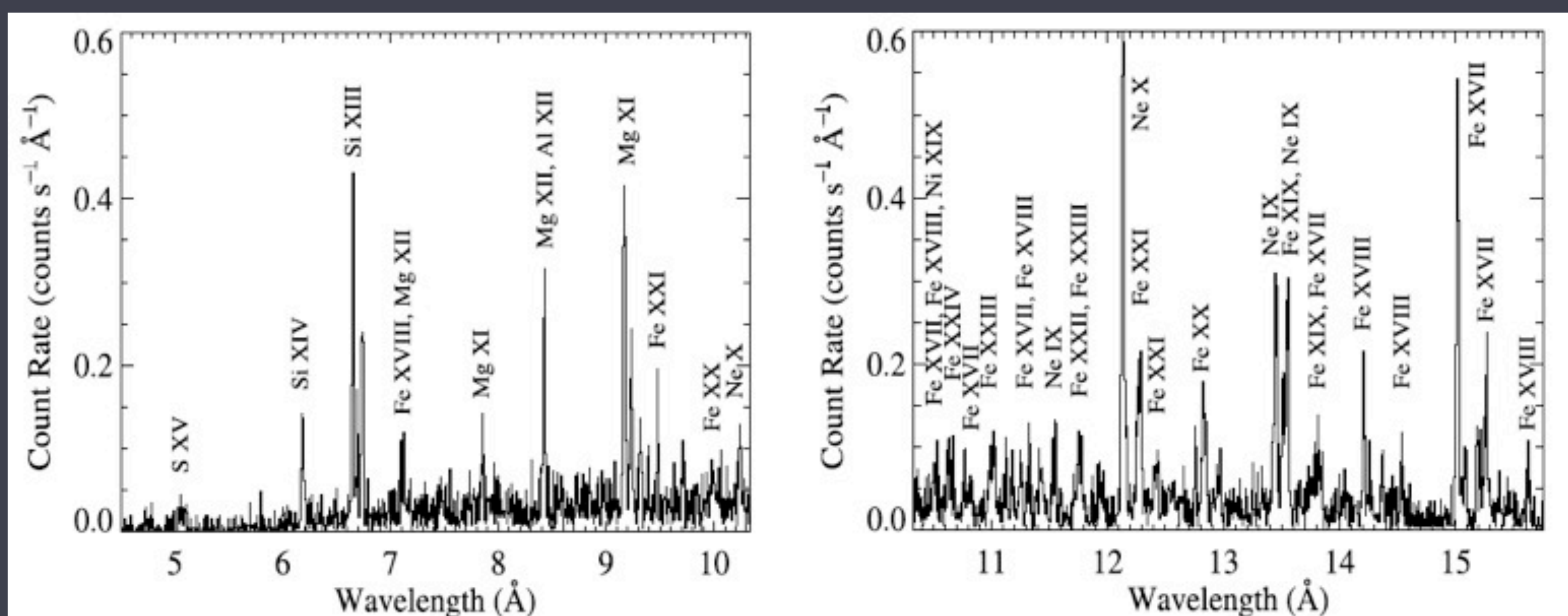

Chandra

small effective area (poor sensitivity) but very low background and very well calibrated

X-ray imaging? > 0.5 arc sec, at best (100s of AU)
spectroscopy (R < 1000 corresp. >300 km/s)

response to photons with hν ~ 0.5 keV up to a few keV
(corresp. ~5Å to 24Å)

Chandra grating spectroscopy (R < 1000)

ζ Pup (O4 If)

cool stars vs. hot stars

starfish, *in situ*, at the Monterey (California) Aquarium

Chandra grating (HETGS/MEG) spectra

ζ Pup (O4 If)

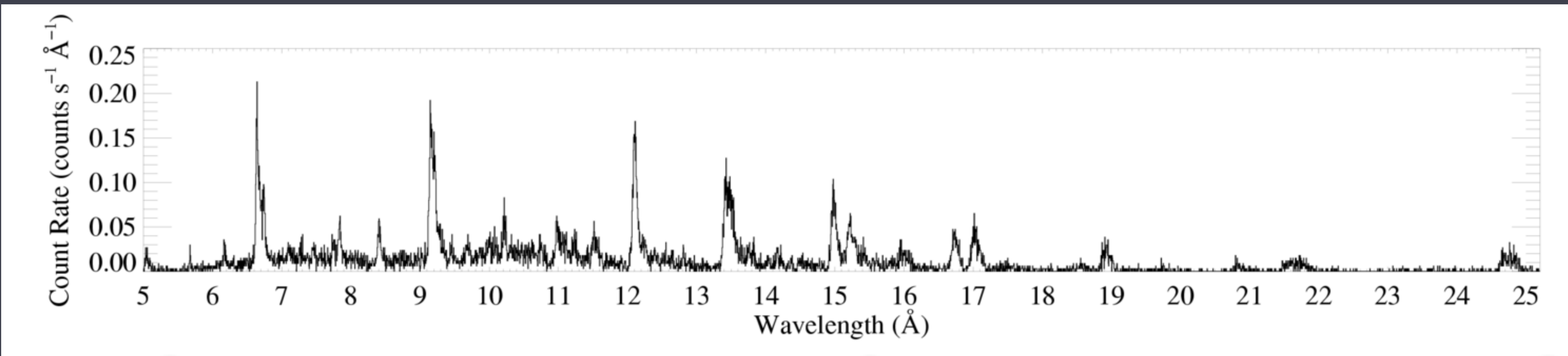

5Å 15Å 25Å

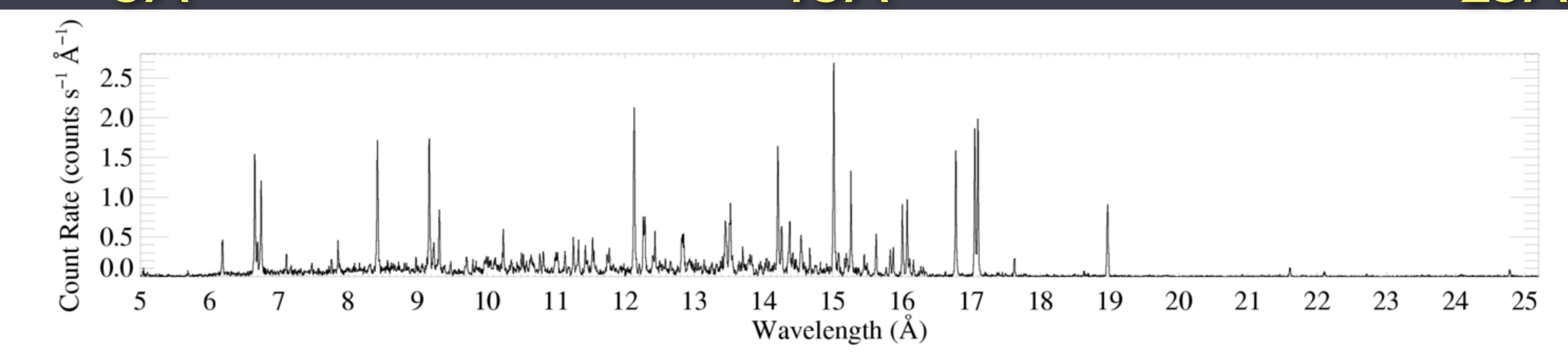

Capella (G5 III)

emission lines + bremsstrahlung + recombination

ζ Pup (O4 If)

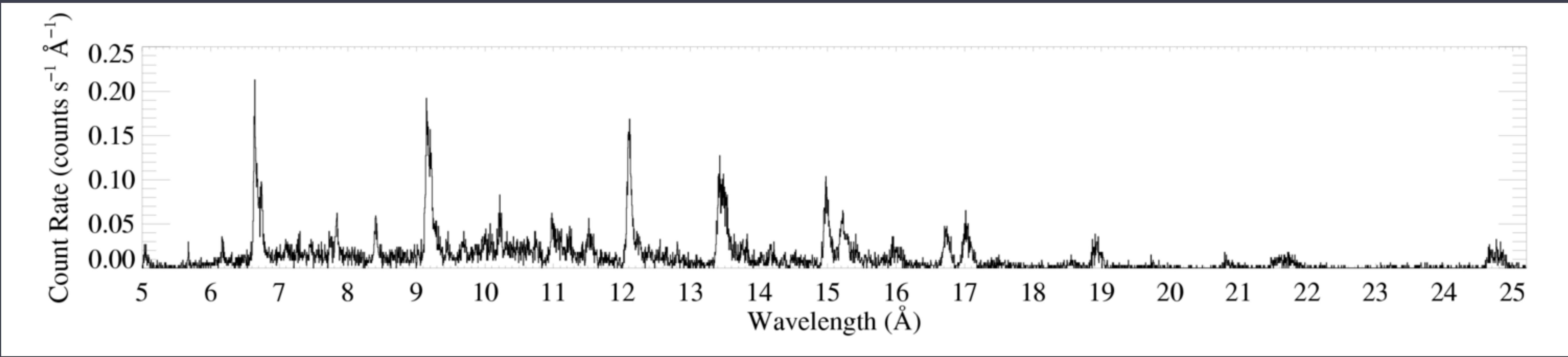

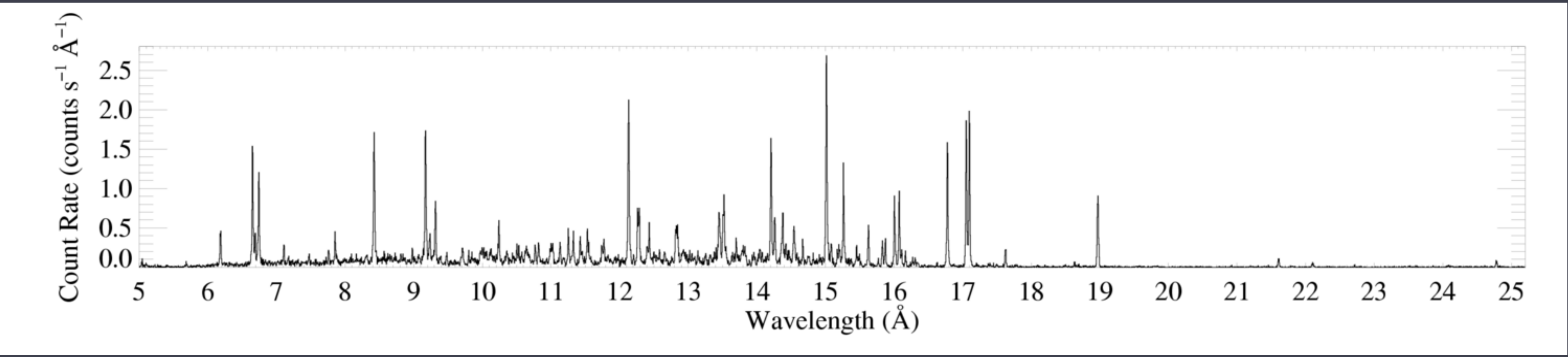

Capella (G5 III)

Chandra grating (HETGS/MEG) spectra

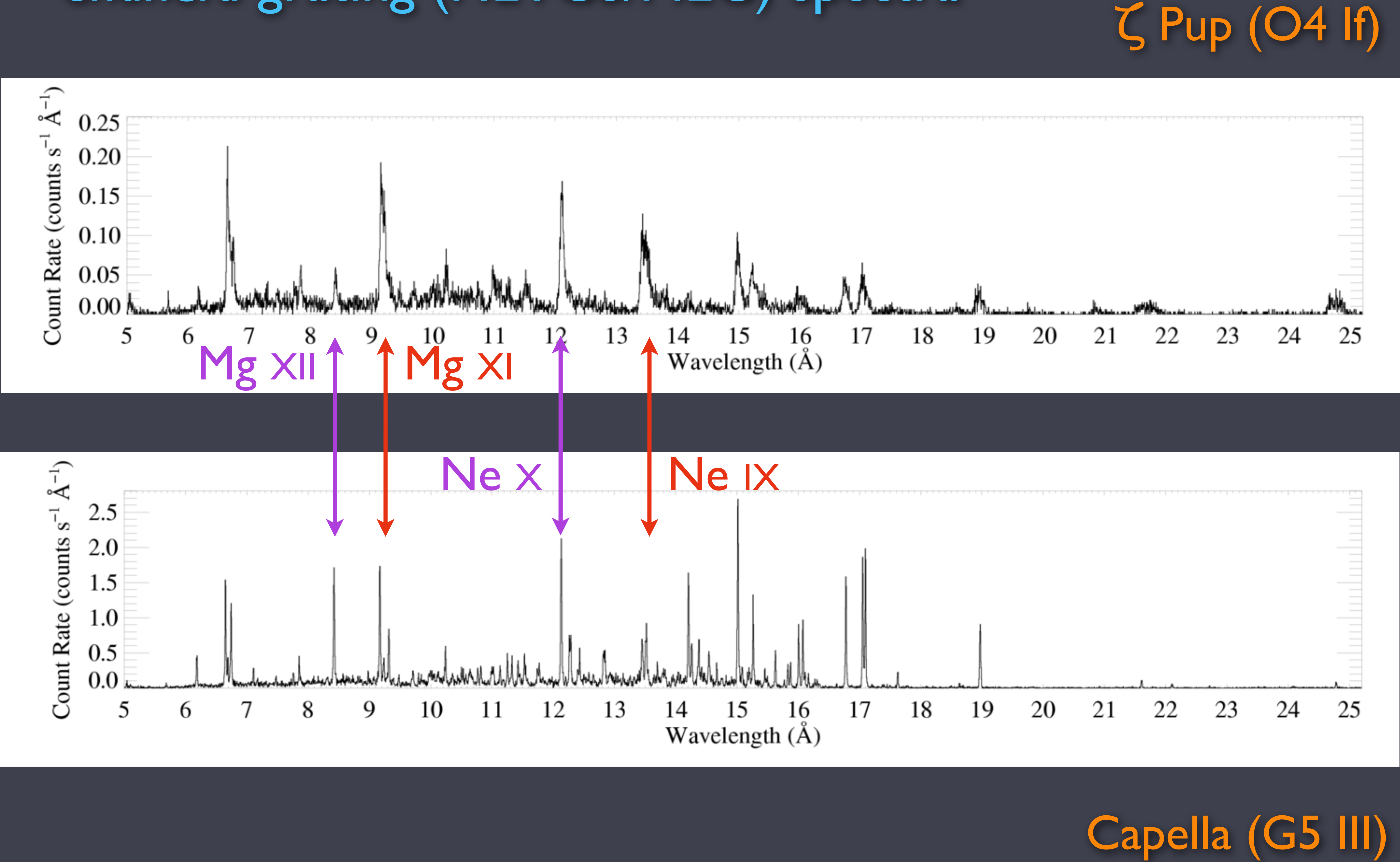

typical temperatures $T \sim$ few 10^6 K
(late-type stellar coronae tend to be hotter)

ζ Pup (O4 If)

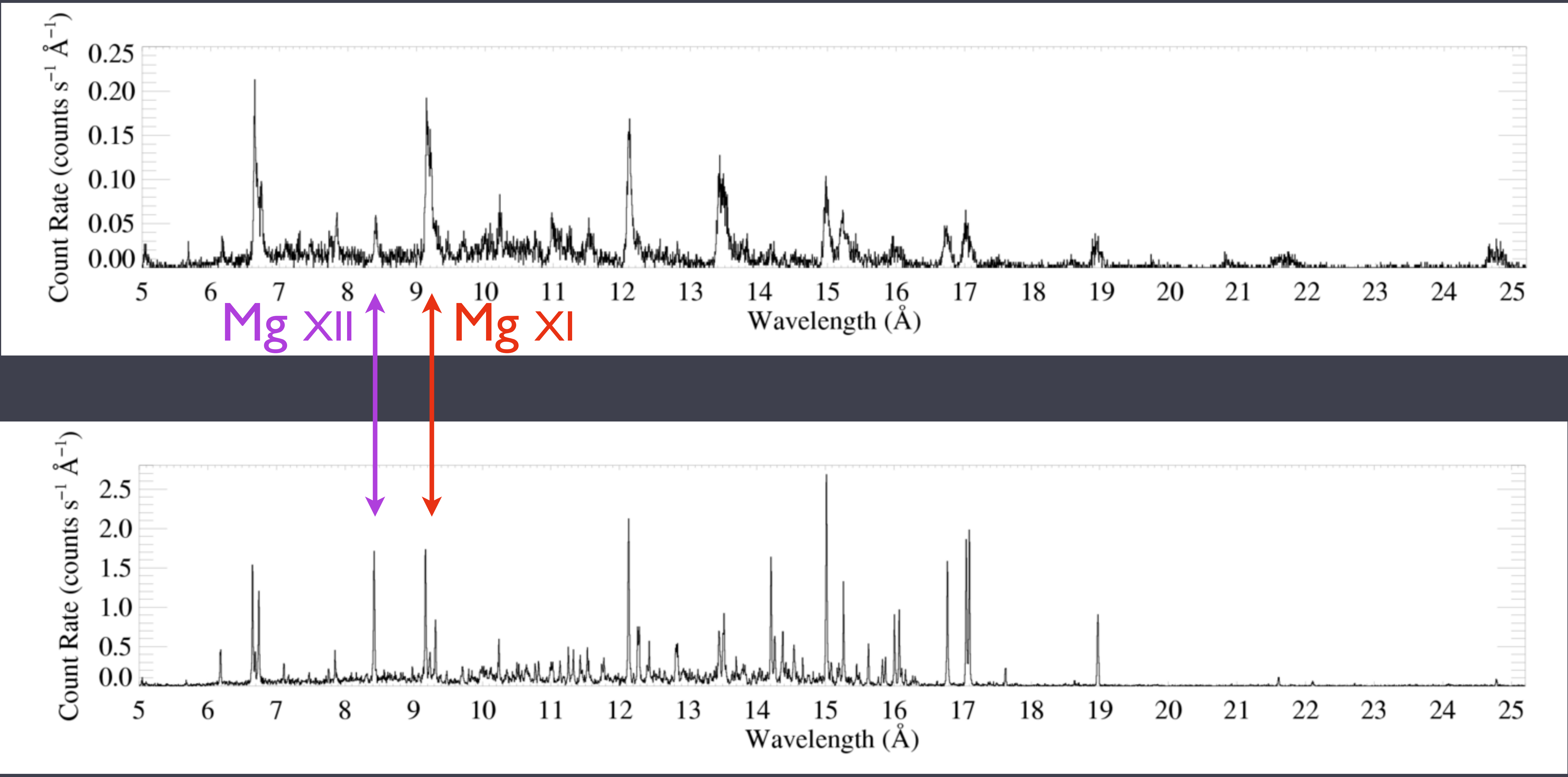

Capella (G5 III)

Zoom in

ζ Pup (O4 If)

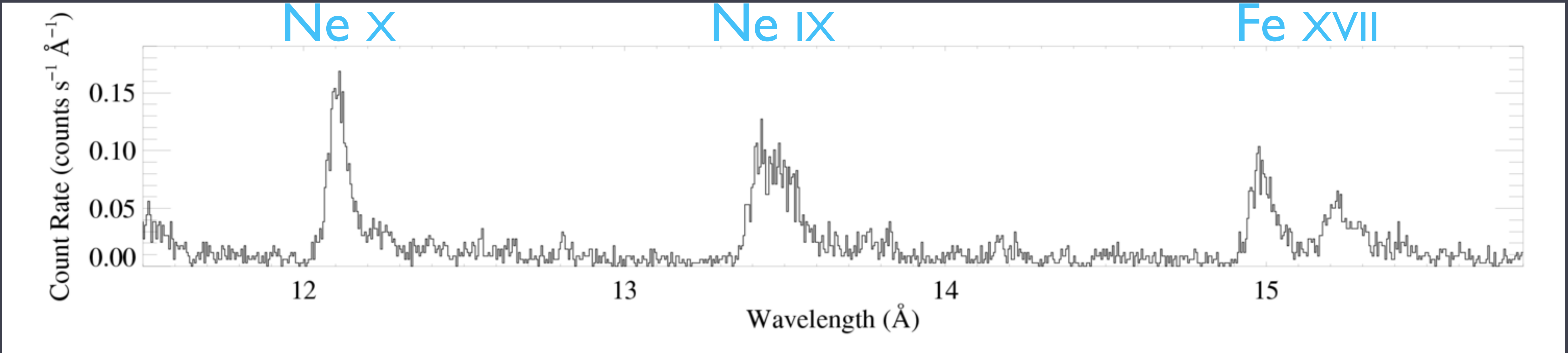

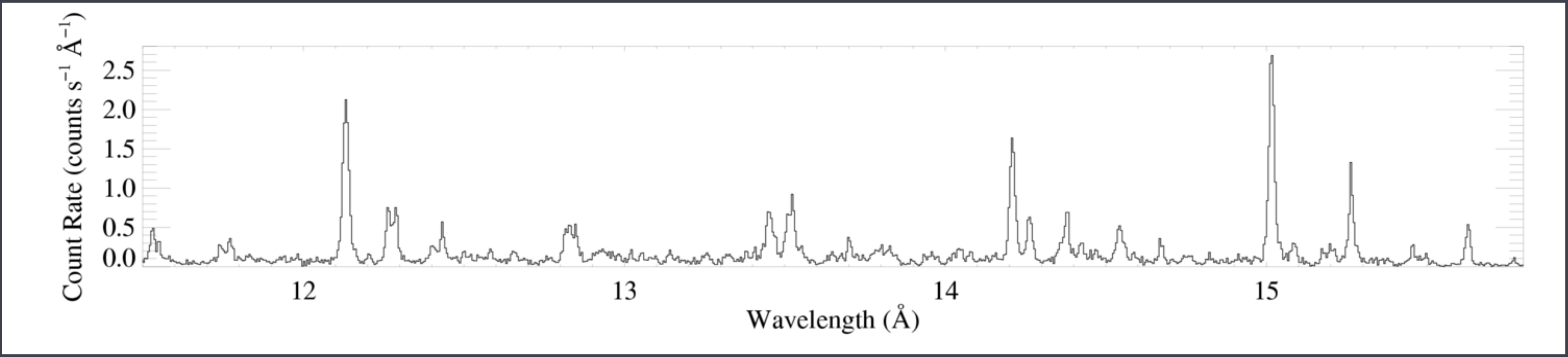

Capella (G5 III)

ζ Pup (O4 If)

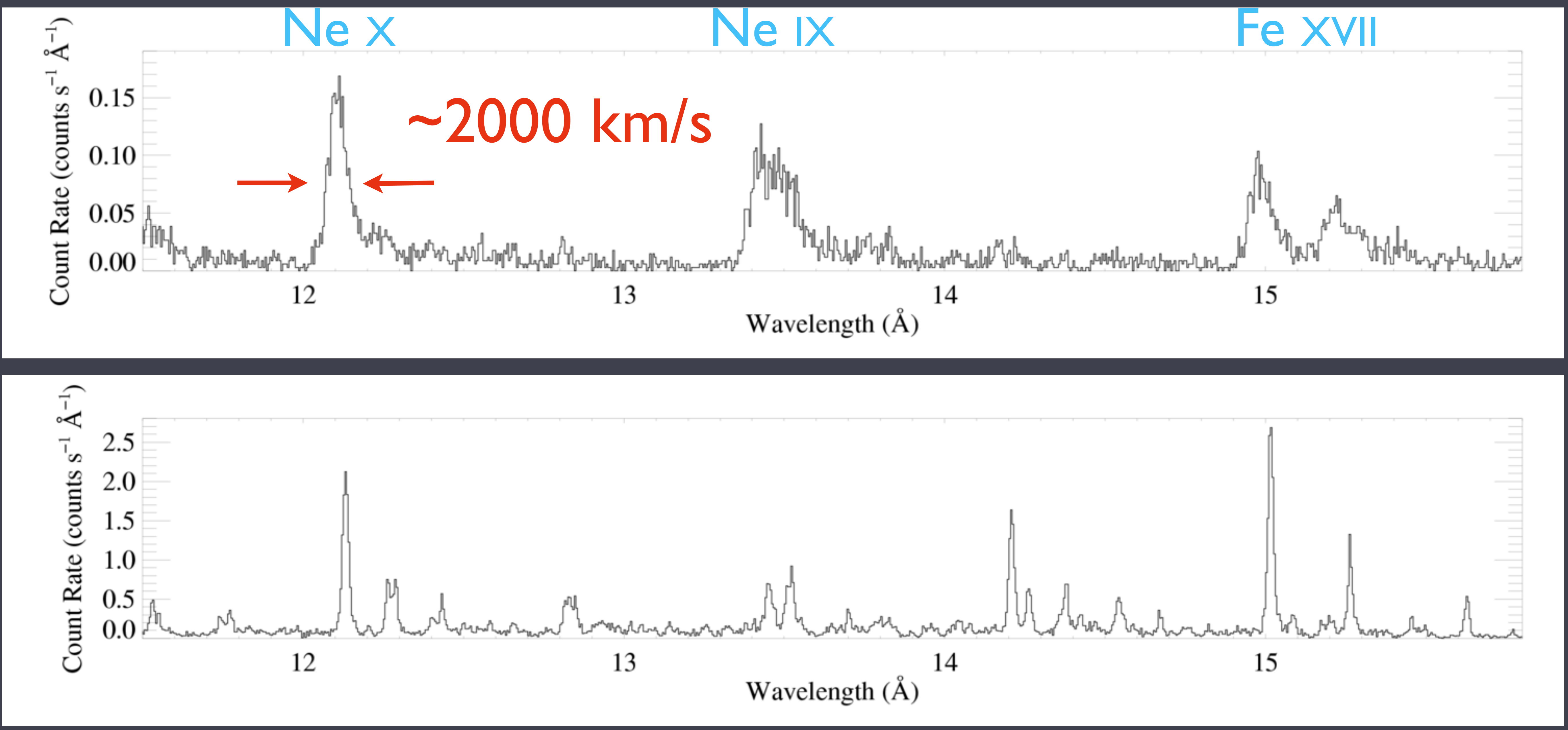

Capella (G5 III)

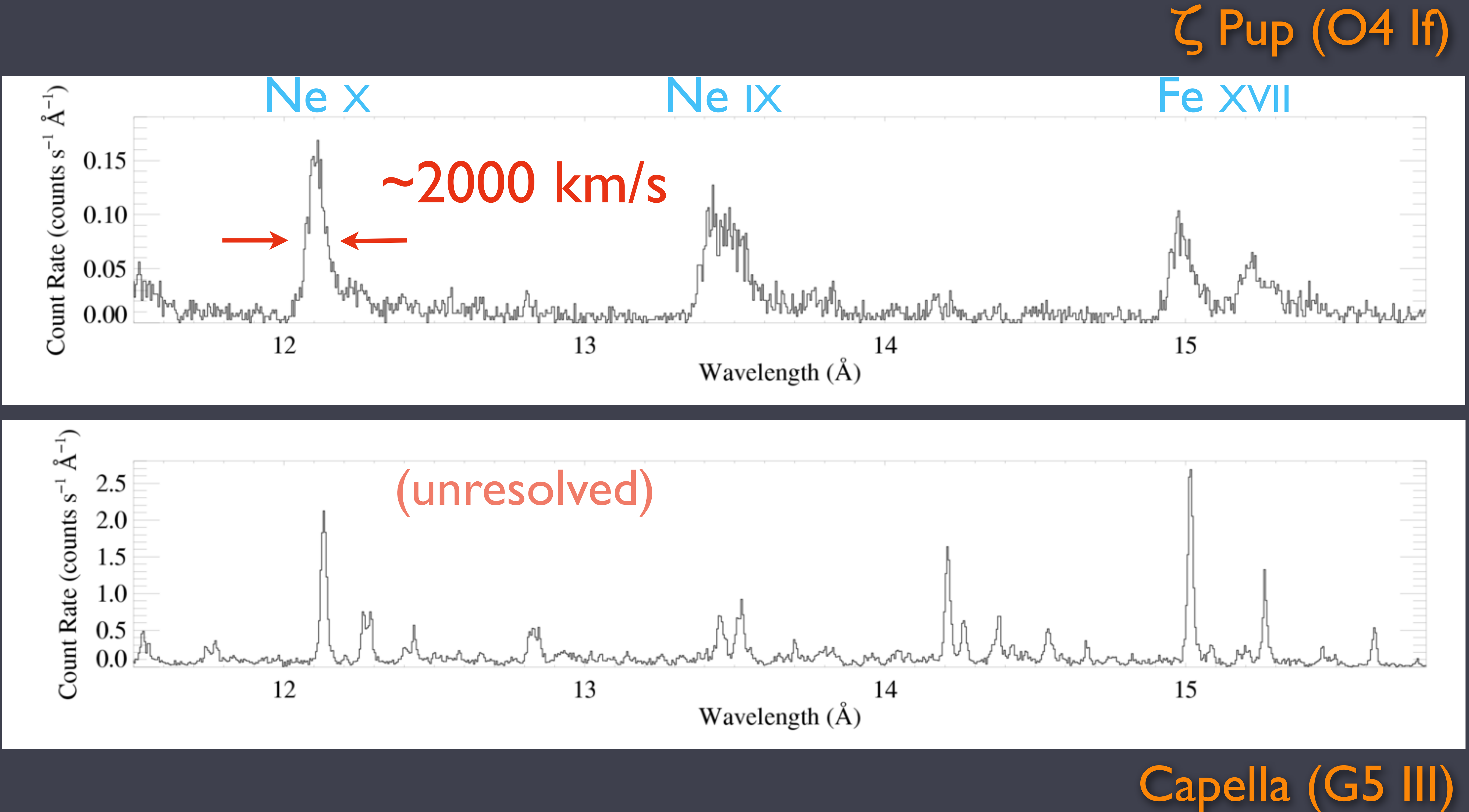
ζ Pup (O4 If)
Ne X
Ne IX
Fe XVII
~2000 km/s
Count Rate (counts s⁻¹ Å⁻¹)
0.15
0.10
0.05
0.00
12
13
14
15
Wavelength (Å)
(unresolved)
Count Rate (counts s⁻¹ Å⁻¹)
2.5
2.0
1.5
1.0
0.5
0.0
12
13
14
15
Wavelength (Å)
Capella (G5 III)

cool stars: narrow lines = magnetically confined coronal plasma

hot stars: broad lines = outflowing, shock-heated wind plasma

lines are asymmetric

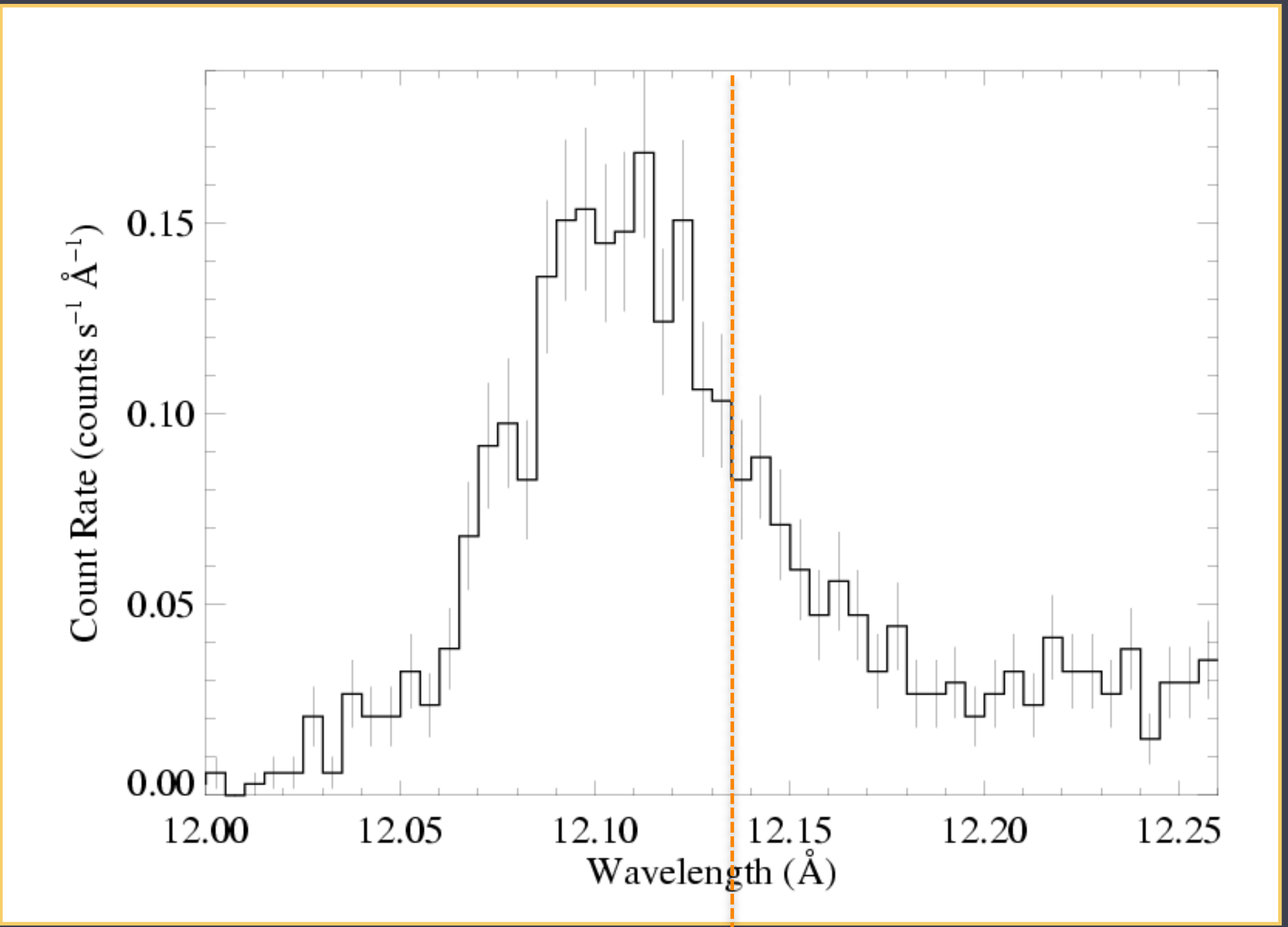

ζ Pup (O4If)

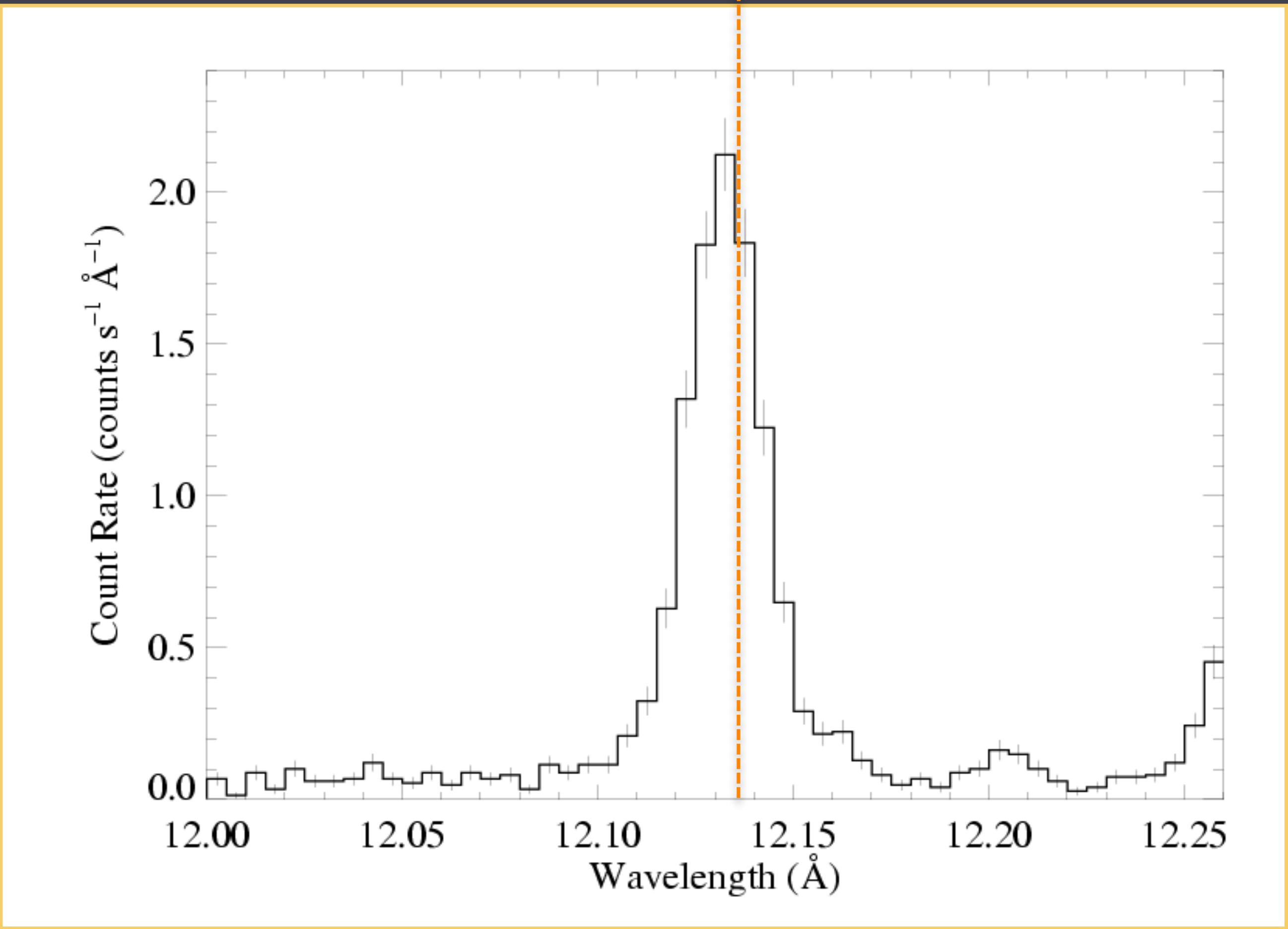

Capella (G5 III)

Line Asymmetry

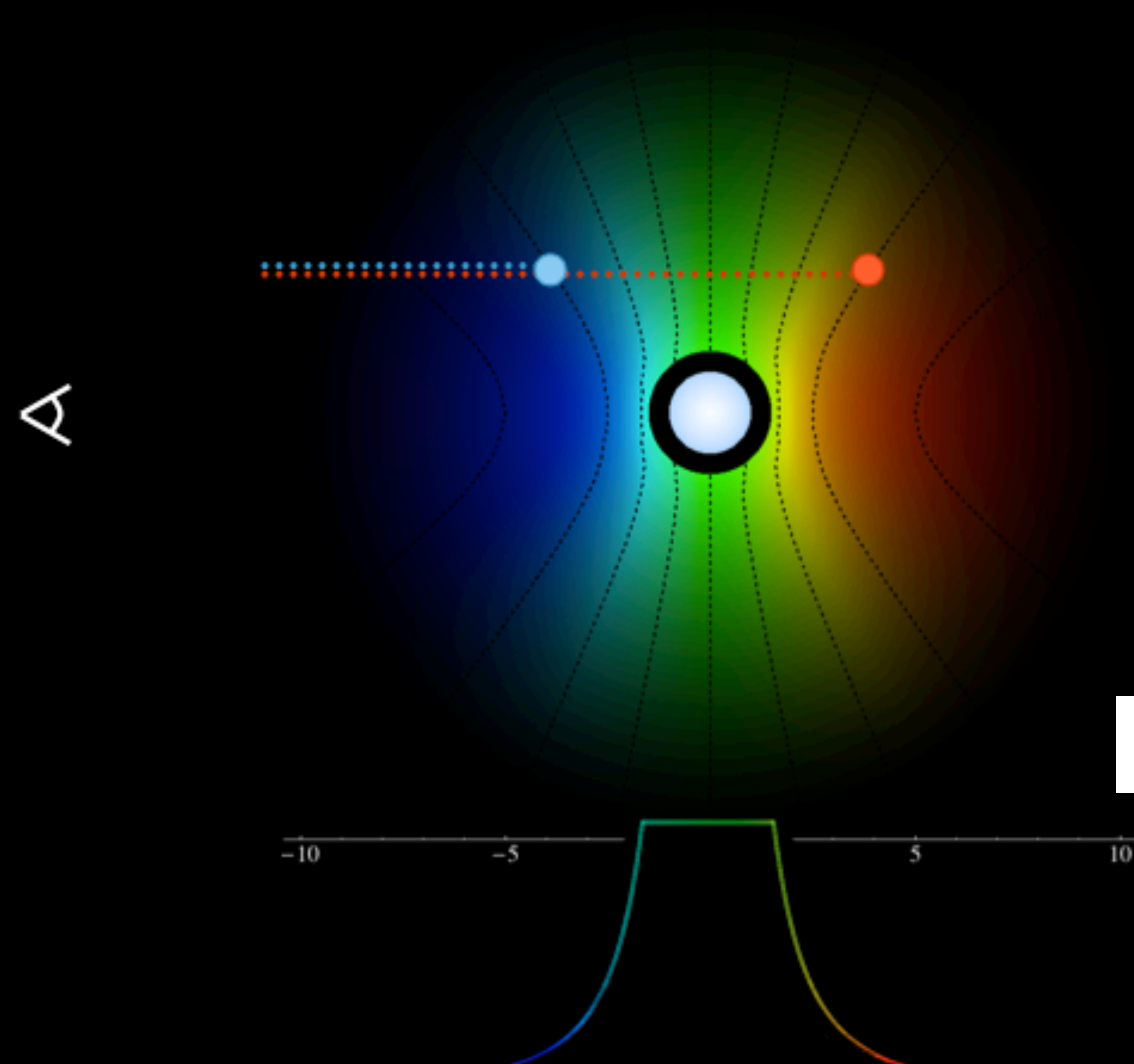

$v = v_\infty(1 - r/R_\star)^\beta$

Line Asymmetry

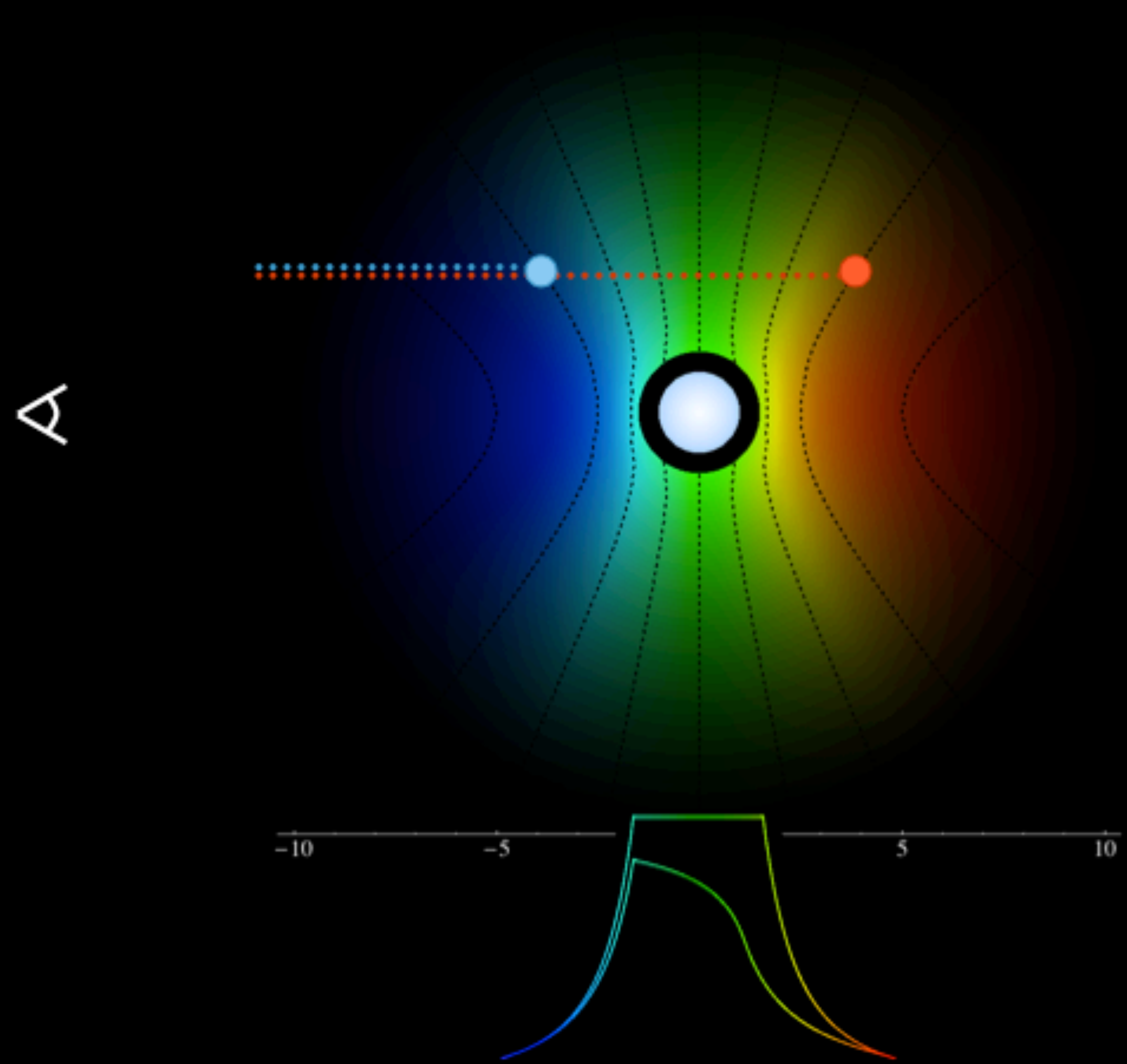

Line Asymmetry

$$\tau = \tau_* \int_z^\infty \frac{R_* dz'}{r'^2 (1 - R_*/r')^\beta}$$

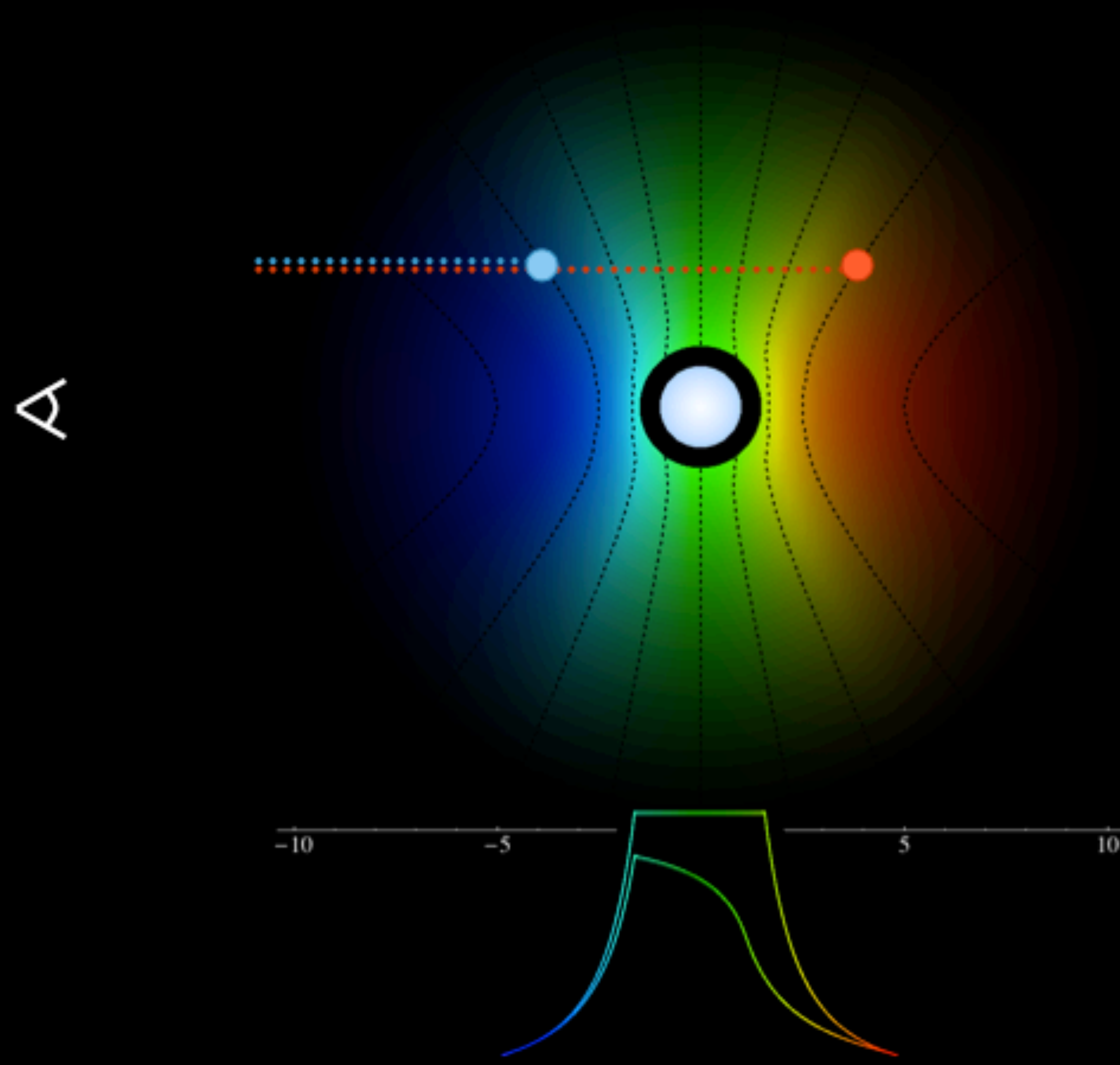

Wind Profile Model

$$\tau_* = \frac{\kappa \dot{M}}{4\pi R_* v_\infty}$$

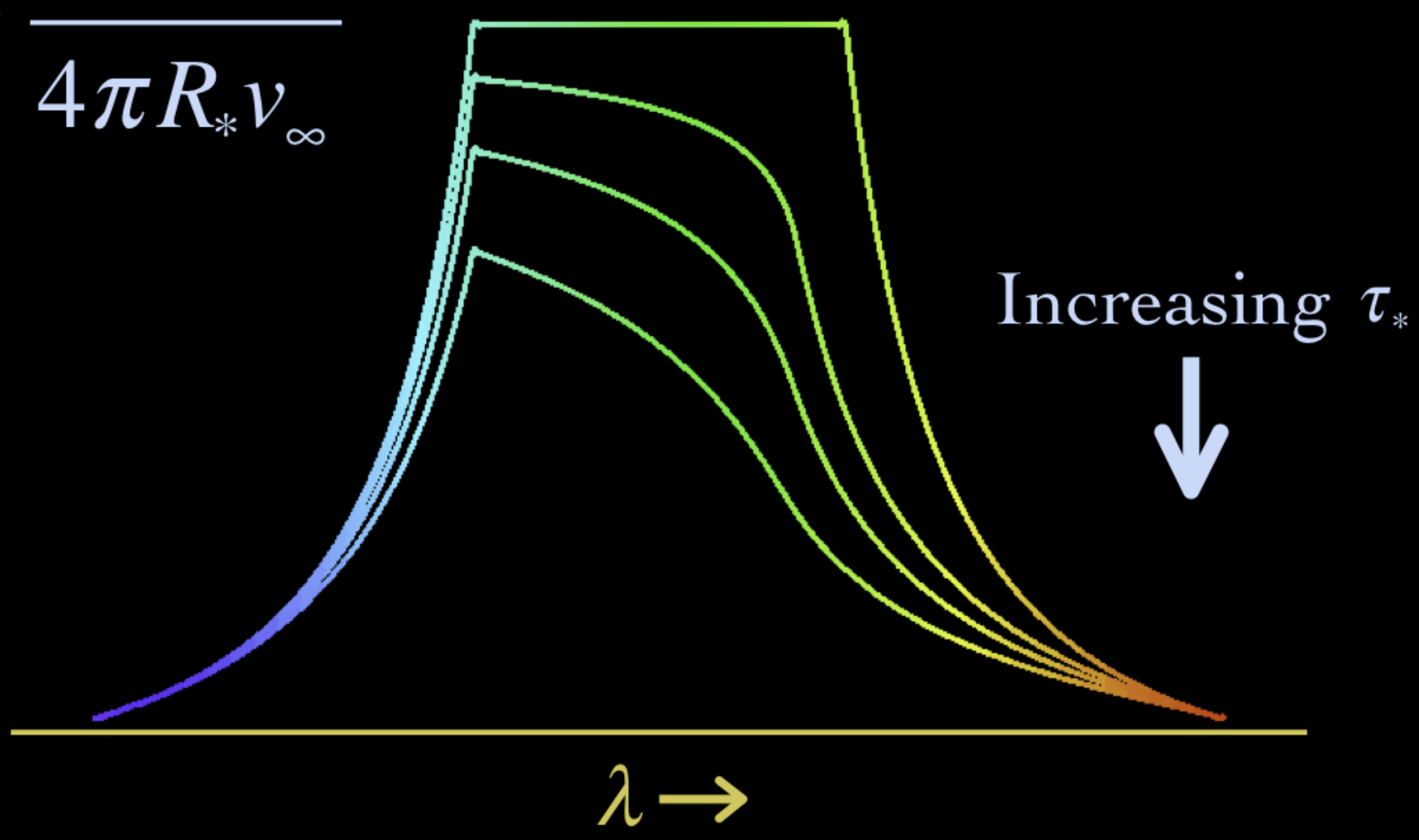

Line profile shapes

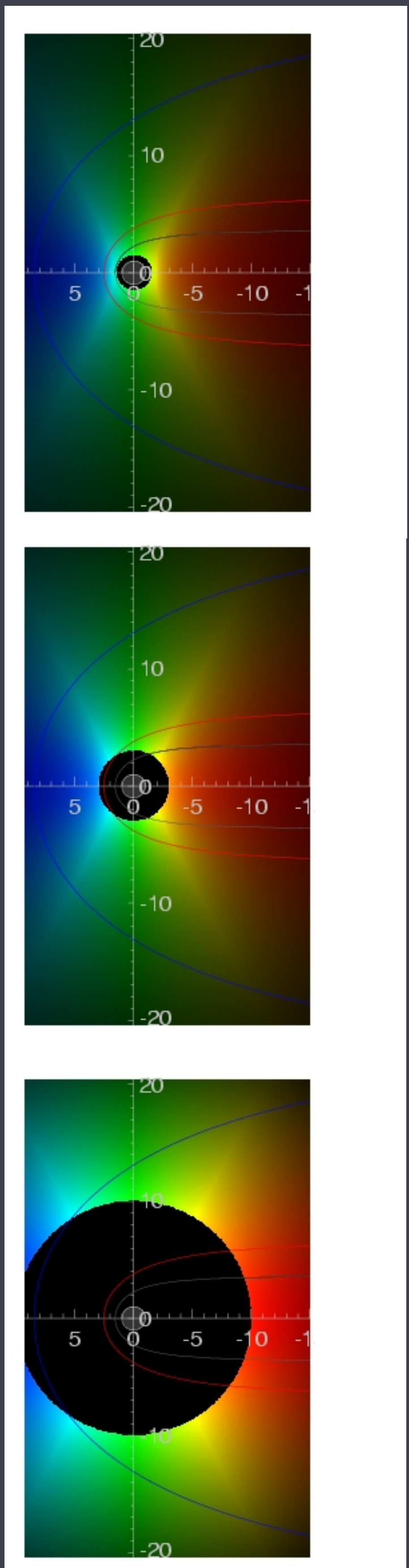

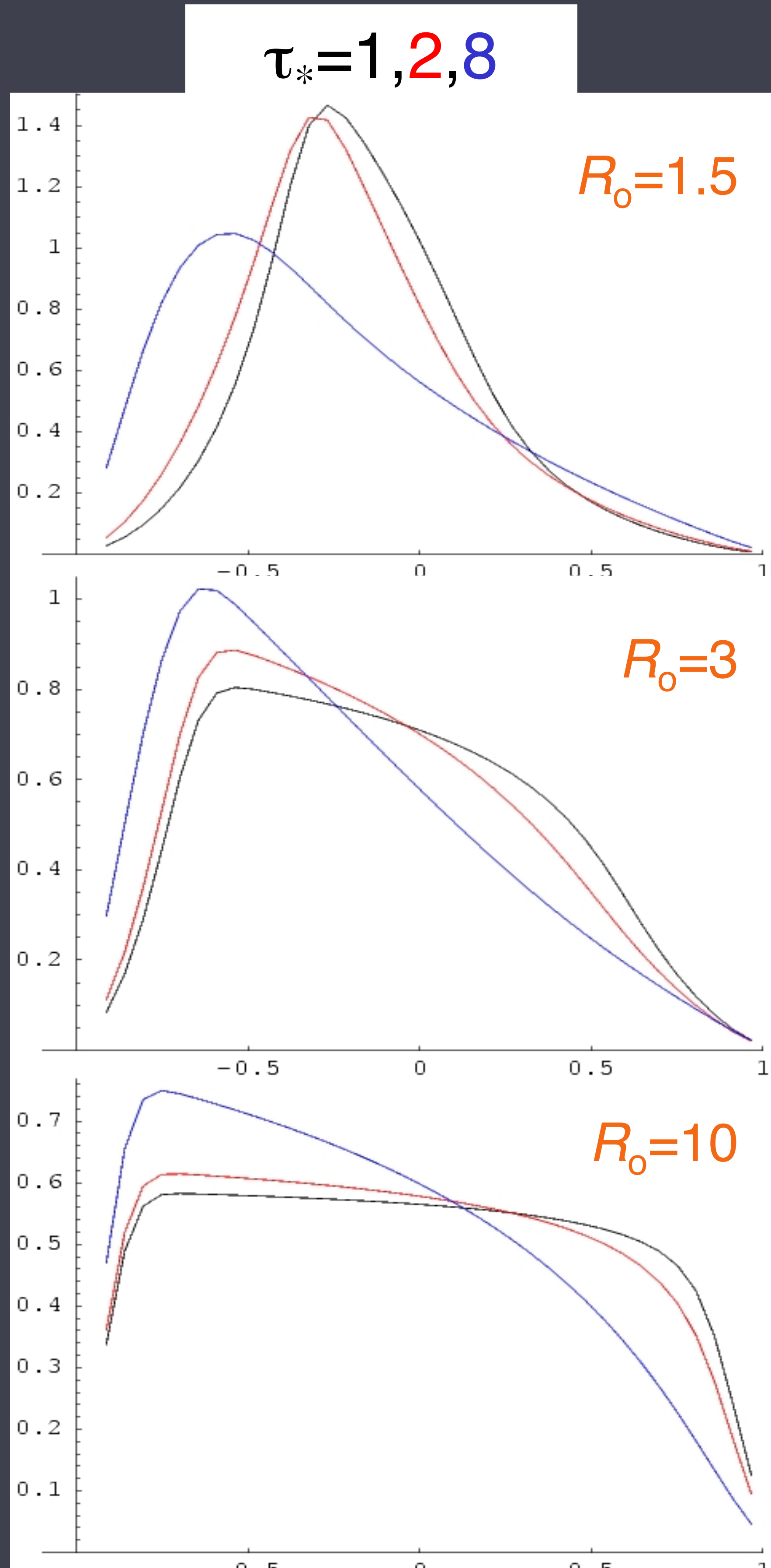

key parameters: R_o & $\tau_\star$

$$v = v_\infty(1 - r/R_\star)^\beta$$

$$j \sim \rho^2 \text{ for } r/R_* > R_o, \quad = 0 \text{ otherwise}$$

$$\tau = \tau_* \int_z^\infty \frac{R_* dz'}{r'^2 (1 - R_*/r')^\beta}$$

$$\tau_* \equiv \frac{\kappa \dot{M}}{4\pi R_* v_\infty}$$

ζ Pup: *Chandra* MEG

Fe XVII

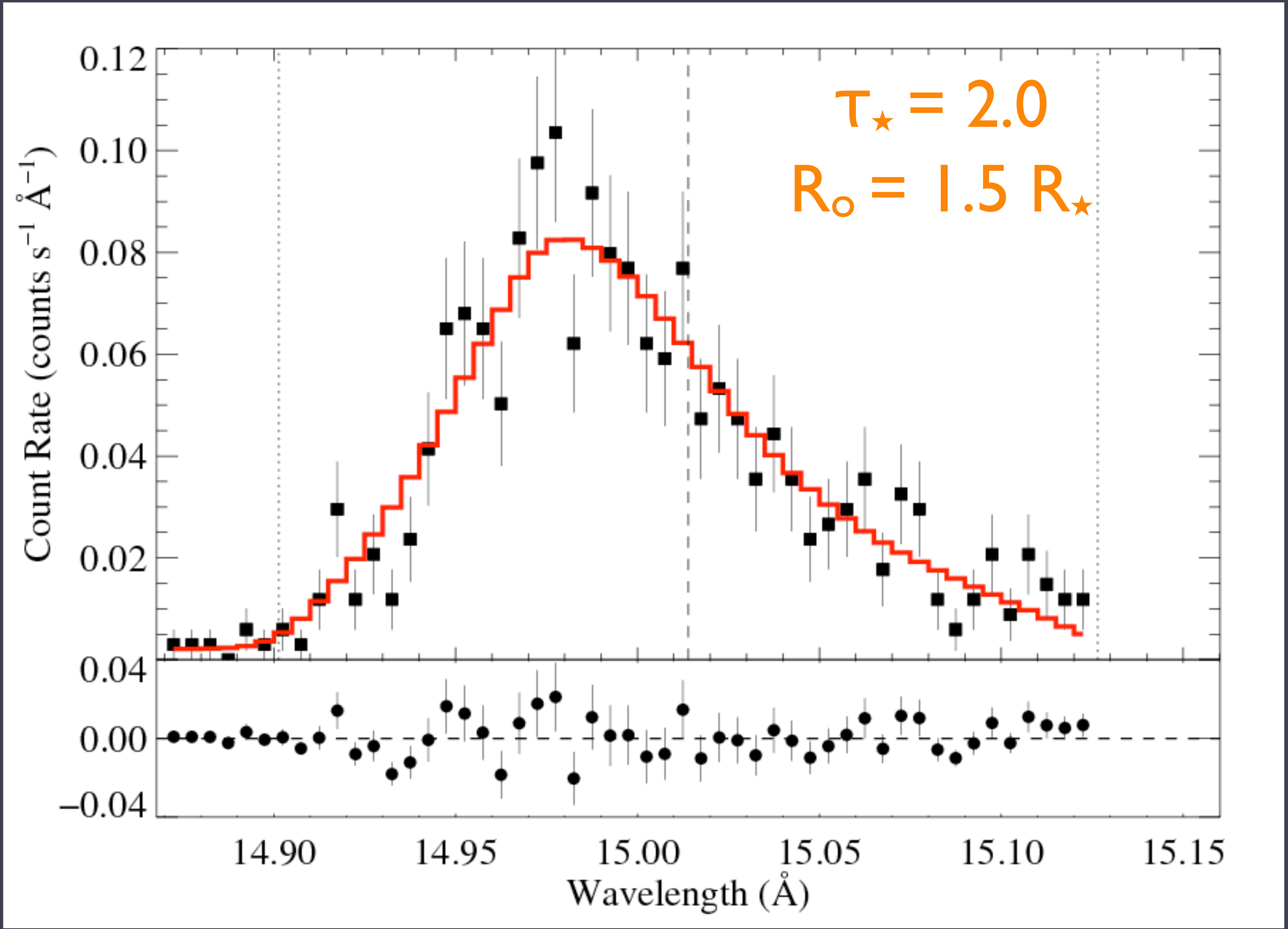

Hot plasma kinematics and location

R_o controls the line width via v(r)

$R_o = 1.5\ R_\star$ $R_o = 3\ R_\star$ $R_o = 10\ R_\star$

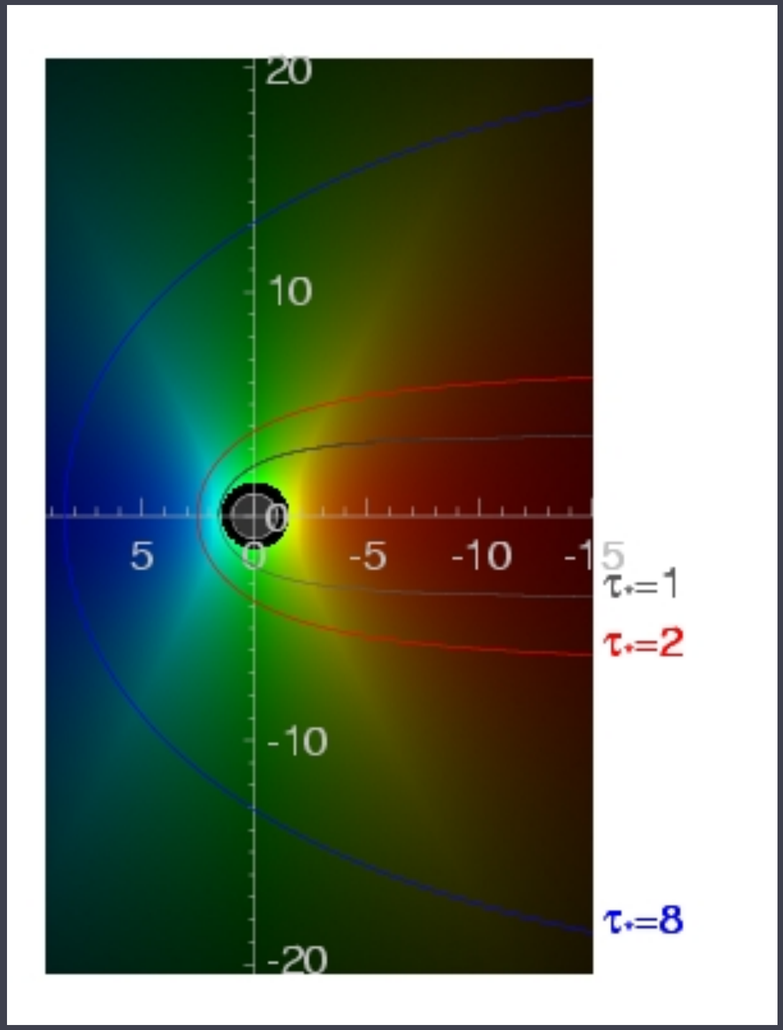

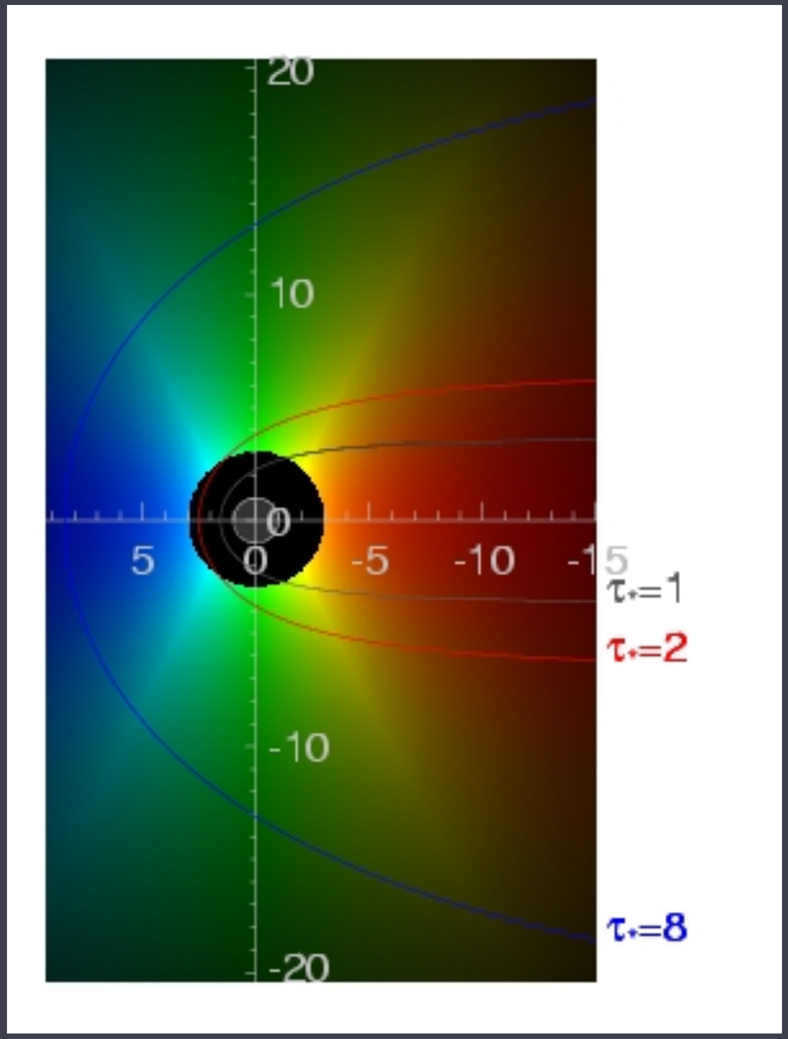

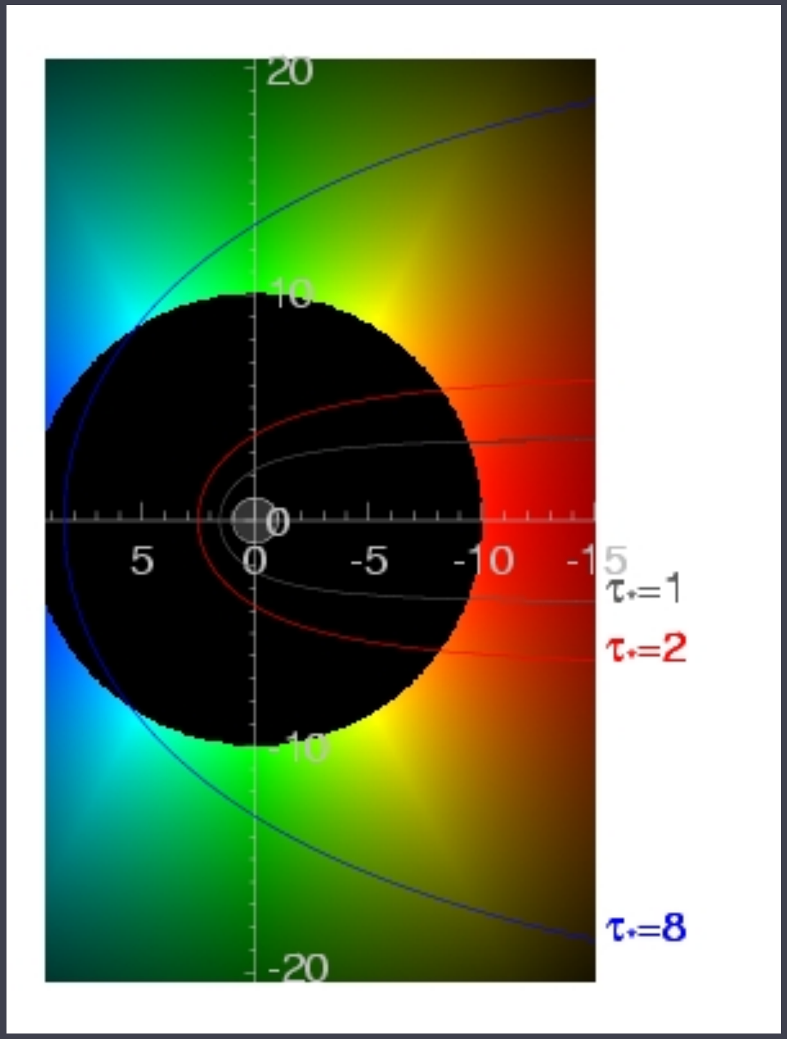

Distribution of R_o values for ζ Pup

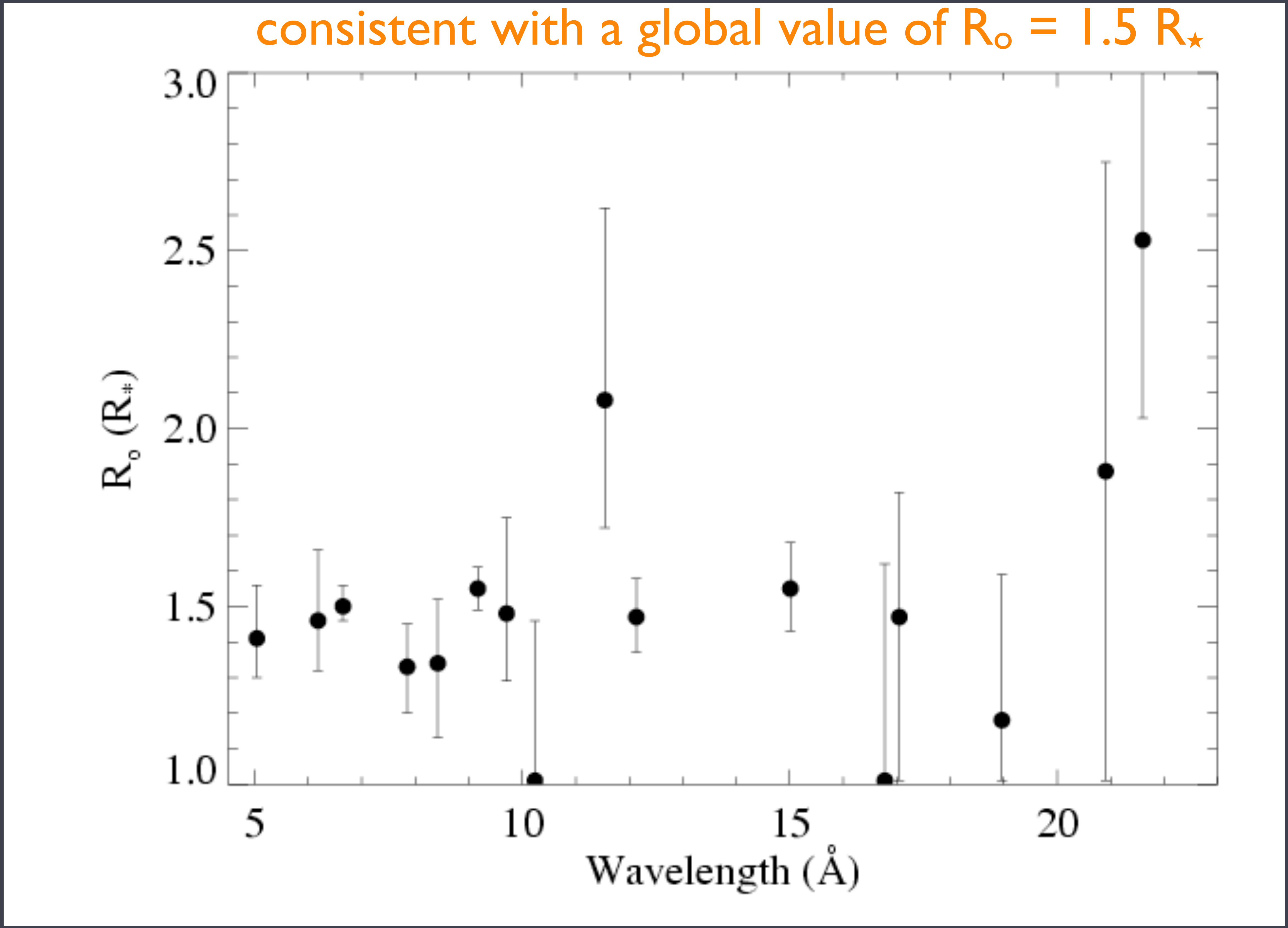

v_∞ can be constrained by the line fitting too

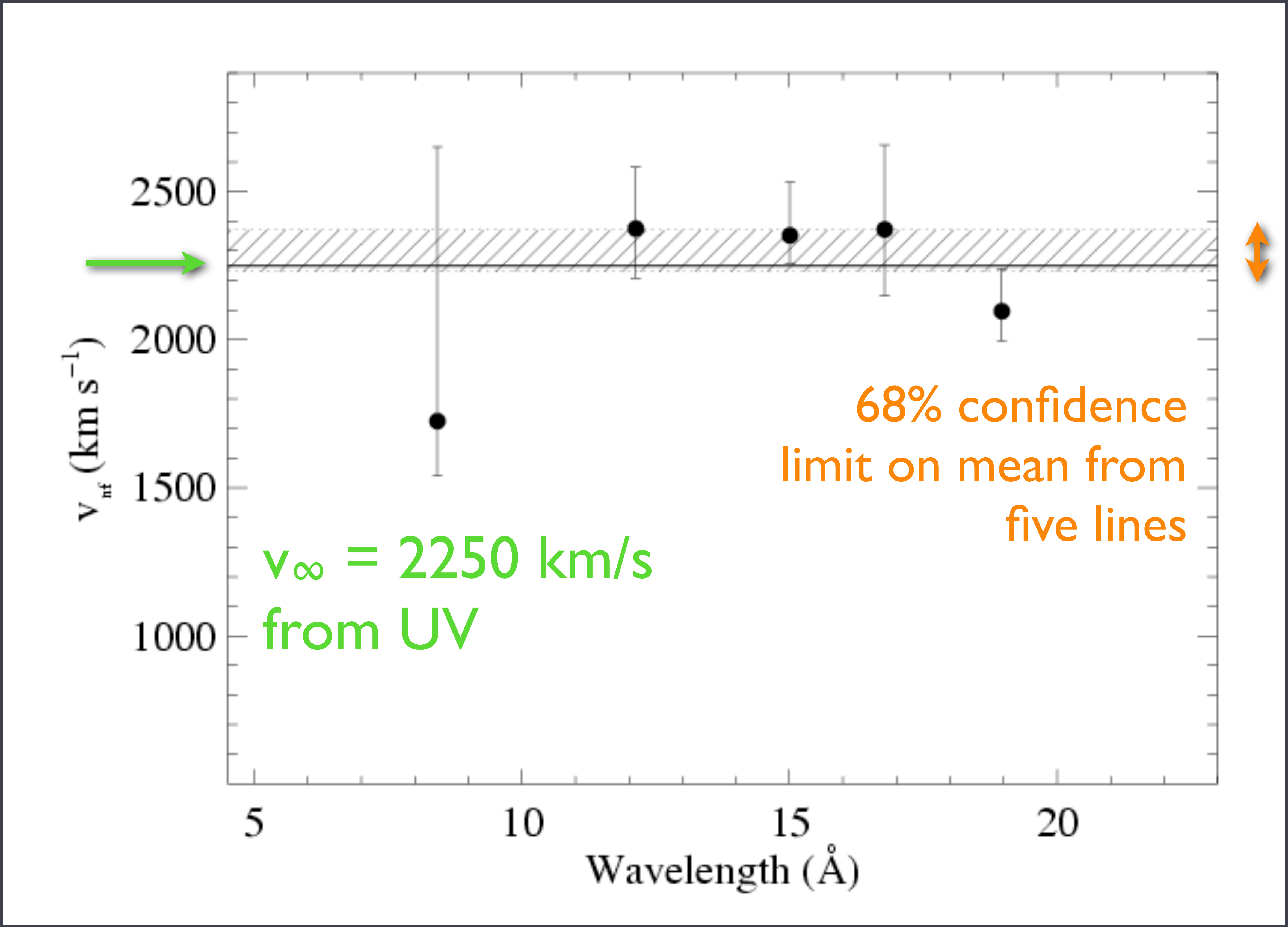

X-ray plasma and mean wind have same kinematics

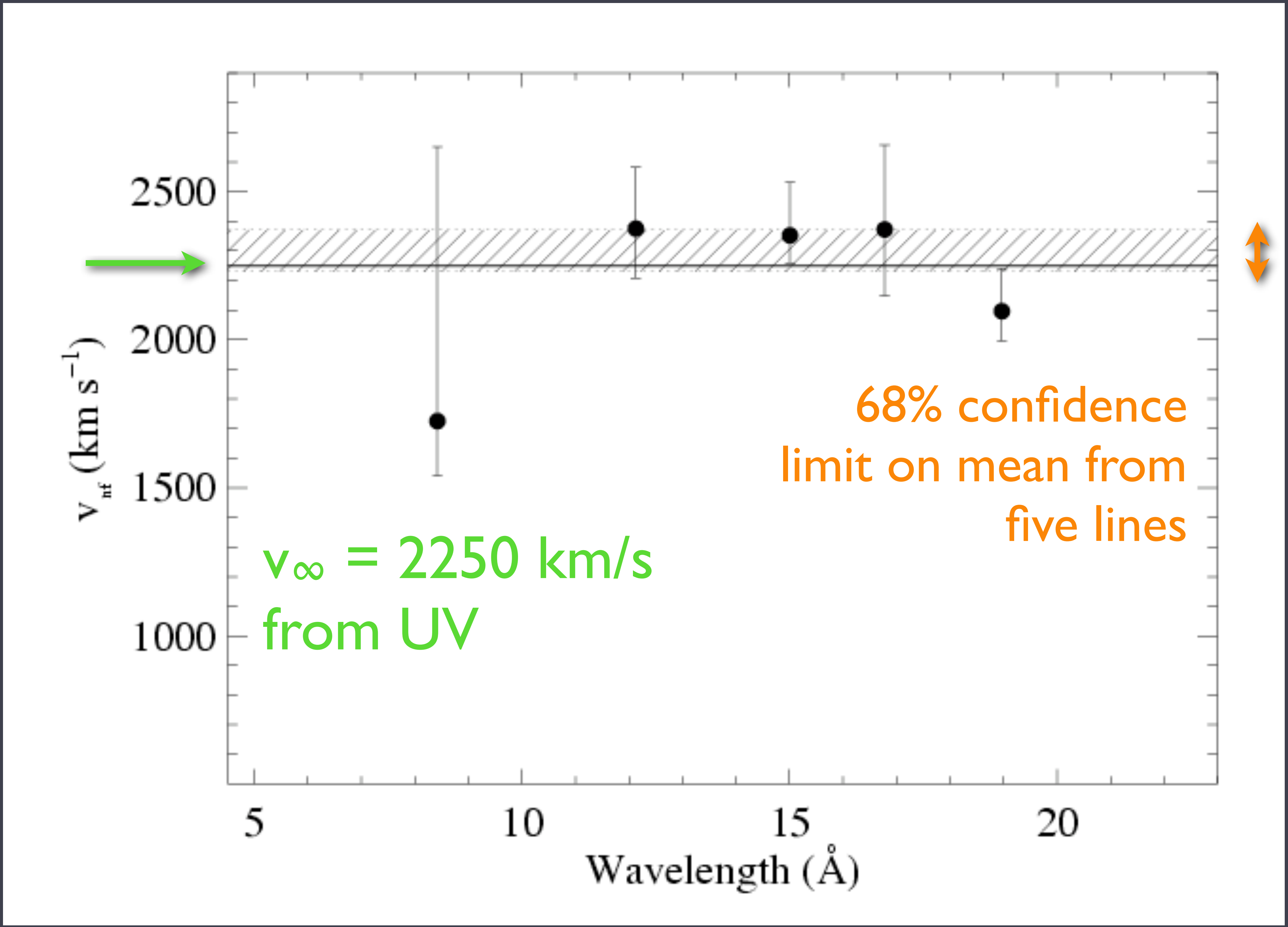

The profiles also tell us about the level of wind absorption

Wind Profile Model

$$\tau_* = \frac{\kappa \dot{M}}{4\pi R_* v_\infty}$$

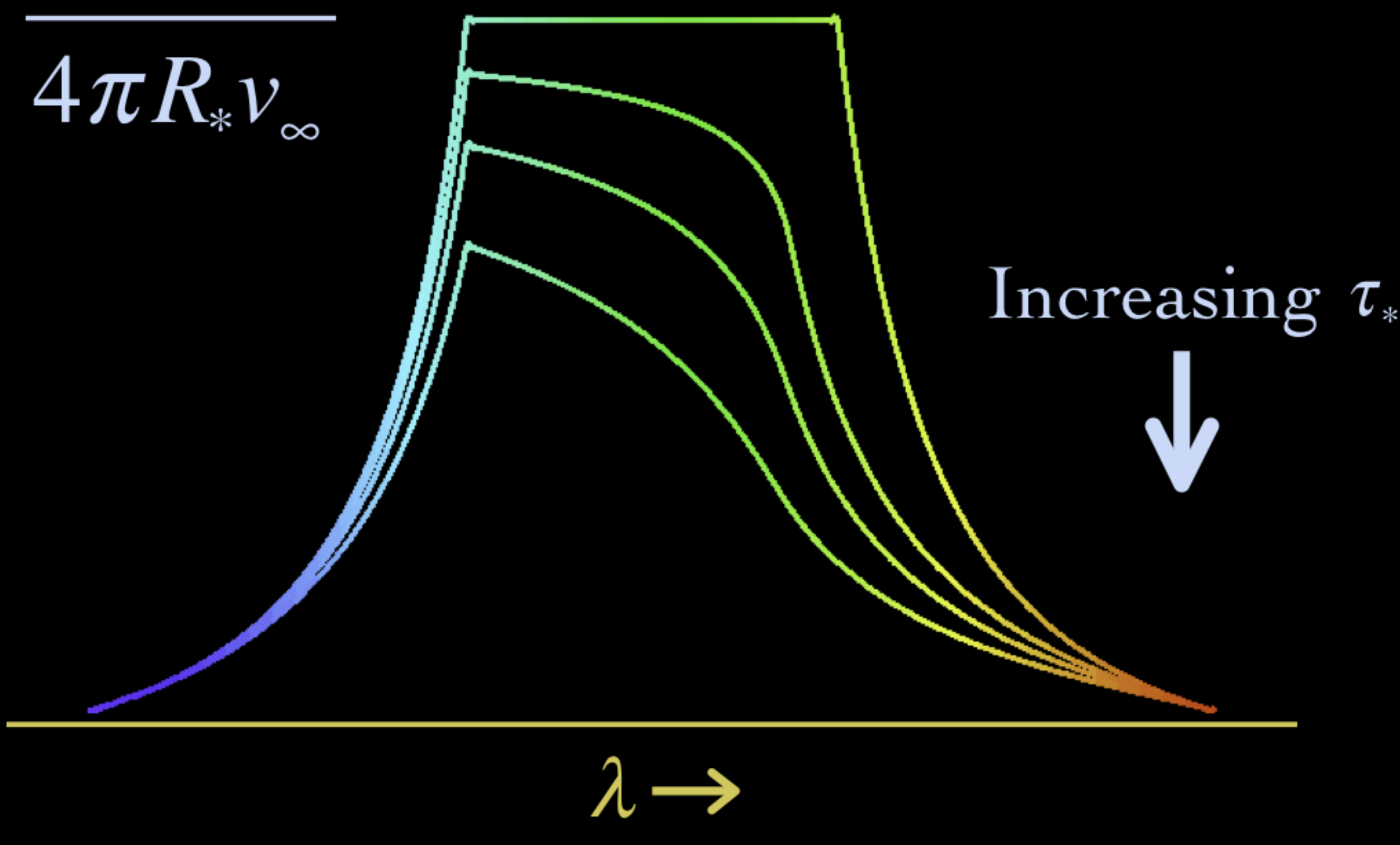

ζ Pup: *Chandra* MEG

Fe XVII

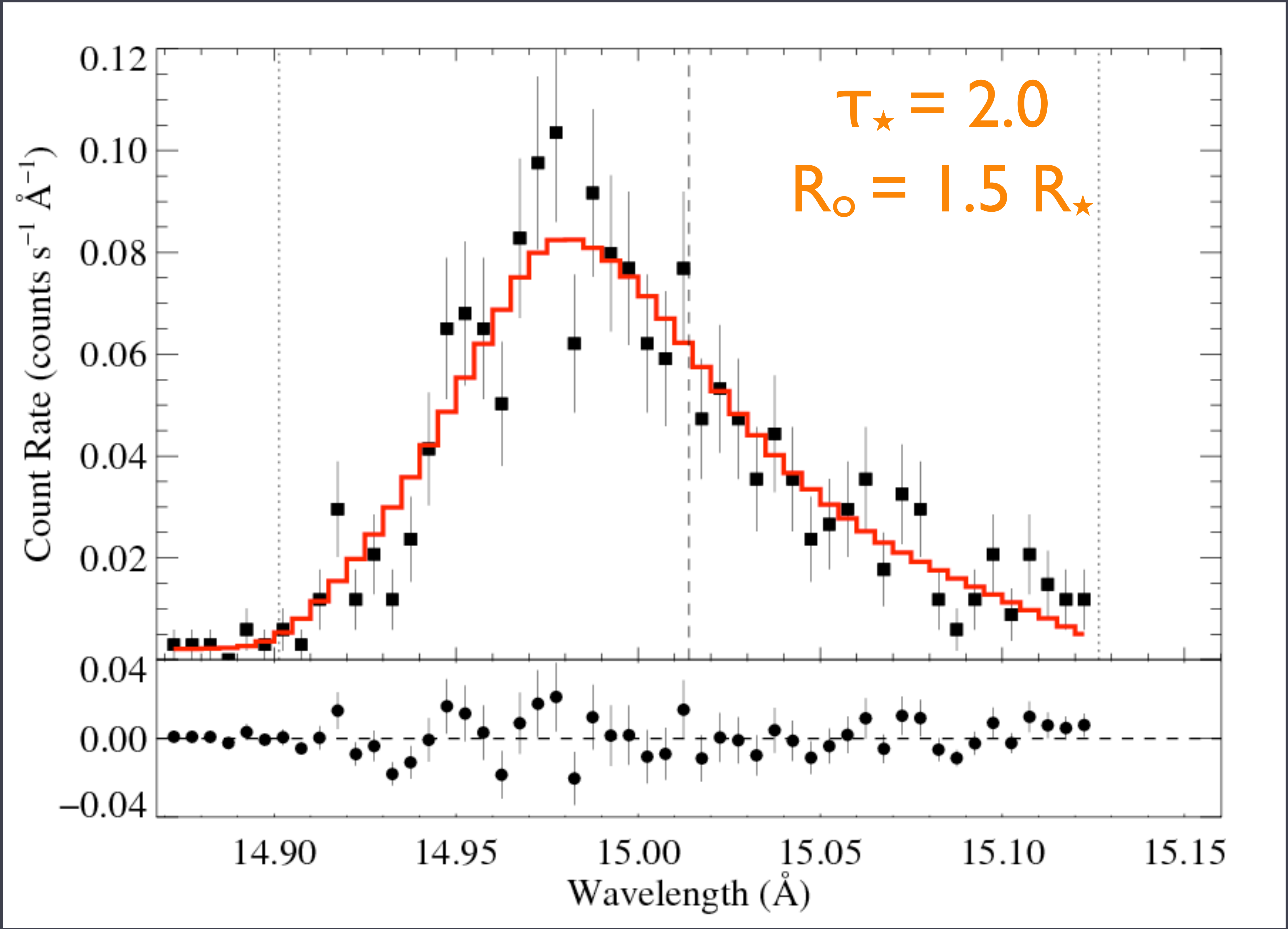

Quantifying the wind optical depth

opacity of the cold wind component (due to bound-free transitions in C, N, O, Ne, Fe)

wind mass-loss rate

$$\dot{M} = 4\pi r^2 v \rho$$

$$\tau_* \equiv \frac{\kappa \dot{M}}{4\pi R_* v_\infty}$$

stellar radius

wind terminal velocity

soft X-ray wind opacity

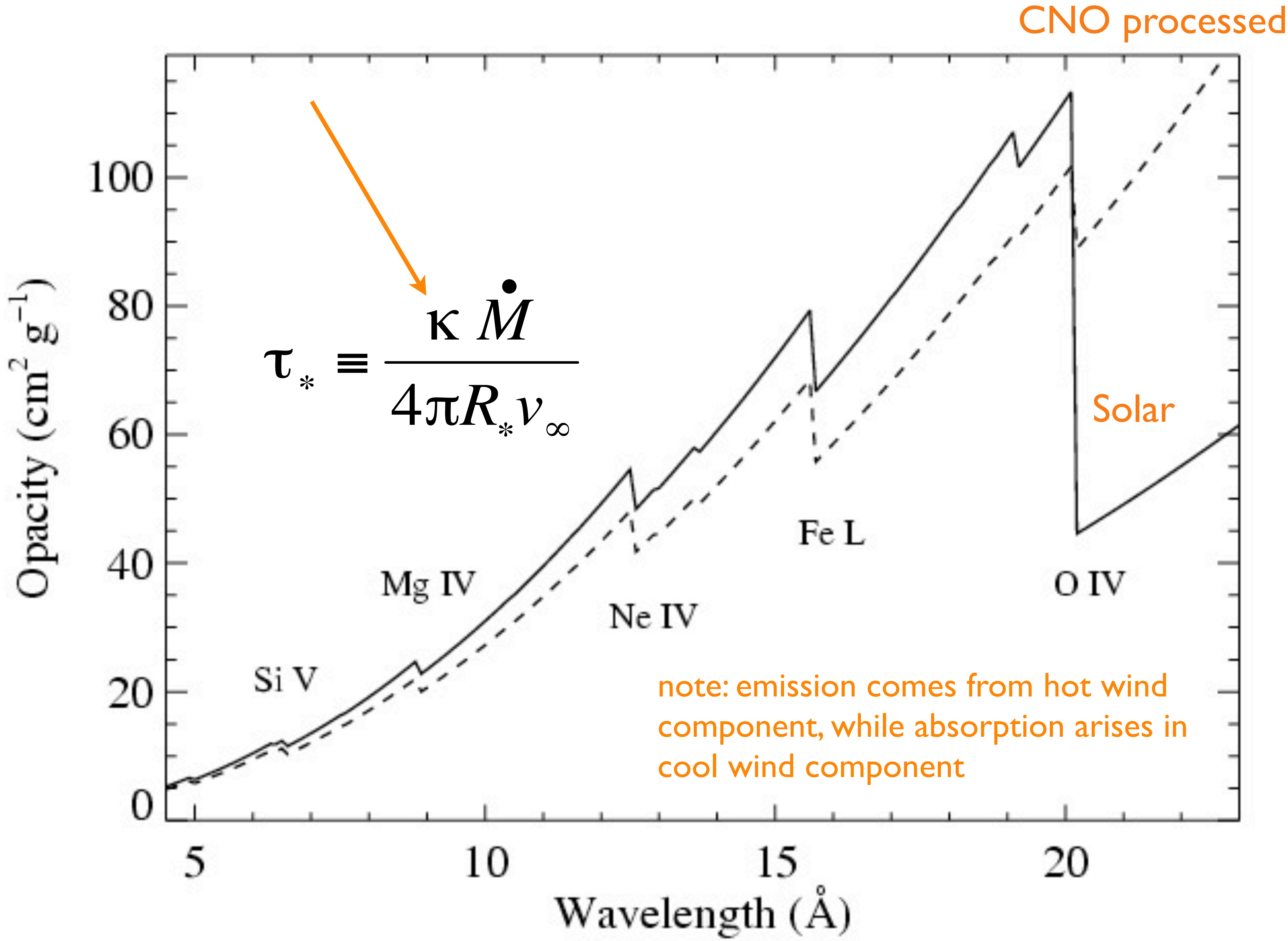

$$\tau_* \equiv \frac{\kappa \dot{M}}{4\pi R_* v_\infty}$$

note: emission comes from hot wind component, while absorption arises in cool wind component

ζ Pup *Chandra*: three emission lines

Mg Lyα: 8.42 Å　　　Ne Lyα: 12.13 Å　　　O Lyα: 18.97 Å

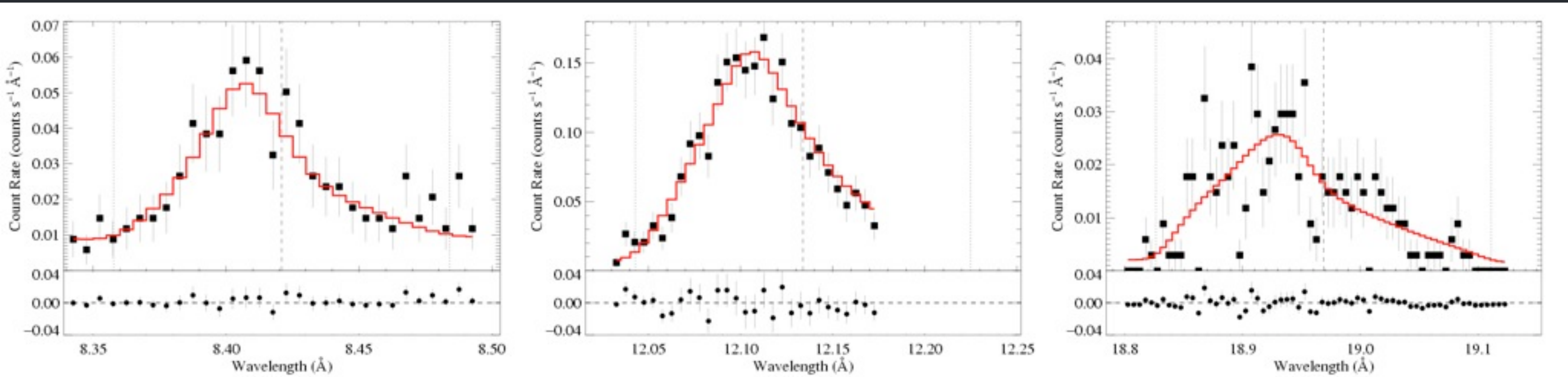

$\tau_* \sim 1$　　　**$\tau_* \sim 2$**　　　**$\tau_* \sim 3$**

Recall:

$$\tau_* \equiv \frac{\kappa \dot{M}}{4\pi R_* v_\infty}$$

Results from the 3 line fits shown previously

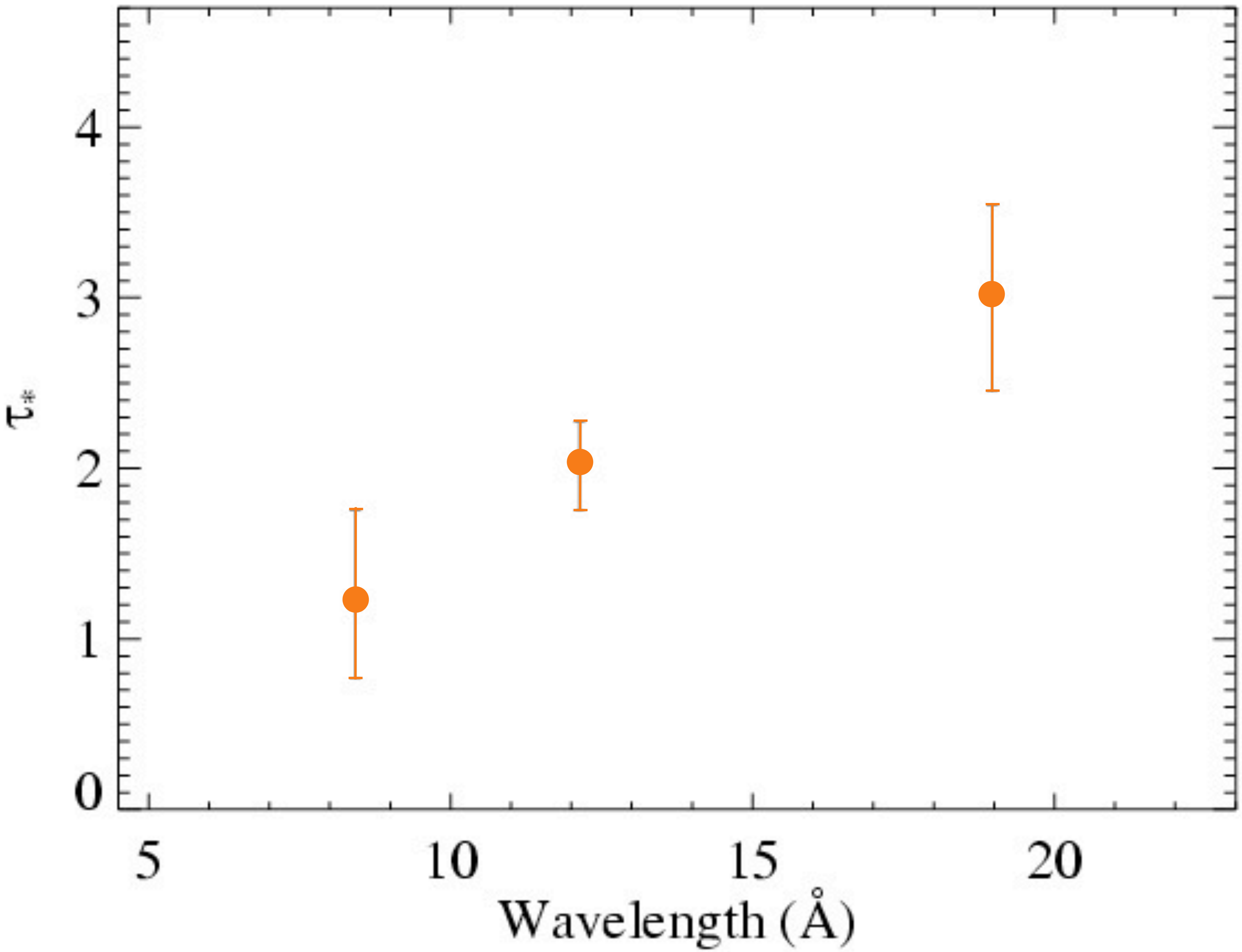

Fits to 16 lines in the *Chandra* spectrum of ζ Pup

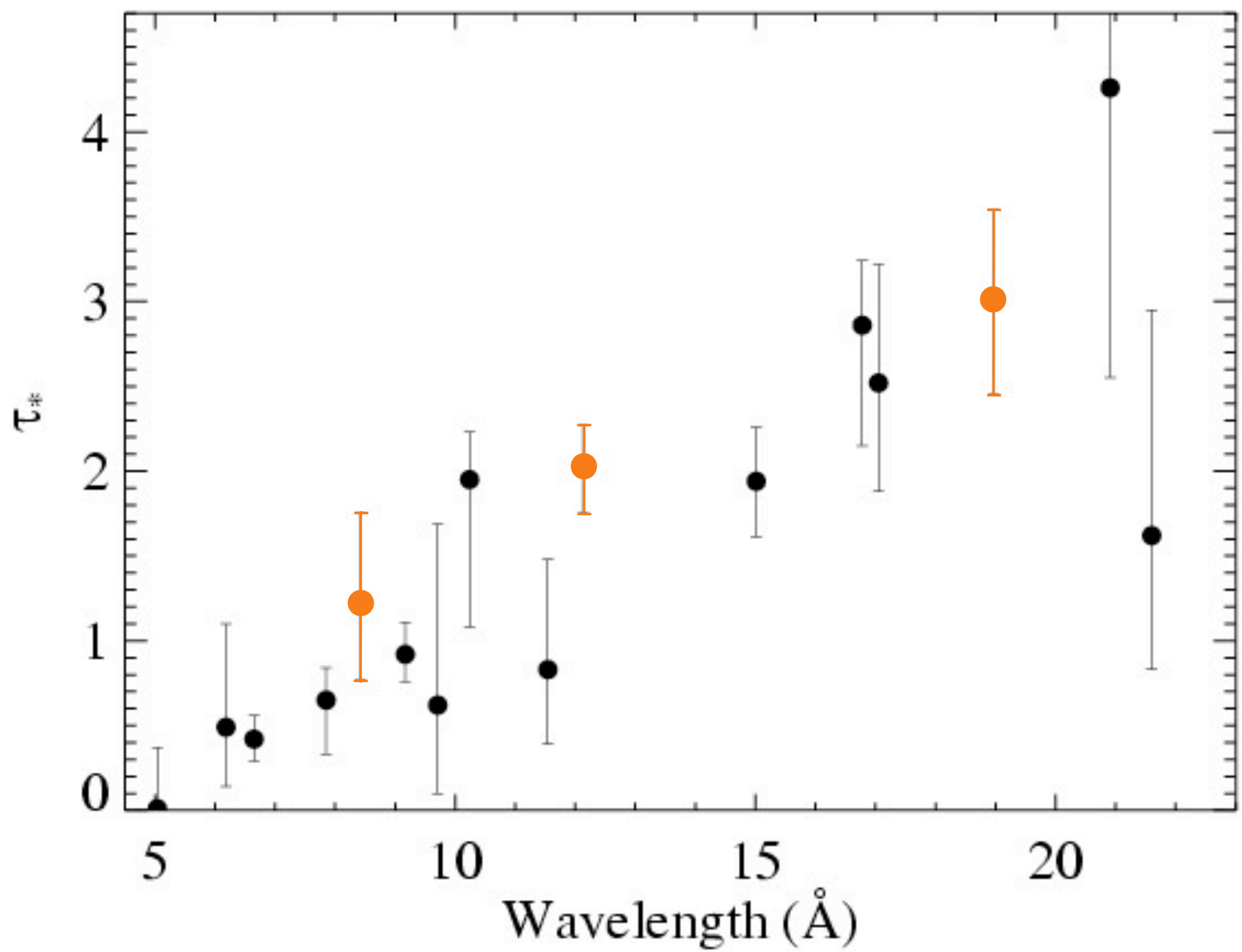

Fits to 16 lines in the *Chandra* spectrum of ζ Pup

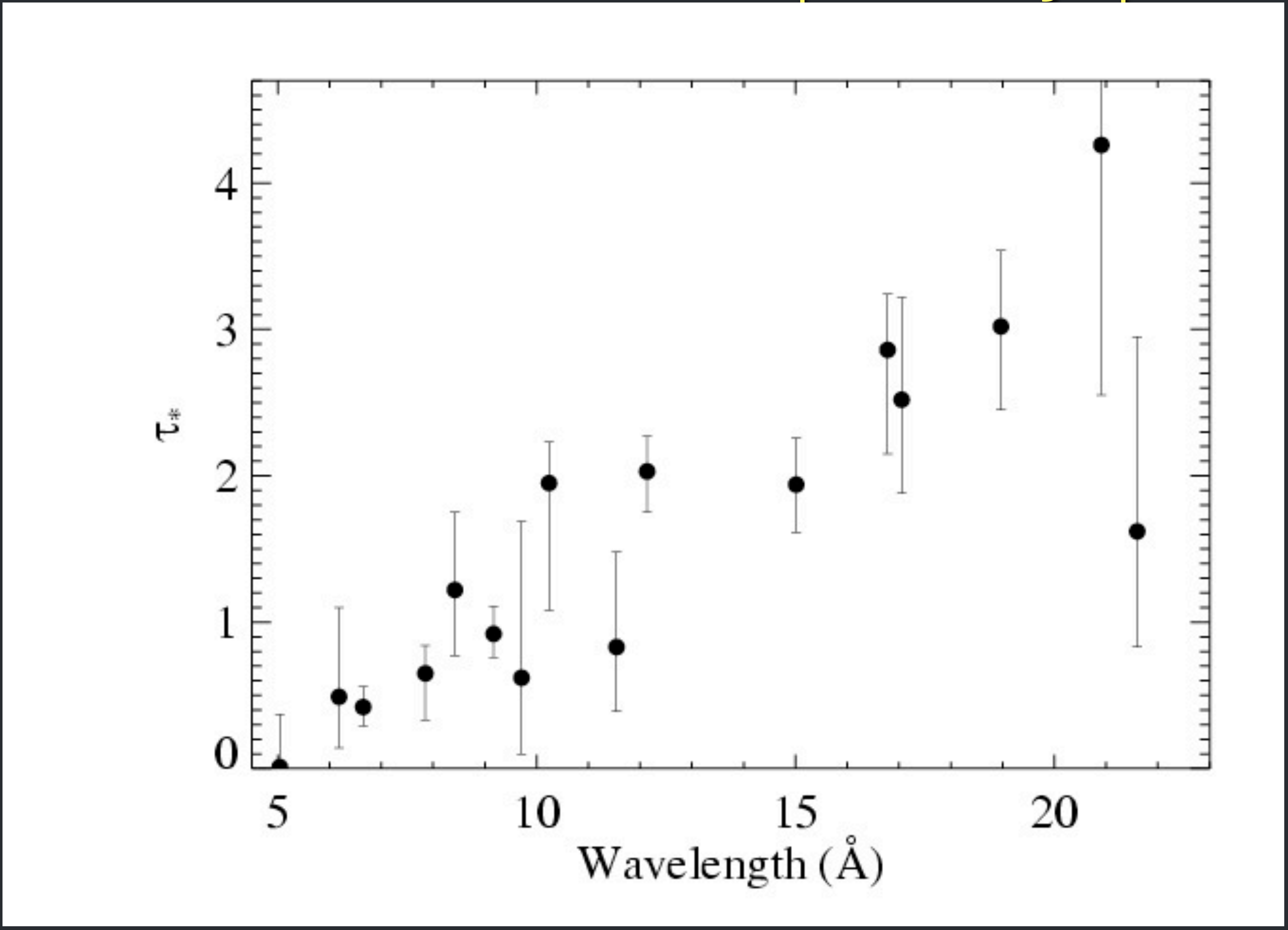

Fits to 16 lines in the *Chandra* spectrum of ζ Pup

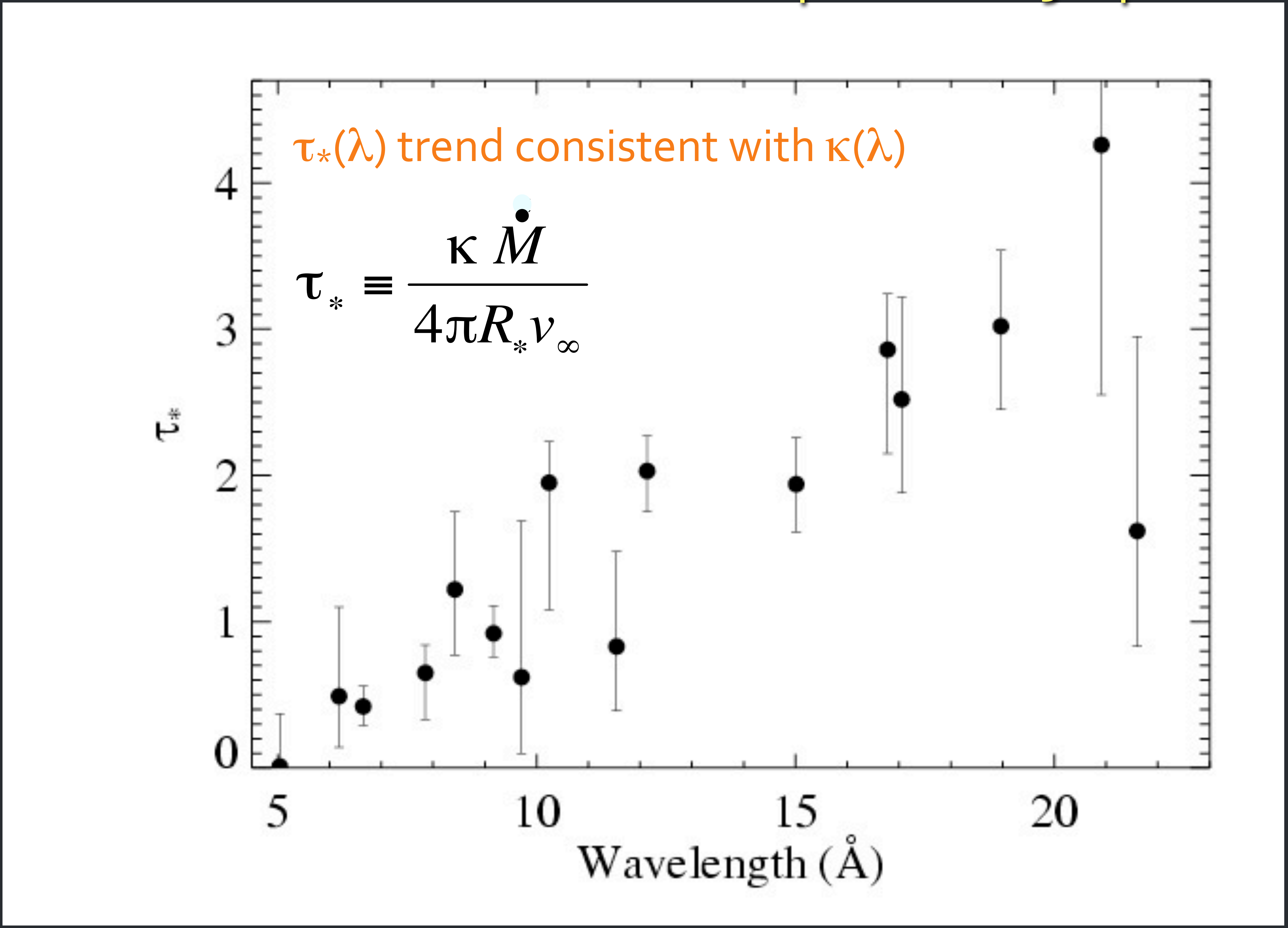

soft X-ray wind opacity

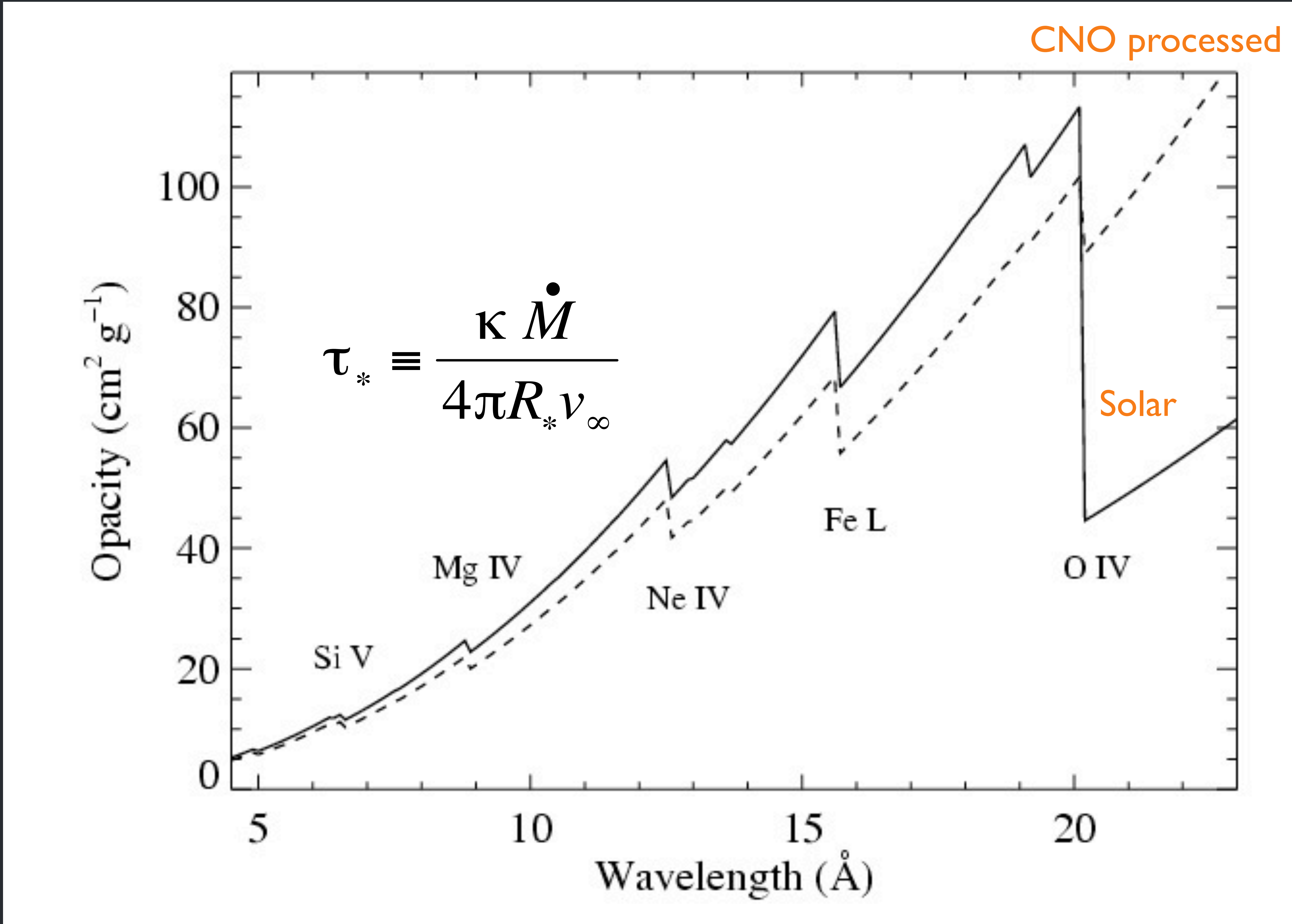

$$\tau_* \equiv \frac{\kappa \dot{M}}{4\pi R_* v_\infty}$$

$\dot{M}$ becomes the free parameter of the fit to the $\tau_*(\lambda)$ trend

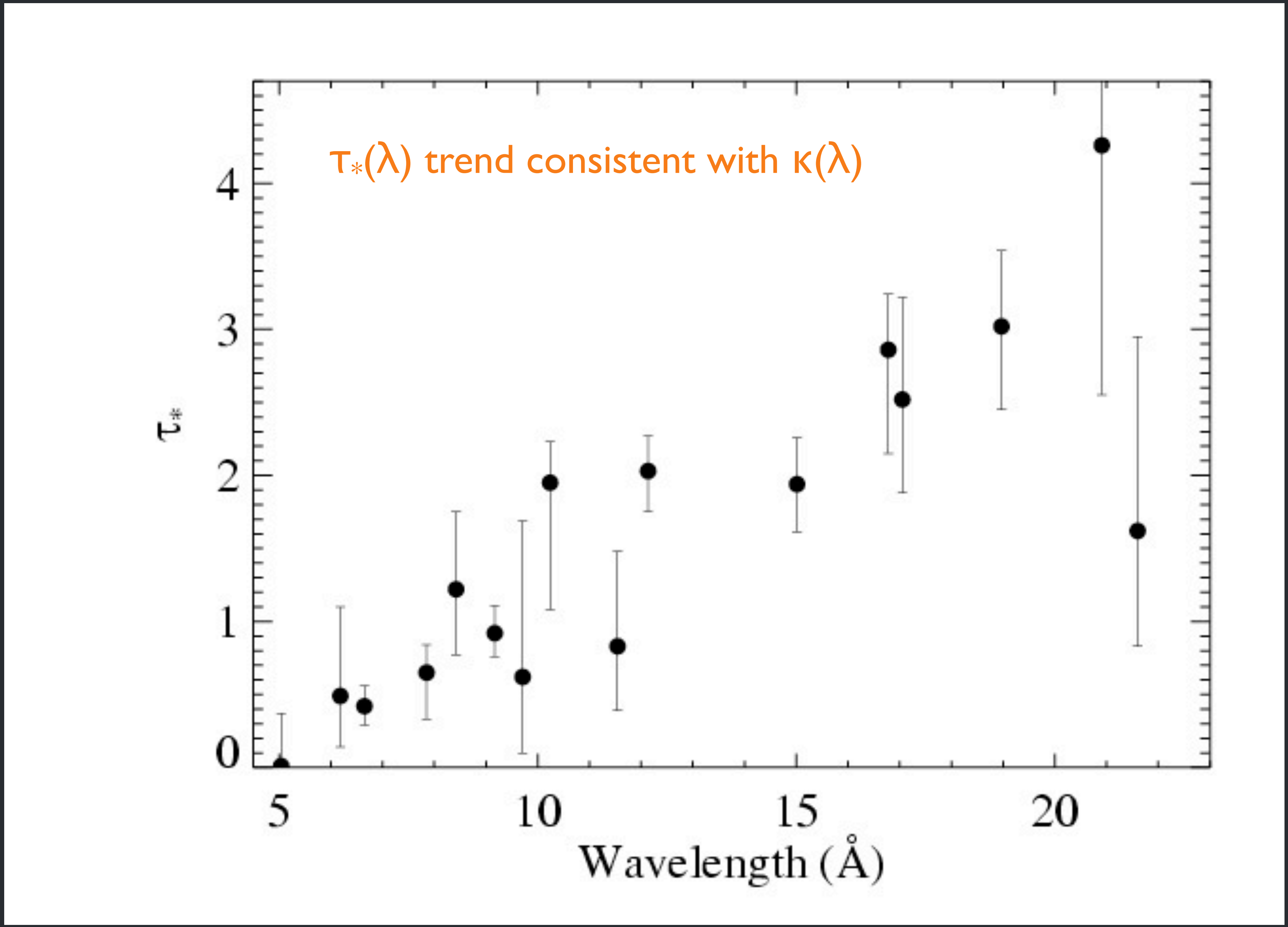

$$\tau_* \equiv \frac{\kappa \dot{M}}{4\pi R_* v_\infty}$$

$\dot{M}$ becomes the free parameter of the fit to the $\tau_*(\lambda)$ trend

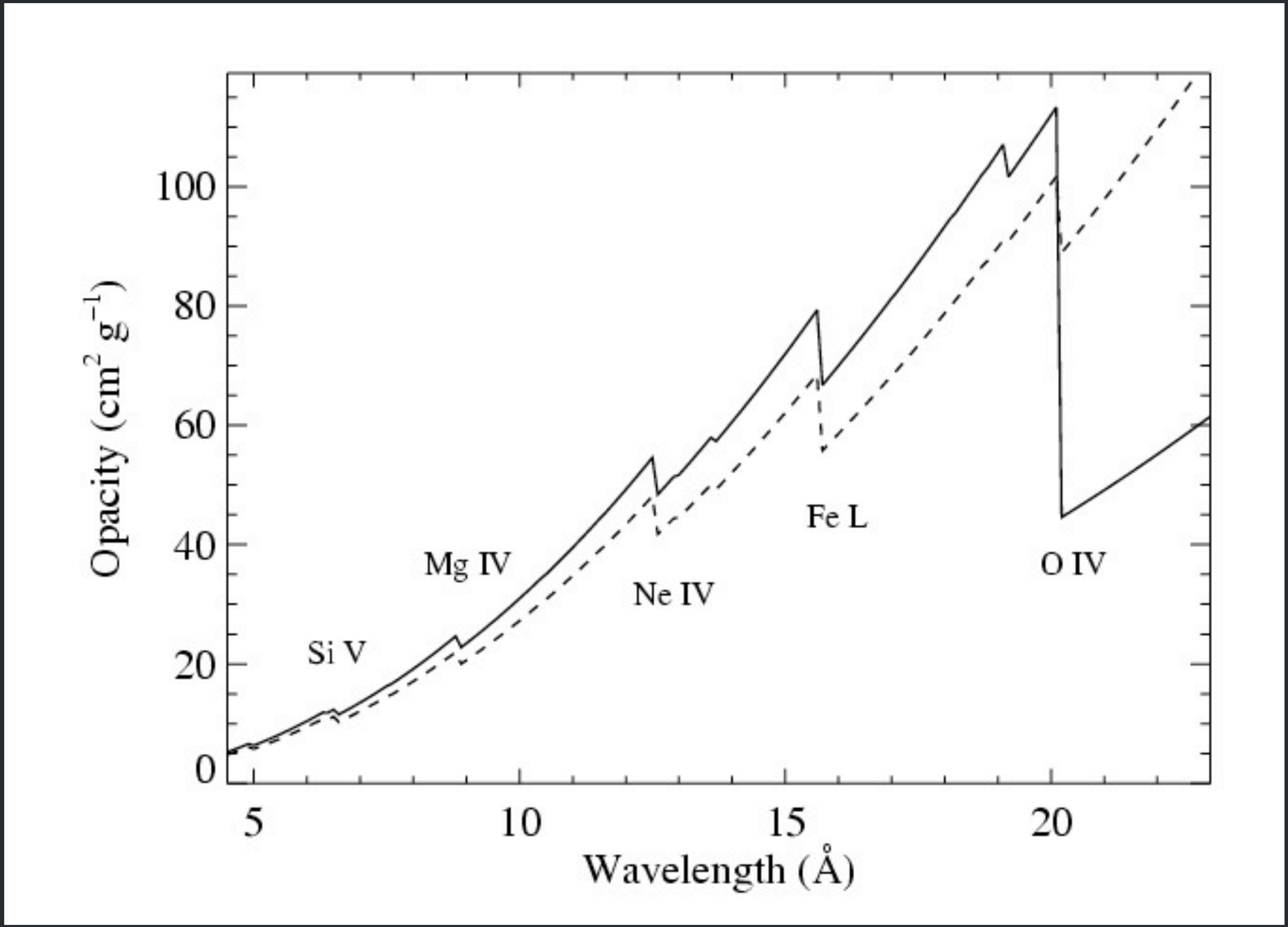

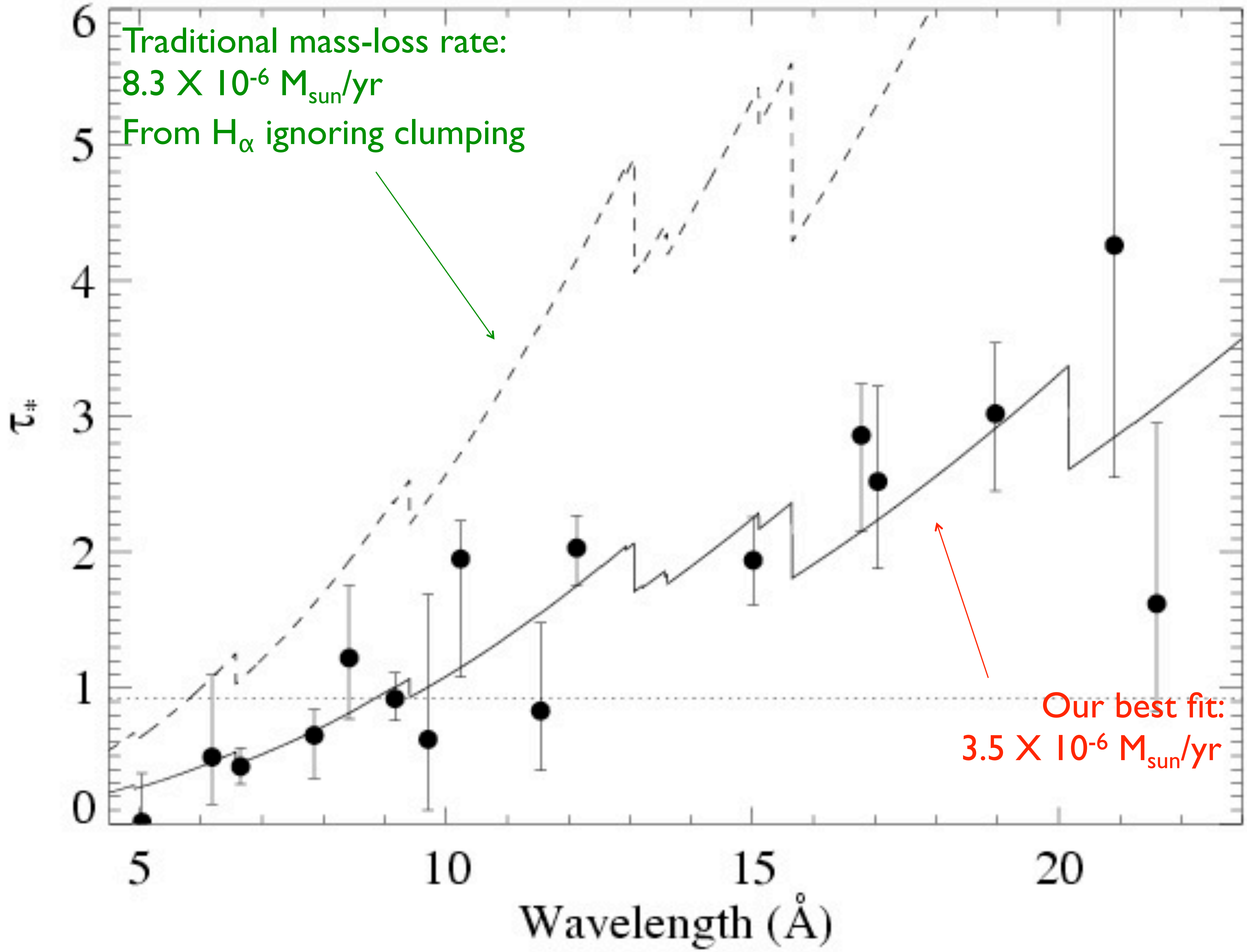

Traditional mass-loss rate:
8.3 X 10-6 Msun/yr
From Hα ignoring clumping
Our best fit:
3.5 X 10-6 Msun/yr
τ*
Wavelength (Å)
0
1
2
3
4
5
6
5
10
15
20

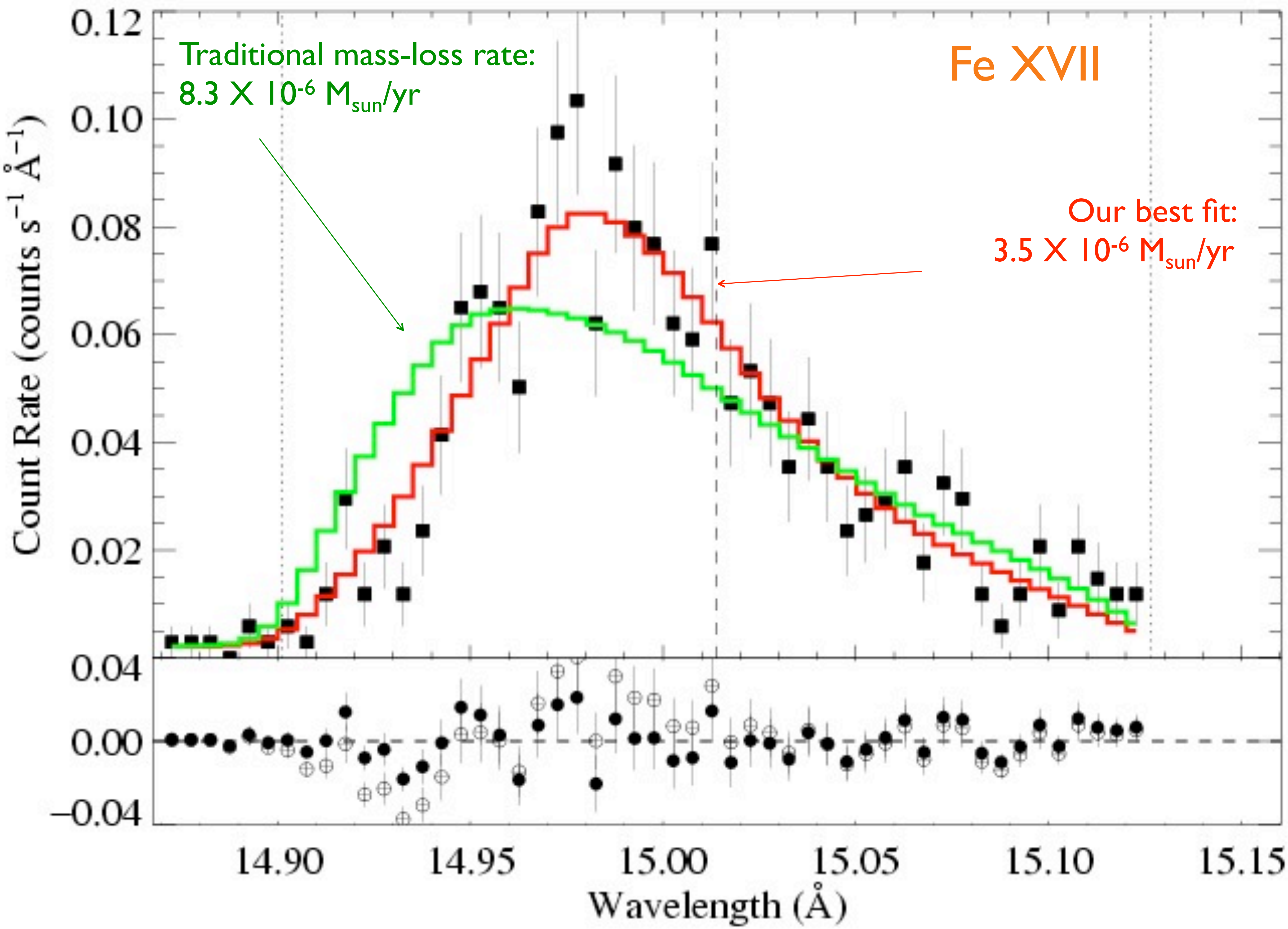

Traditional mass-loss rate:
8.3 X 10-6 Msun/yr
Fe XVII
Our best fit:
3.5 X 10-6 Msun/yr
Count Rate (counts s−1 Å−1)
0.12
0.10
0.08
0.06
0.04
0.02
0.04
0.00
−0.04
14.90
14.95
15.00
15.05
15.10
15.15
Wavelength (Å)

X-ray line profile based mass-loss rate: implications for clumping

basic definition: $f_{cl} \equiv \langle\rho^2\rangle / \langle\rho\rangle^2$

clumping factor

X-ray line profile based mass-loss rate: implications for clumping

basic definition: $f_{cl} \equiv \langle\rho^2\rangle/\langle\rho\rangle^2$

from density-squared diagnostics like Hα, IR & radio free-free

from (column) density diagnostic like $\tau_\star$ from X-ray profiles

ζ Pup mass-loss rate < 4.2 x 10^{-6} M_{sun}/yr

Bright OB stars in the Galaxy

III. Constraints on the radial stratification of the clumping factor in hot star winds from a combined H_{α}, IR and radio analysis*

J. Puls[1], N. Markova[2], S. Scuderi[3], C. Stanghellini[4], O. G. Taranova[5], A. W. Burnley[6] and I. D. Howarth[6]

[1] Universitäts-Sternwarte München, Scheinerstr. 1, D-81679 München, Germany, e-mail: uh101aw@usm.uni-muenchen.de
[2] Institute of Astronomy, Bulgarian National Astronomical Observatory, P.O. Box 136, 4700 Smoljan, Bulgaria, e-mail: nmarkova@astro.bas.bg
[3] INAF - Osservatorio Astrofisico di Catania, Via S. Sofia 78, I-95123 Catania, Italy, e-mail: scuderi@oact.inaf.it
[4] INAF - Istituto di Radioastronomia, Via P. Gobetti 101, I-40129 Bologna, Italy, e-mail: c.stanghellini@ira.inaf.it
[5] Sternberg Astronomical Institute, Universitetski pr. 13, Moscow, 119992, Russia, e-mail: taranova@sai.msu.ru
[6] Department of Physics and Astronomy, University College London, Gower Street, London WC1E 6BT, UK, e-mail: awxb@star.ucl.ac.uk, idh@star.ucl.ac.uk

Received; accepted

Abstract. Recent results strongly challenge the canonical picture of massive star winds: various evidence indicates that currently accepted mass-loss rates, $\dot{M}$, may need to be revised downwards, by factors extending to one magnitude or even more. This is because the most commonly used mass-loss diagnostics are affected by "clumping" (small-scale density inhomogeneities), influencing our interpretation of observed spectra and fluxes.
Such downward revisions would have dramatic consequences for the evolution of, and feedback from, massive stars, and thus robust determinations of the clumping properties and mass-loss rates are urgently needed. We present a first attempt concerning this objective, by means of constraining the radial stratification of the so-called clumping factor.
To this end, we have analyzed a sample of 19 Galactic O-type supergiants/giants, by combining our own and archival data for H_{α}, IR, mm and radio fluxes, and using approximate methods, calibrated to more sophisticated models. Clumping has been included into our analysis in the "conventional" way, by assuming the inter-clump matter to be void. Because (almost) all our diagnostics depends on the square of density, we cannot derive absolute clumping factors, but only factors normalized to a certain minimum.
This minimum was usually found to be located in the outermost, radio-emitting region, i.e., the radio mass-loss rates are the lowest ones, compared to $\dot{M}$ derived from H_{α} and the IR. The radio rates agree well with those predicted by theory, but are only upper limits, due to unknown clumping in the outer wind. H_{α} turned out to be a useful tool to derive the clumping properties inside $r < 3 \ldots 5 R_{\star}$. Our most important result concerns a (physical) difference between denser and thinner winds: for denser winds, the innermost region is more strongly clumped than the outermost one (with a normalized clumping factor of 4.1 ± 1.4), whereas thinner winds have similar clumping properties in the inner and outer regions.
Our findings are compared with theoretical predictions, and the implications are discussed in detail, by assuming different scenarios regarding the still unknown clumping properties of the outer wind.

trade-off/degeneracy between clumping factor and mass-loss rate

$$\dot{M}_{cl} \equiv \dot{M}_{smooth} / f_{cl}^{0.5}$$

Puls et al. (2006) : relative clumping (vs. radius), but free scale factor

ζ Pup mass-loss rate < 4.2×10^{-6} M_{sun}/yr

X-ray mass-loss rate breaks degeneracy and sets the scale factor

ζ Pup: radially varying clumping

for $\dot{M} = 3.5 \times 10^{-6}$ M_{sun}/yr

$$f_{cl} \equiv \langle\rho^2\rangle / \langle\rho\rangle^2$$

$$\dot{M}_{cl} \equiv \dot{M}_{smooth} / f_{cl}^{0.5}$$

$f_{cl} = 1.3$ @ $r < 1.12\ R_*$ Hα

$f_{cl} = 6.0$ @ $1.12 < r < 1.5\ R_*$ Hα

$f_{cl} = 3.7$ @ $1.5 < r < 2\ R_*$ Hα

$f_{cl} = 2.6$ @ $2 < r < 15\ R_*$ IR

$f_{cl} = 1.3$ @ $r > 15\ R_*$ radio

Hα

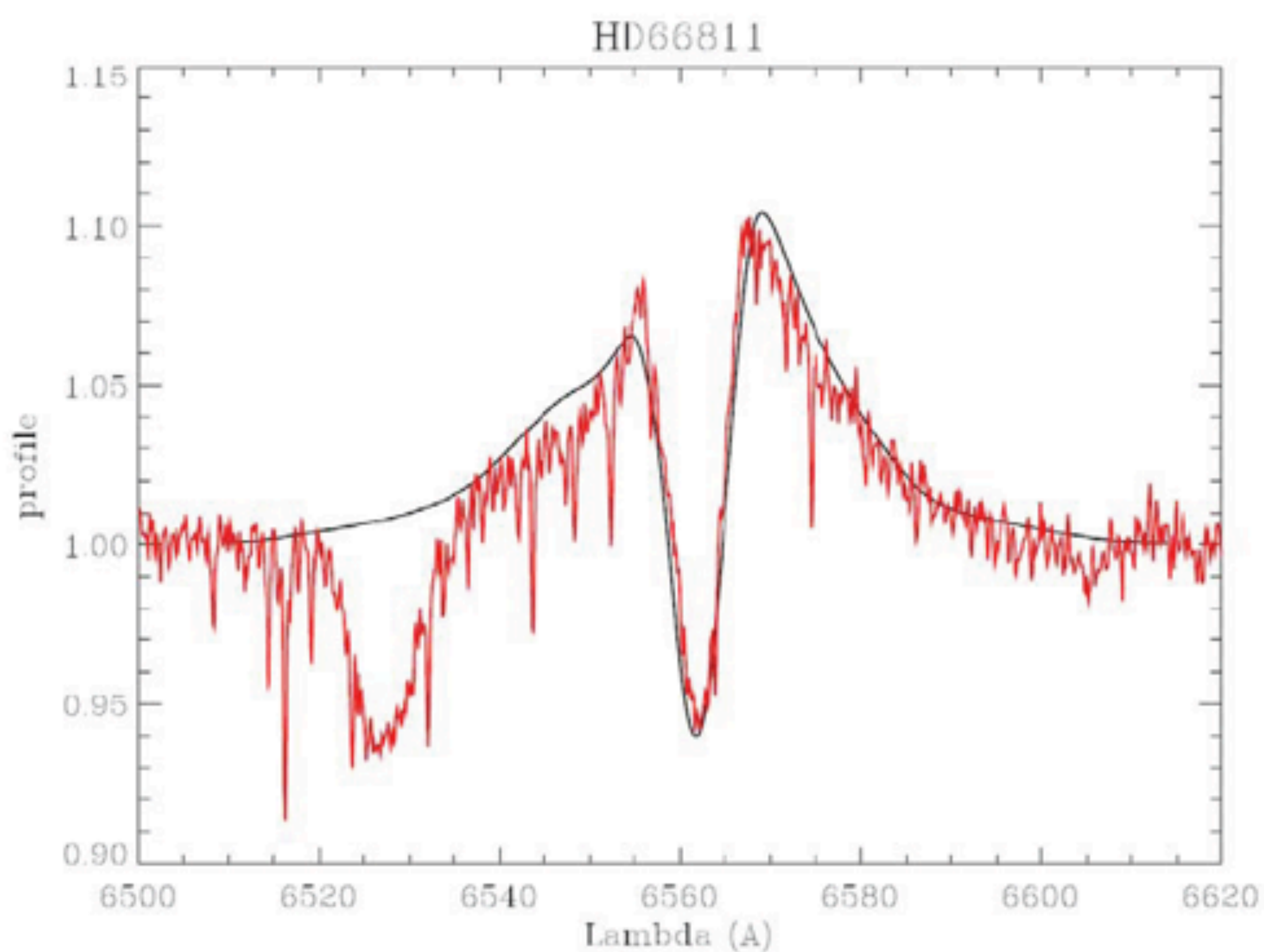

IR radio

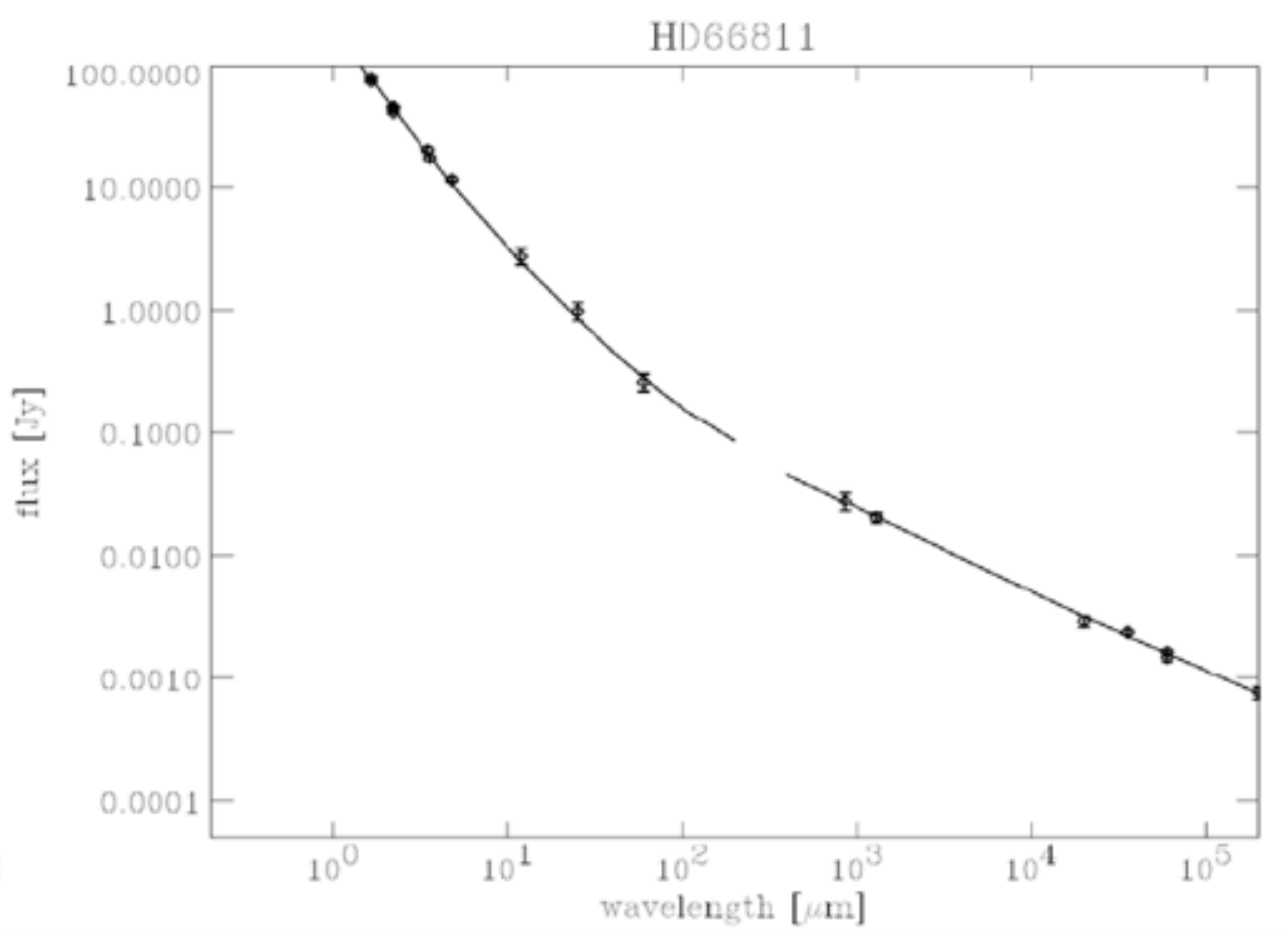

base of the wind ($r < 1.5\ R_\star$)

is clumped

...but...

recall: X-ray $R_o = 1.5\ R_\star$

$f_{cl} = 1.3$ @ $r < 1.12\ R_*$ Hα

$f_{cl} = 6.0$ @ $1.12 < r < 1.5\ R_*$ Hα

$f_{cl} = 3.7$ @ $1.5 < r < 2\ R_*$ Hα

$f_{cl} = 2.6$ @ $2 < r < 15\ R_*$ IR

$f_{cl} = 1.3$ @ $r > 15\ R_*$ radio

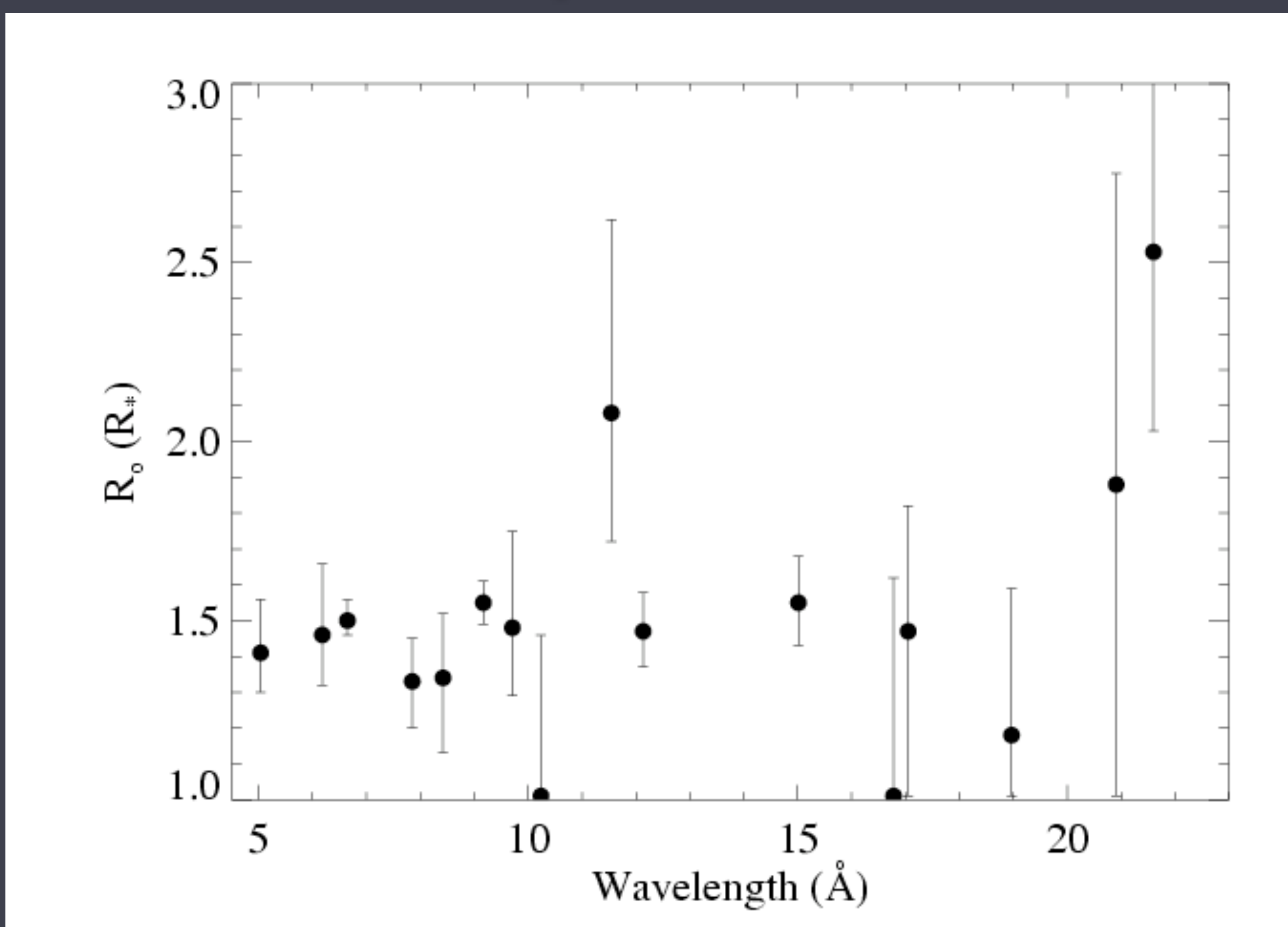

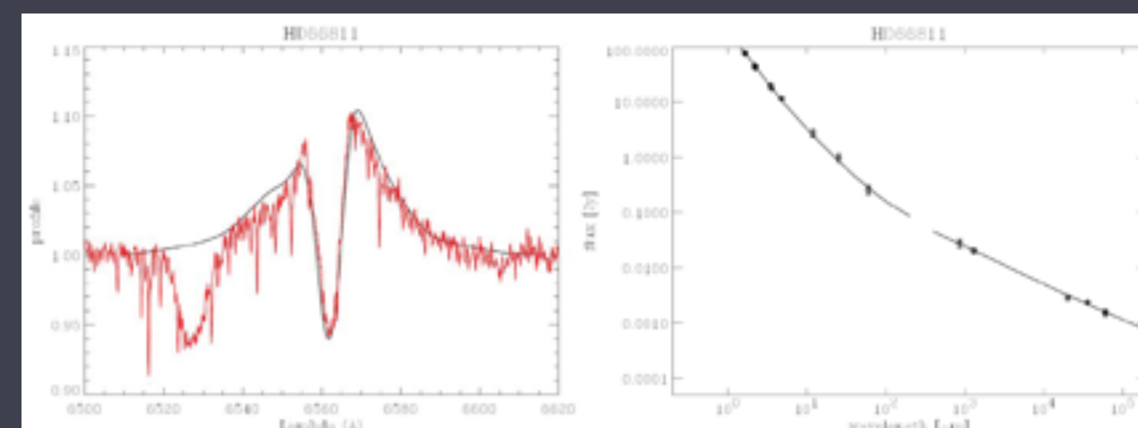

Other Stars?

HD 93129A

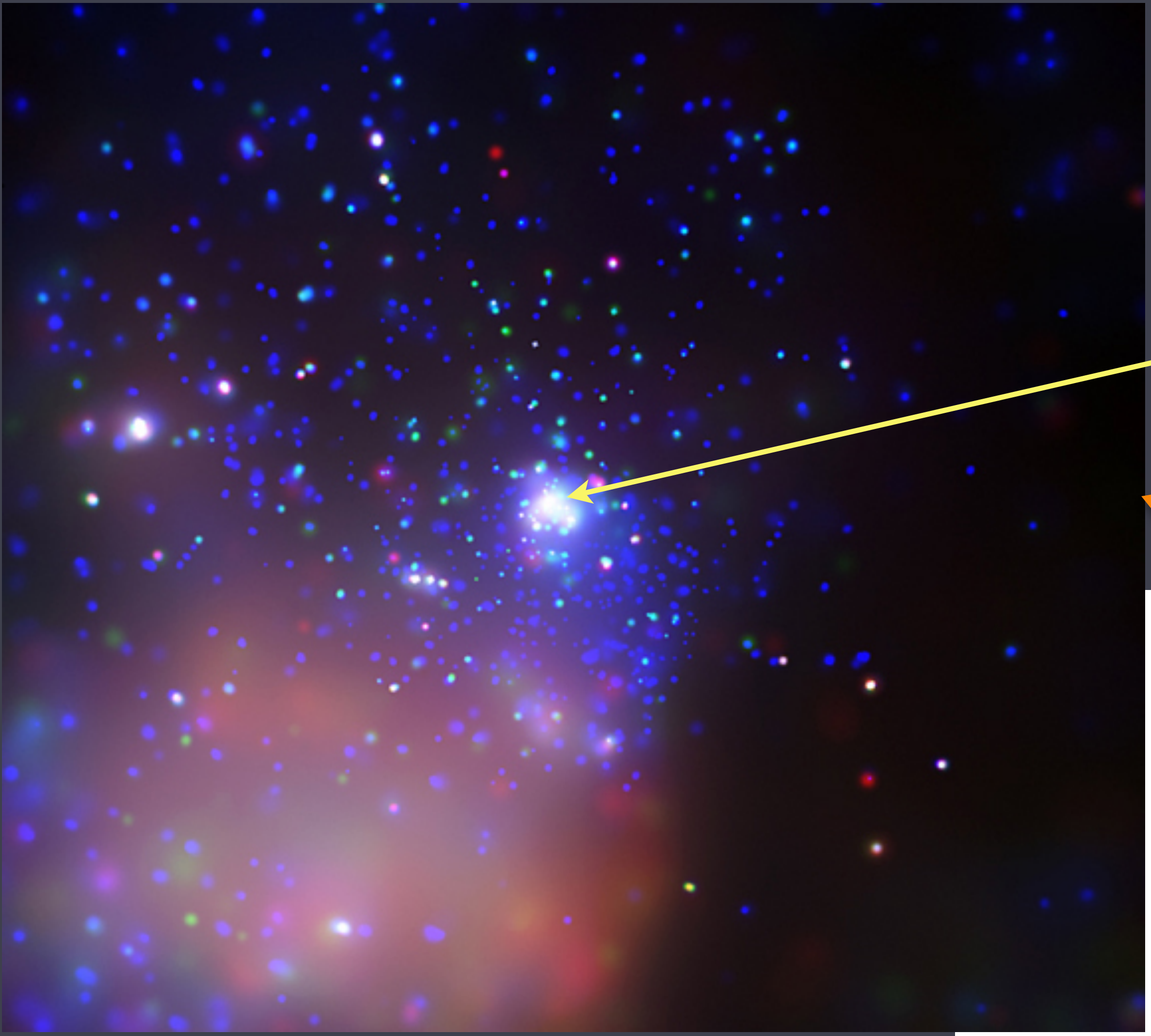

Tr 14: *Chandra*

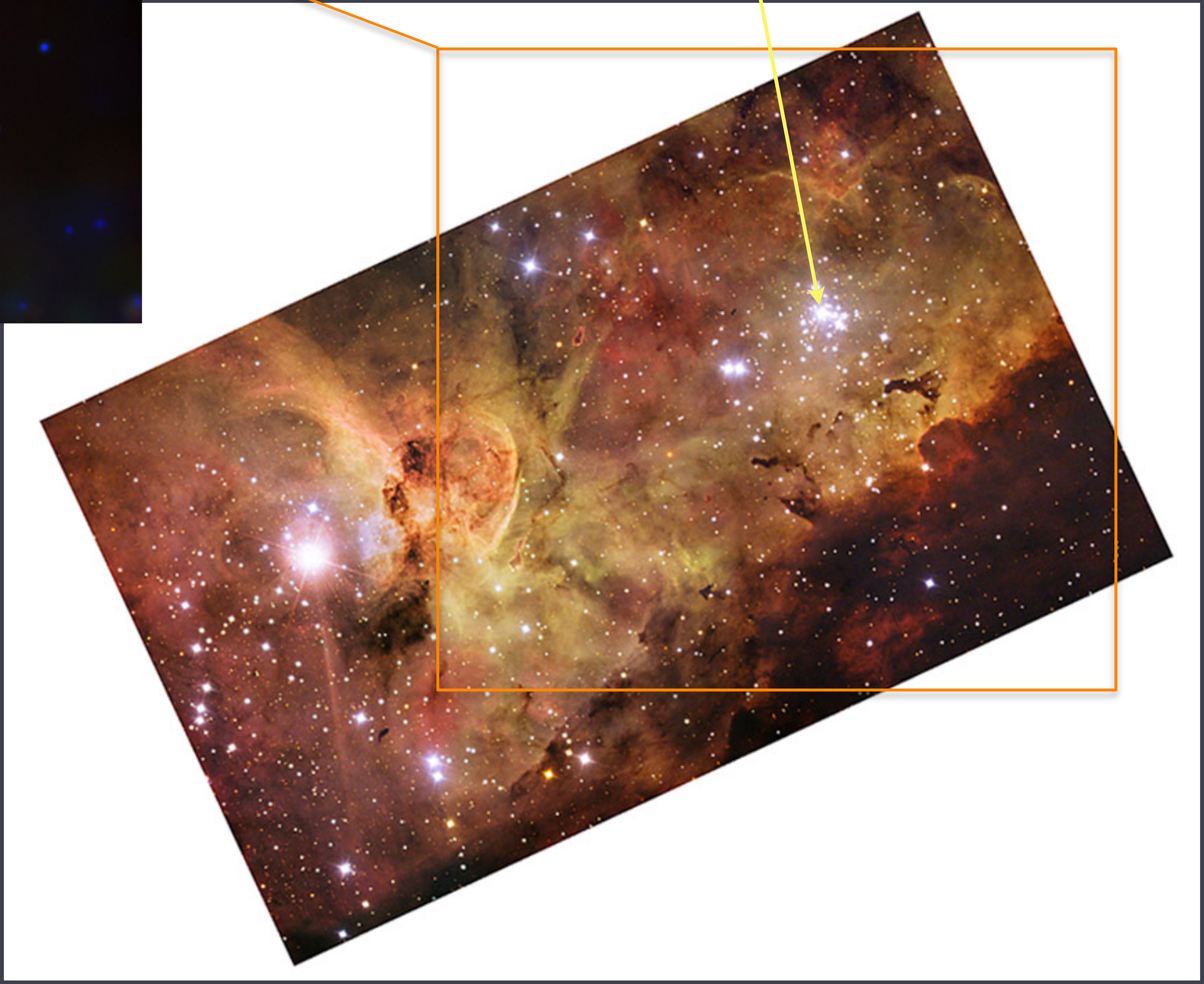

Carina: ESO

Tr 14: *Chandra*

$L_X \sim 7 \times 10^{32}$

$\langle h\nu \rangle \sim 1$ keV

: $kT \sim 10^7$ K

$L_{bol} \sim 2 \times 10^6 L_{sun}$ so $\mathbf{L_X/L_{bol} \sim 10^{-7}}$

Strong stellar winds: traditional diagnostics

UV

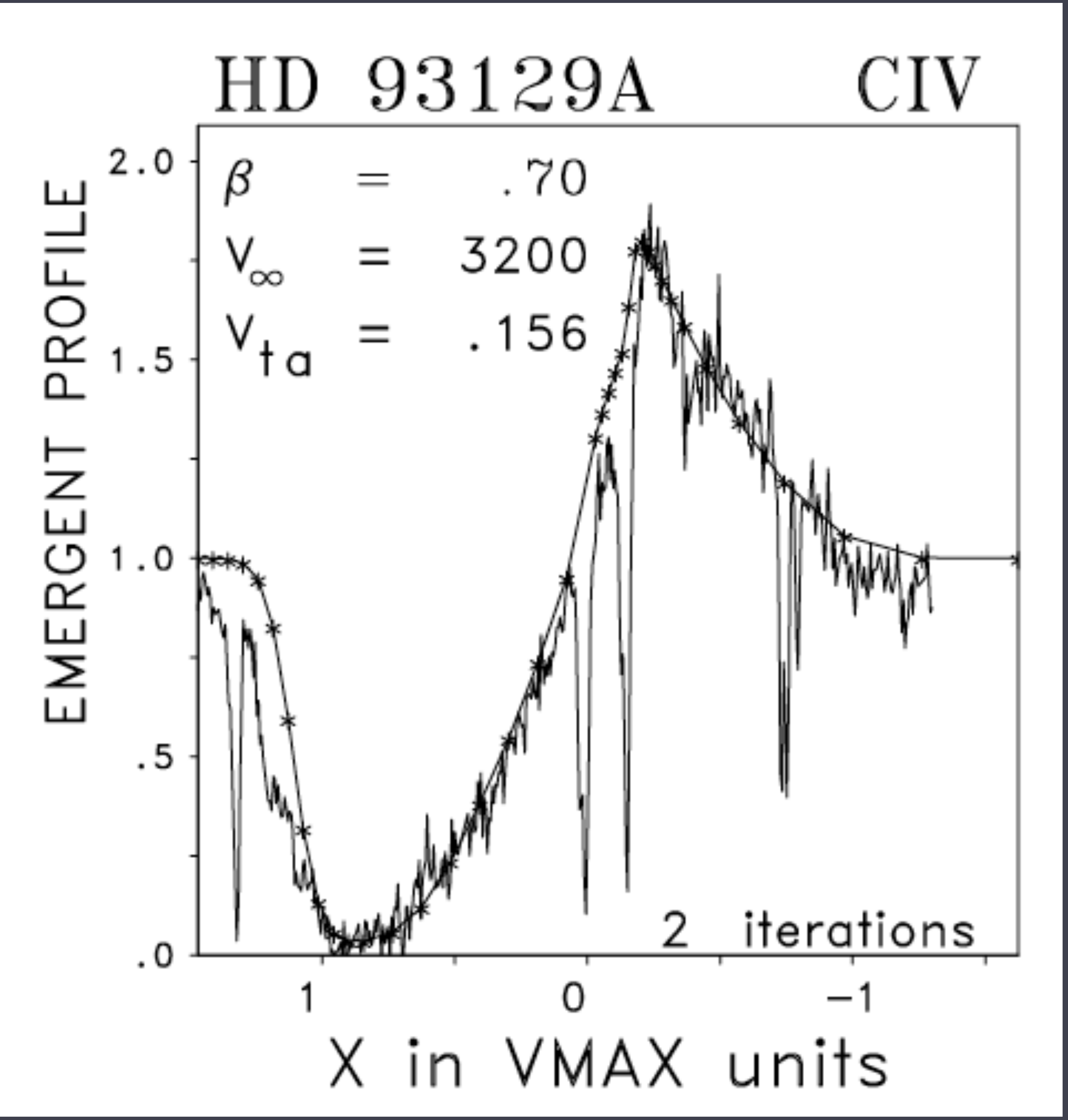

Taresch et al. (1997)

$\dot{M} = 2 \times 10^{-5}\ M_{sun}/yr$

$v_\infty = 3200$ km/s

Hα

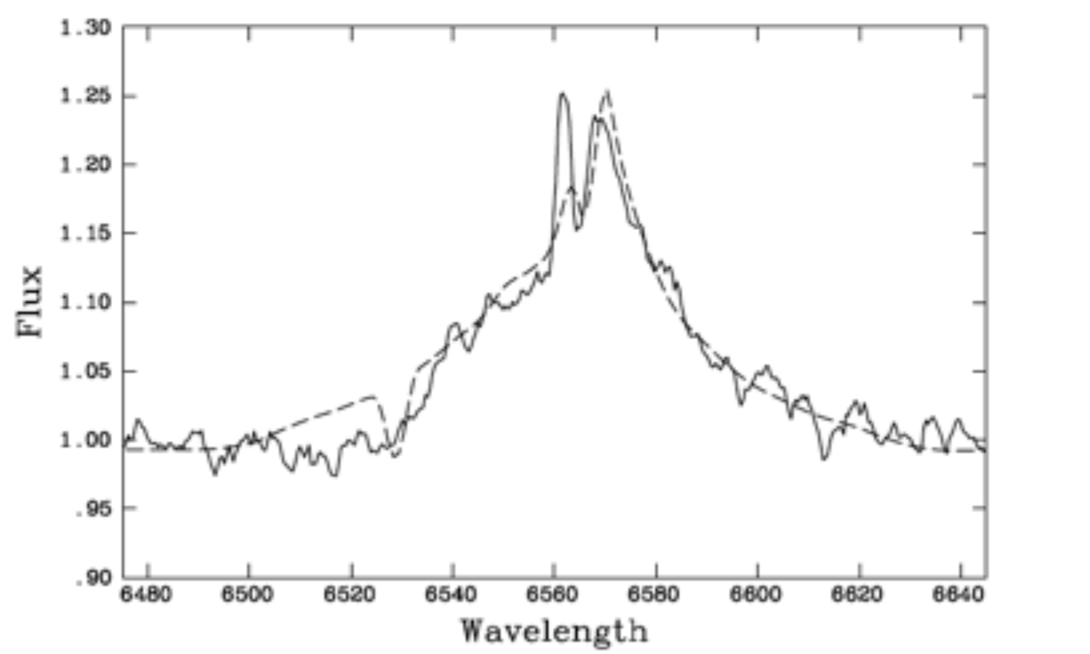

Fig. 13. Observed Hα profile (**solid**) compared with the calculation assuming a mass loss of $18 \times 10^{-6}\ M_\odot$/yr (dashed). Note that the blue narrow emission peak originates from the H II-region emission.

HD 93129A: strongest wind measured in an O star

Hα

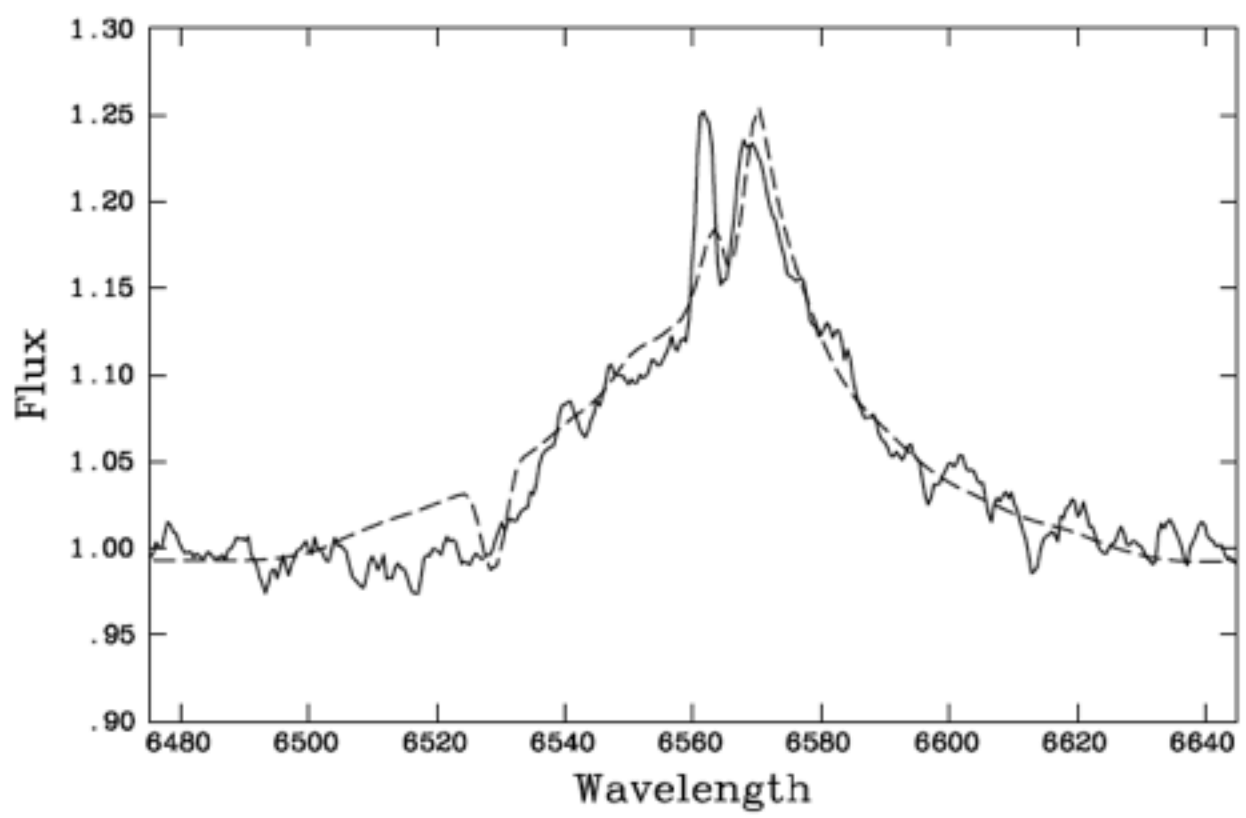

Fig. 13. Observed Hα profile (**solid**) compared with the calculation assuming a mass loss of $18 \times 10^{-6}\ M_{\odot}$/yr (dashed). Note that the blue narrow emission peak originates from the H II-region emission.

Taresch et al. (1997)

$\dot{M} = 2 \times 10^{-5}\ M_{sun}/yr$

assuming a *smooth* wind

i.e. no clumping

Tr 14: *Chandra*

HD 93129A

$L_X \sim 7 \times 10^{32}$

$\langle h\nu \rangle \sim 1$ keV
: $kT \sim 10^7$ K

$L_{bol} \sim 2 \times 10^6 \, L_{sun}$ so $\mathbf{L_X/L_{bol} \sim 10^{-7}}$

H-like vs. He-like soft emission absent: wind attenuation

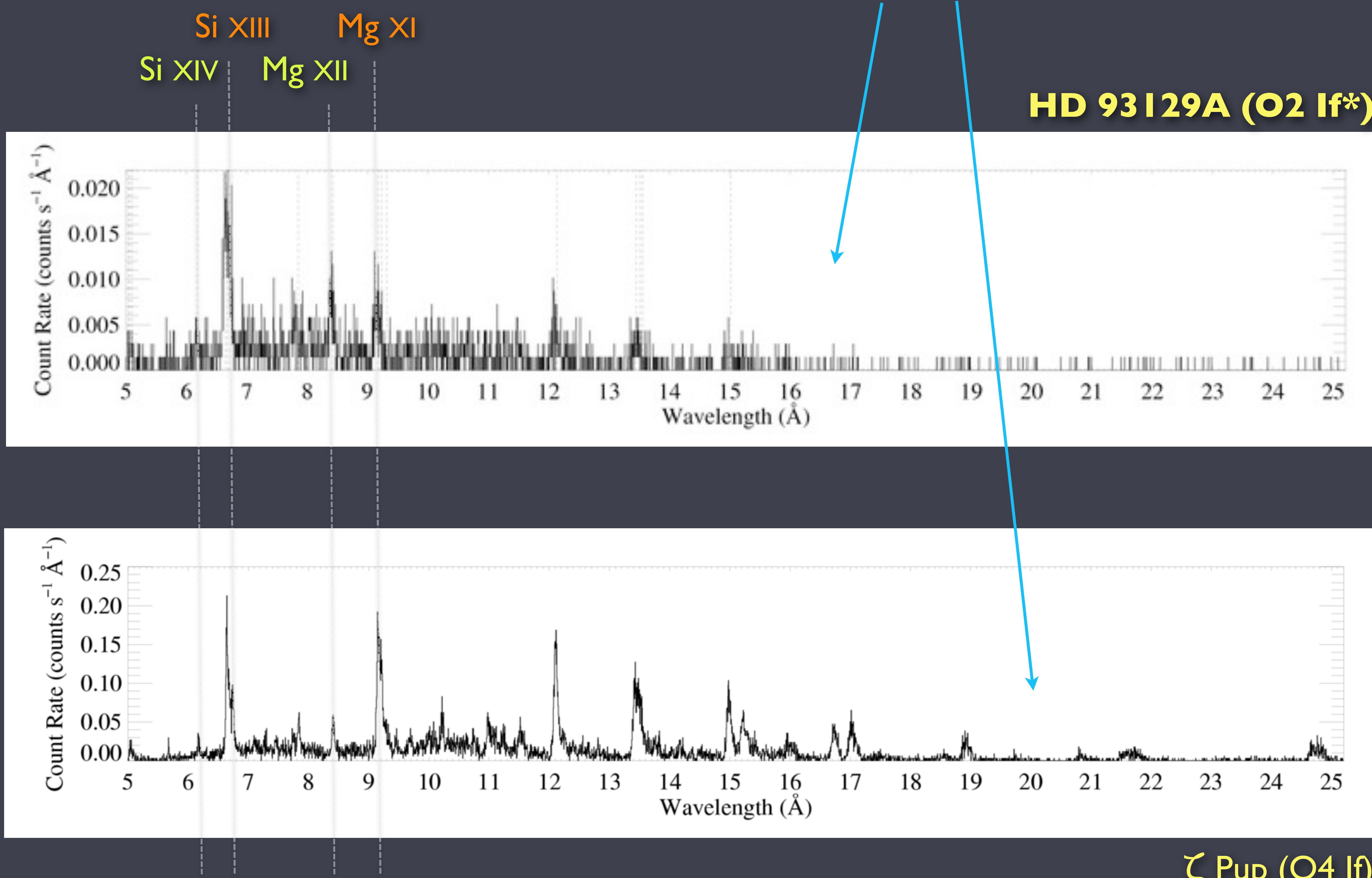

HD 93129A

Mg XII Lyman-alpha

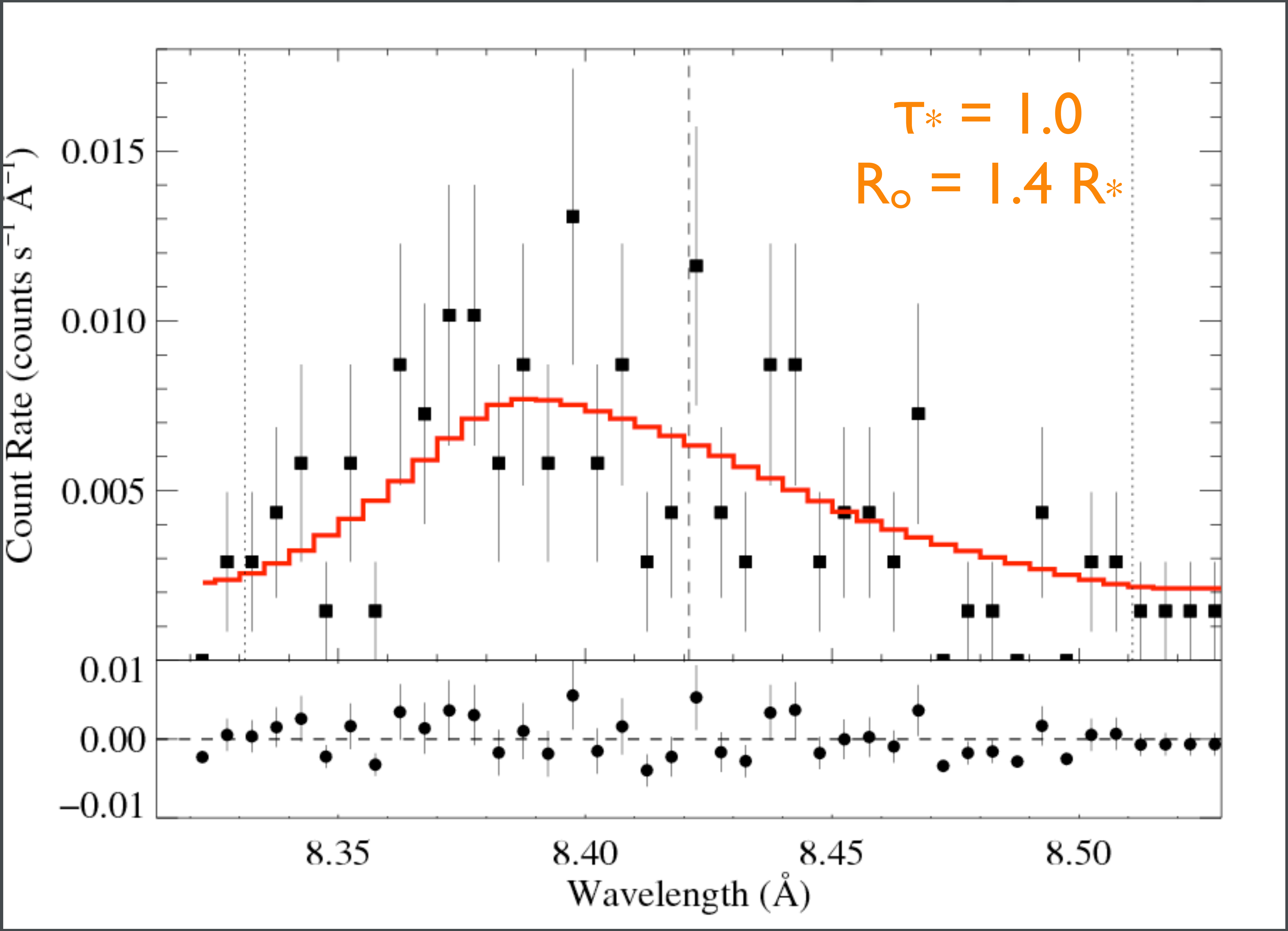

R_o = onset radius of X-ray emission

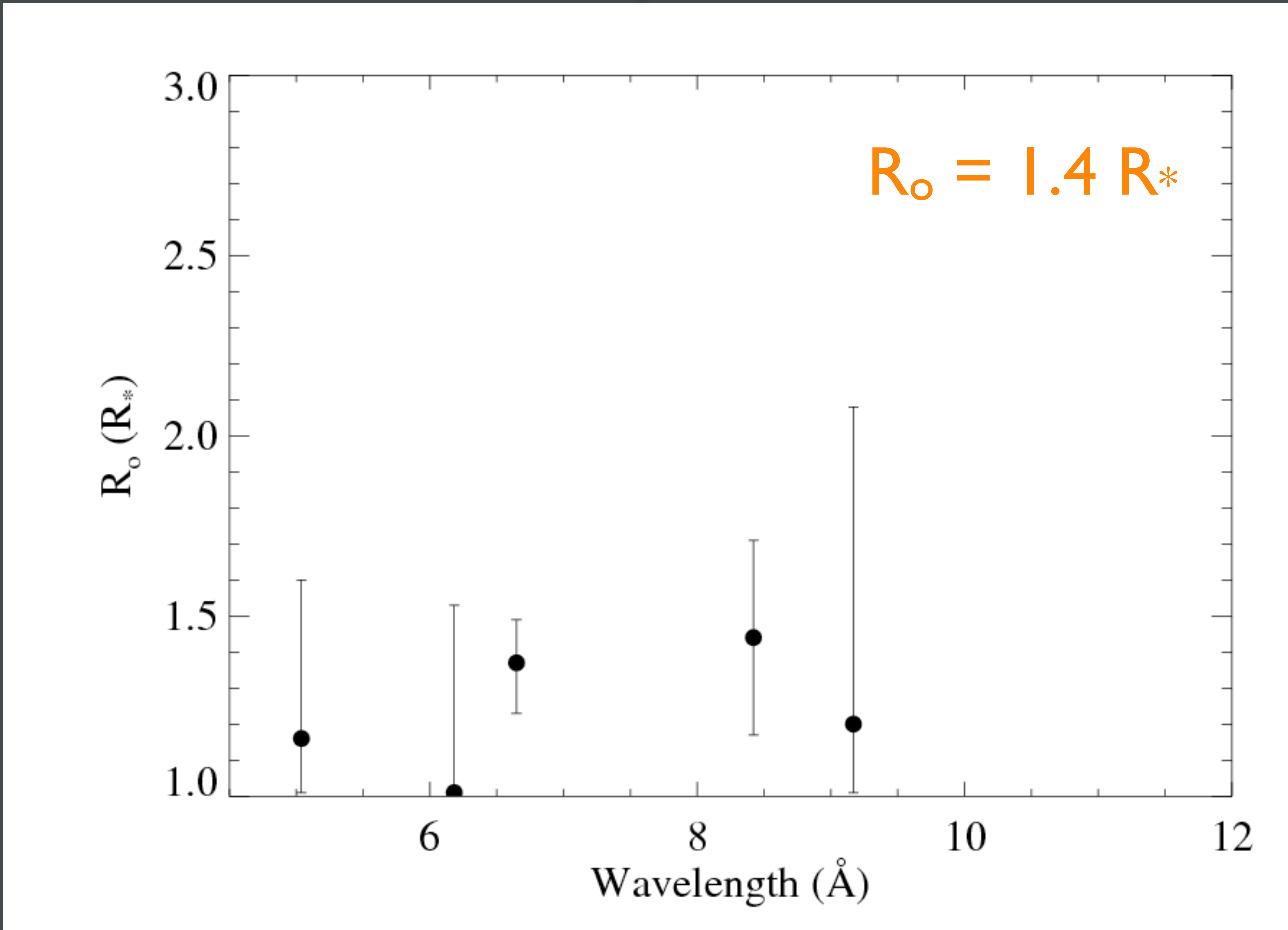

HD 93129A

τ_* from five emission lines

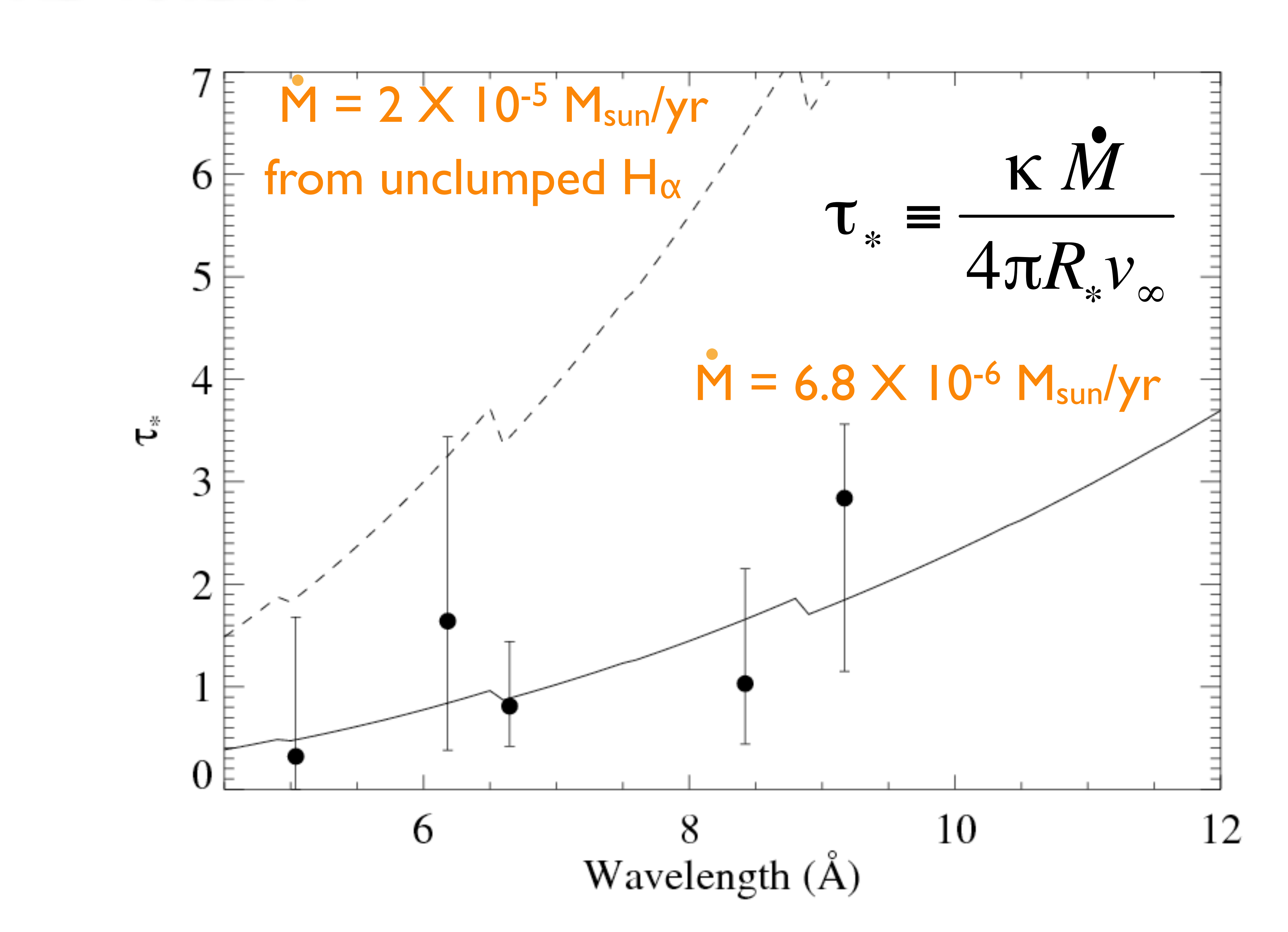

Lower mass-loss rate: consistent with Hα?

Lower mass-loss rate: consistent with Hα?

Yes! With clumping factor of f_{cl} = 12

$\dot{M} = 7 \times 10^{-6}\ M_{sun}/yr$

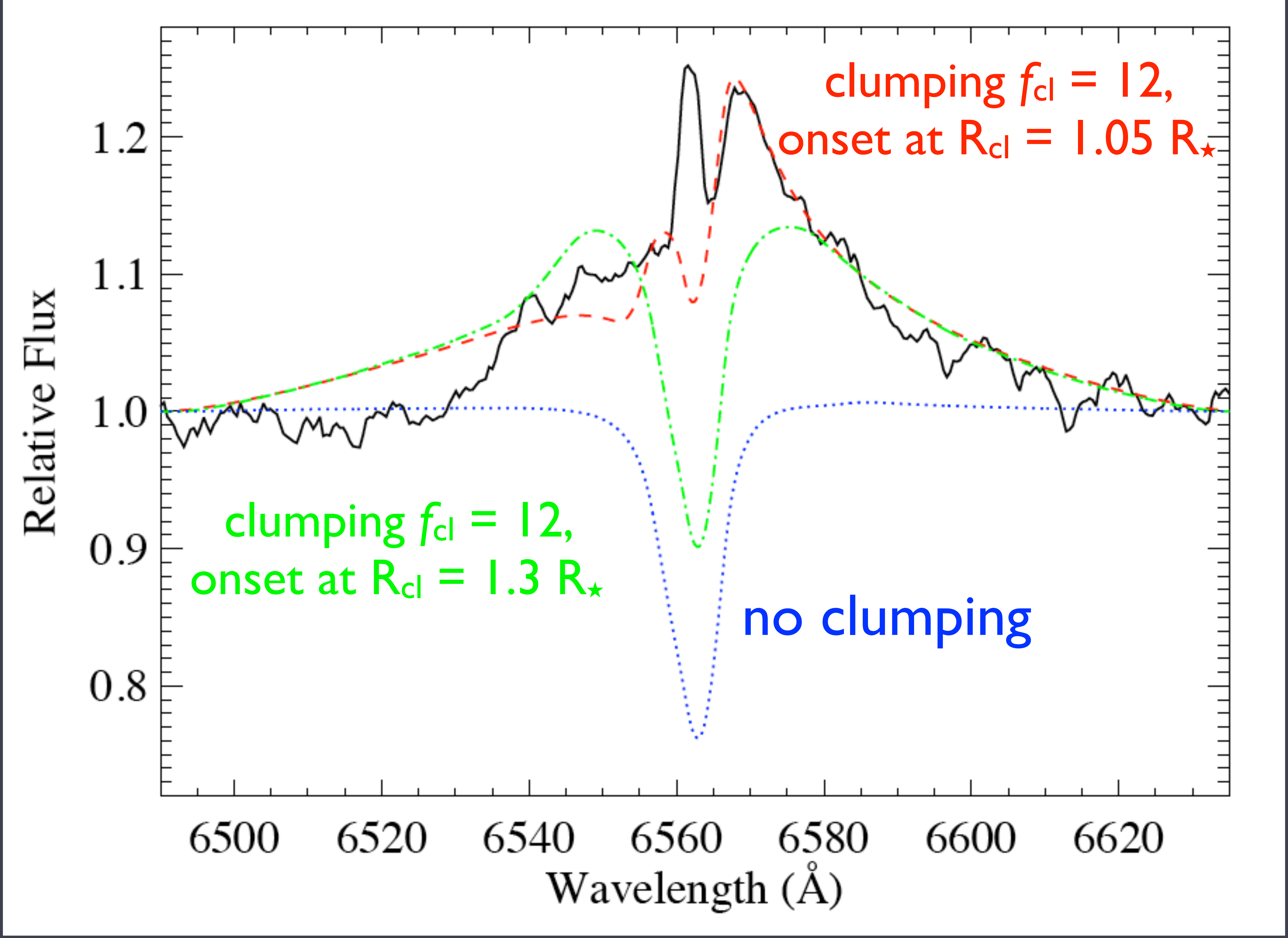

Conclusions

- X-ray emission is consistent with the LDI mechanism leading to shocks distributed throughout the wind
- Little or no X-ray emission at the base of the wind ($r < 1.5\ R_{\star}$), though clumping extends lower
- Absorption signatures in line profiles enable a mass-loss rate measurement
- Mass-loss rates are lower (factor of 3 to 5) than traditionally thought (from density-squared diagnostics)
- This is consistent with clumping factors, $f_{cl} \sim 10$